

Dissertation zur Erlangung des Doktorgrades
der Fakultät für Chemie und Pharmazie
der Ludwig-Maximilians-Universität München

**Thermoregulation of gene expression in encapsulated cells
by magnetic field-directed, nanoparticle-mediated
heat induction**

Cornelius Jakob Kaspar

aus München

2011

Erklärung

Diese Dissertation wurde im Sinne von § 13 Abs. 3 bzw. 4 der Promotionsordnung vom 29. Januar 1998 (in der Fassung der sechsten Änderungssatzung vom 16. August 2010) von Herrn Professor Dr. Ernst Wagner betreut.

Ehrenwörtliche Versicherung

Diese Dissertation wurde selbständig, ohne unerlaubte Hilfe erarbeitet.

München, den 20.12.2011

.....

Cornelius Kaspar

Dissertation eingereicht am 14.10.2011

1. Gutacher: Prof. Dr. Ernst Wagner

2. Gutacher: PD Dr. Christine Hohenadl

Mündliche Prüfung am 08.12.2011

TABLE OF CONTENT

1. SUMMARY	7
2. INTRODUCTION	9
2.1. Gene and cell-based therapy	10
2.2. Microencapsulation of cells.....	11
2.3. Magnetic nanoparticles in biomedicine.....	16
2.4. Heat generation by magnetic nanoparticles	18
2.5. Heat responsive promoters	19
2.6. A novel promoter for gene and cell-based therapy	20
2.7. Regulation of heat shock response	22
2.8. Aim of the project.....	24
3. MATERIALS AND METHODS.....	25
3.1. Materials	25
3.1.1. Chemicals and reagents	25
3.1.2. Enzymes and Kits	27
3.1.3. Cell culture materials	27
3.1.3.1. Tubes	27
3.1.3.2. Cell culture flask	27
3.1.3.3. Pipettes	28
3.1.3.4. Multi-well-plates.....	28
3.1.3.5 Syringes and accessories.....	28
3.1.4. Laboratory devices.....	29
3.1.5. Nanoparticles.....	30

3.1.6. Cells.....	31
3.1.6.1. Cell line: HEK293	31
3.1.6.2. Single cell clone: HEK293 pSGH2lucpuro C5	31
3.1.6.3. Cell populations: HEK293 pCMVluc and HEK293 pCMVegfp	31
3.2. Methods.....	31
3.2.1. Cell culture	32
3.2.1.1. Maintenance of cells.....	32
3.2.1.2. Storage of eukaryotic cell lines.....	32
3.2.1.3. Thawing of cells.....	33
3.2.2. Encapsulation	34
3.2.2.1. Encapsulation apparatus und process principles	34
3.2.2.2. Encapsulation with alginate.....	37
3.2.2.3. Encapsulation with sodium cellulose sulphate.....	37
3.2.2.4. Maintenance of encapsulated cells	38
3.2.2.5. Freezing of encapsulated cells	39
3.2.2.6. Thawing of encapsulated cells	40
3.2.3. Determination of capsule properties	40
3.2.3.1. Investigation of capsule membrane thickness	40
3.2.3.2. Determination of capsule pore size	41
3.2.4. Determination of viscosity	41
3.2.5. Analysis of cell viability.....	42
3.2.5.1. Determination of cell viability by analysis of metabolic activity (AlamarBlue assay)	42
3.2.5.2. Determination of cell viability by analysing cell membrane integrity (TrypanBlue assay)	43

3.2.5.3. Determination of cell viability by analysing intracellular esterase activity and membrane integrity by co-staining with calcein and propidium iodide.....	44
3.2.6. Magnetic field treatment.....	45
3.2.7. Analysis of gene expression	47
3.2.7.1. Analysis of luciferase expression by luciferase assay	47
3.2.7.2. Analysis of GFP expression by FACS	48
3.2.8. Electron microscopy.....	48
3.2.9. Immunohistochemistry	49
3.2.9.1. Preparation of paraffin-embedded samples.....	49
3.2.9.2. Hematoxylin/Eosin staining	50
3.2.9.3. TUNEL assay	50
3.2.9.4. Caspase 3 staining.....	51
3.2.10. Animal experiments	52
3.2.10.1. Maintenance of mice	52
3.2.10.2. Anaesthesia and euthanasia	52
3.2.10.3. Experimental accomplishment.....	52

4. RESULTS.....54

4.1. Analysis of heat-induced expression in genetically modified cells.....	54
4.2. Characterisation of magnetic nanoparticles with respect to physical properties, heat generation capacity and tendency to aggregate.....	57
4.3. Co-encapsulation of cells and nanoparticles.....	61
4.3.1. Characterisation of physicochemical properties of capsules with and without nanoparticles	62
4.4. Characterisation of encapsulated cells	68
4.4.1. Characterisation of encapsulated cells with respect to nanoparticle localisation	68

4.4.2. Characterisation of encapsulated cells concerning biocompatibility of nanoparticles.....	71
4.4.3. Characterisation of encapsulated cells with respect to heat inducibility.....	75
4.5. Effects of magnetic field treatment on cell integrity and cell viability of encapsulated cells.....	83
4.6. Magnetic field-induced, nanoparticle-mediated, gene expression in encapsulated cells.....	91
4.7. Heat inducible expression in encapsulated cells <i>in vivo</i>.....	96
4.8. Summary of the results.....	99
5. DISCUSSION	101
6. REFERENCES	115
7. APPENDIX	123
7.1. Abbreviations.....	123
7.2. List of figures.....	125
7.3. List of tables	126
7.4. Plasmids.....	127
7.5. Own publications.....	129
7.5.1. Scientific paper	129
7.5.2. Oral presentation	129
7.5.3. Poster presentations	131
8. ACKNOWLEDGEMENTS	134
9. CURRICULUM VITAE	136

1. SUMMARY

The objective of this project was to establish a system facilitating externally controlled gene expression within encapsulated cells. This project may allow production of a potential therapeutic protein from genetically modified heterologous cells inside a patient's body at the place of therapeutic relevance without rejection by the host's immune system. To this aim, magnetic field-directed, nanoparticle-mediated heat induction of reporter gene expression in encapsulated cells was evaluated.

In a first step, genetically modified HEK293 cells, which harboured a heat-inducible expression construct, were analysed with respect to inducibility in response to incubation at elevated temperature, revealing robust induction of reporter gene expression.

A set of 13 different nanoparticle formulations was investigated with regard to critical parameters such as heat generation capacity in an alternating magnetic field as well as their general tendency to aggregate. Taking into account both parameters, two nanoparticle formulations were selected for further experiments.

The co-encapsulation of cells with the two nanoparticle formulations in biologically inert sodium cellulose sulphate (SCS) was successfully established by modifying encapsulation parameters. Modified encapsulation parameters were shown to have no impact on microcapsule diameter and membrane thickness of the microcapsules as well as on pore size of the microcapsules compared to unmodified standard capsules.

Encapsulated cells were characterised regarding biocompatibility of nanoparticle formulations as well as heat inducibility. Nanoparticle localisation in SCS capsules, cell viability and metabolic activity during long-term cultivation as well as proliferation of encapsulated cells demonstrated acceptable tolerability of magnetite nanoparticles. Investigation of heat inducibility of reporter gene expression in encapsulated cells revealed general inducibility of gene expression also in encapsulated cells as well as ongoing inducibility of gene expression in encapsulated

cells for four weeks of cultivation. Additionally, the possibility of repeated induction for three weeks of cultivation was demonstrated.

Finally, the survival of encapsulated cells after magnetic field treatment was investigated revealing that magnetic field treatment was well tolerated by HEK293 cells.

Proof-of-principle for this novel cell therapy concept could be provided *in vitro* by magnetic field-directed, nanoparticle-mediated heat induction of reporter gene expression in encapsulated cells. Additionally, preliminary *in vivo* experiments confirmed repeated heat-inducible expression of reporter genes within encapsulated cells that had been implanted into mice, being indication for a general applicability for potential therapeutic approaches.

2. INTRODUCTION

For the treatment of many diseases using cell-based therapy approaches, externally induced therapeutic gene expression is of great interest. In this project a strictly external regulation of gene expression should be achieved within encapsulated cells. Thereby, therapeutic protein levels can be generated in a controlled manner by genetically modified heterologous cells inside a patient's body at the place of therapeutic relevance.

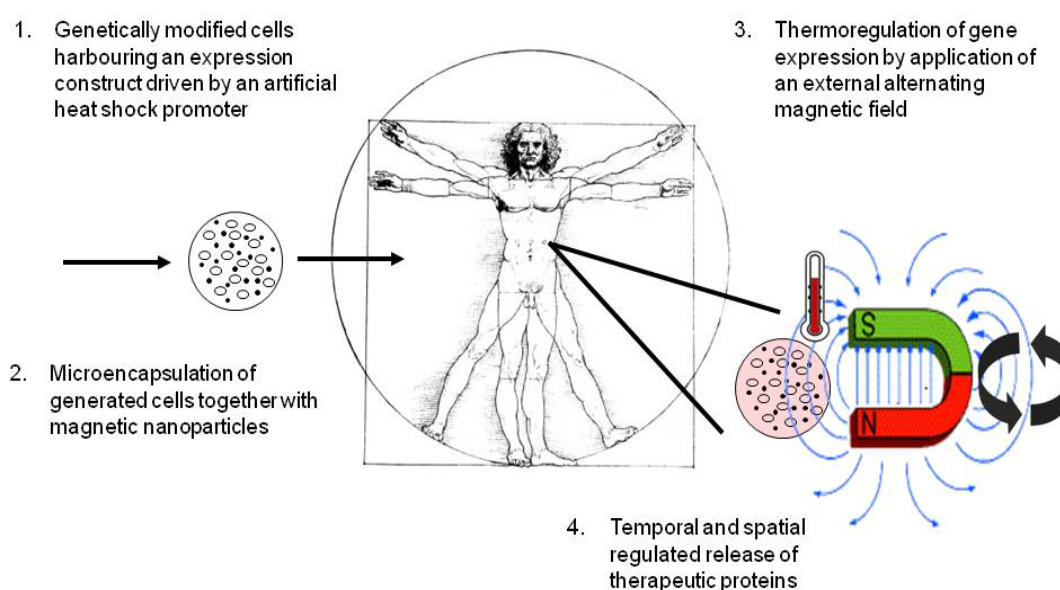


Fig. 2.1.: Nanoparticle-mediated thermoregulation of gene expression within encapsulated cells by applying an alternating magnetic field.

For this purpose (see Fig. 2.1.), genetically modified cells harbouring a highly inducible artificial heat shock promoter are co-encapsulated together with magnetite nanoparticles in biologically inert sodium cellulose sulphate (SCS). These capsules can be instilled at the site of therapeutic relevance bearing the advantage of not being rejected by the patient's immune system because of immunoisolation by a semipermeable SCS capsule membrane. Once *in situ* placement of the capsules has been performed, an alternating magnetic field induces heat within the capsules due to co-encapsulated magnetite nanoparticles: This in turn switches on gene

expression of encapsulated cells. The proposed concept might accomplish a spatial and temporal regulation of therapeutic gene expression inside a patient's body.

2.1. Gene and cell-based therapy

Recent breakthroughs in molecular medicine have made gene therapy one of the most rapidly advancing fields of biotechnology, with a great outlook on promising treatment for both inherited and acquired diseases (Somia, et al., 2000). During the last years and despite some disappointments, considerable progress was made, which culminated in the first market approval of a gene therapy product in 2003 (reviewed in Günzburg, et al., 2004). Current strategies mainly focus on therapeutic genes, which are active over a wide range of expression levels. Gene therapy though would have the potential to interfere with biochemical or genetic pathways of the organism in a quantitative manner. However, for applications of transgenes encoding products with a narrow therapeutic range, a stringent regulation of expression is required. Rigorous control of transgene activity will therefore be essential for the next generation of gene therapy applications. Ideally, this activity should be regulated from the outside of the organism and has to be restricted to the target cells. (please refer to Czerny, et al., 2006)

Cell therapy is considered a promising variation of this technique (Orive, et al., 2004), initially developed to protect transplanted heterologous cells from the host's immune system (Chang, 2005). The focus of this method shifted to the transplantation of genetically engineered cells. Preventing cellular attacks of the immune system, encapsulation of cells within a permeable membrane enables continuous nutrition of the cells. Thereby, survival in the host can be reached over several months (Hauser, et al., 2004). In gene therapy approaches a stable and prolonged gene expression can be accomplished by using retroviral vectors (Ferry, et al., 2011). These vectors integrate into the host cell DNA, which might result in disruption of gene function and potentially cause cancer (Hacein-Bey-Abina, et al., 2003). Moreover, viral vectors in conventional gene therapy bear the risk of reaching germ cells, thus inheriting the modified genome. These risks are avoided, applying encapsulated cells for

therapeutic approaches. Here, clones of cells with optimal expression characteristics can be selected in cell culture, which is considered an ideal strategy of achieving reproducible expression levels in the proposed concept. (please refer to Czerny et al., 2006)

2.2. Microencapsulation of cells

Today, one of the most exciting fields in translational medicine is cell therapy. Cell therapy applying microencapsulation technology targets aspects of a variety of evolving scientific disciplines: molecular biology, biotechnology, biomaterials, immunology, tissue engineering, transplantation biology, regenerative medicine, and clinical research (Hernandez, et al., 2010). “Cell encapsulation is a strategy that aims to physically isolate a cell mass from an outside environment within the confines of a semipermeable membrane barrier (Orive, et al. 2003, Hunt, et al., 2010, Fig. 2.2) without the use of long-term therapies of modulating and/or immunosuppressive agents, which have potentially severe side effects (Hernandez, et al., 2010).”

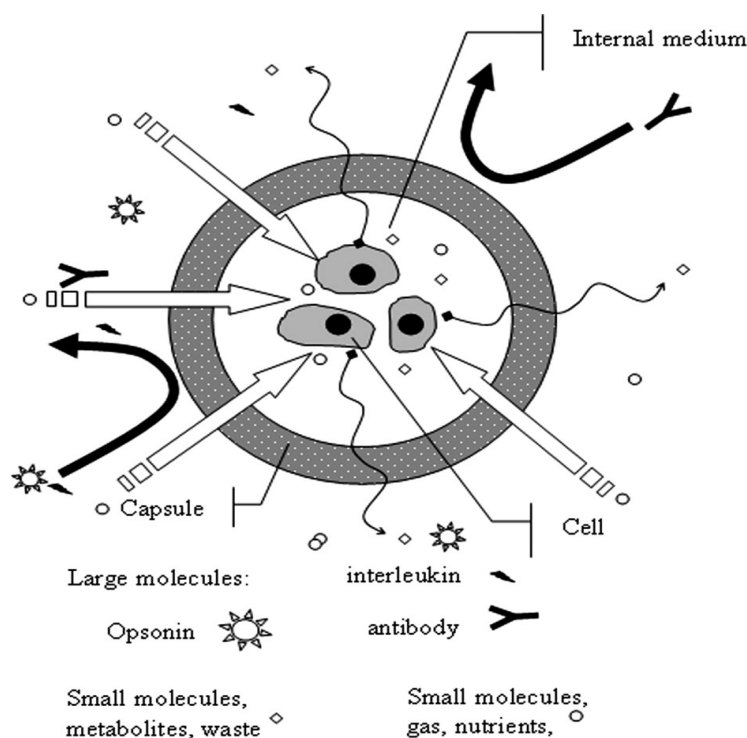


Fig. 2.2.: Concept of cell therapy and cell immunoisolation in microcapsules. (Rabanel, et al., 2009)

Microcapsules are almost exclusively generated as hydrogels. Hydrogels have some attractive properties. Hydrogels exhibit (reviewed by Hernandez, et al., 2010):

- A highly hydrated microenvironment for encapsulated cells that can mimic biochemical, cellular, and physical stimuli that direct cellular processes such as differentiation, proliferation, and migration.
- A soft and pliable characteristic that diminishes mechanical irritation of the surrounding tissue.
- Virtually no interfacial tension with the surrounding tissues and fluids which diminishes cell adhesion and protein adsorption.
- Permeability for low molecular weight molecules as nutrients, therapeutics and metabolic waste.

These properties in turn result in high biocompatibility of hydrogels.

Encapsulation technology has two major advantages: on the one hand the transplantation of potential therapeutic cells and tissue without the need of immunosuppressive agents and on the other hand the potential use of cells and tissue from a variety of different sources such as primary cells and stem cells or genetically modified cells (Hernandez, et al., 2010).

Different immunoisolation procedures have been established over the years. Immunoisolation procedures can be distinguished in macroencapsulation (large usually flat-sheet and hollow-core fibers) and microencapsulation (small spherical vehicles and coated tissue). Here, special attention should be drawn to microencapsulation because of their use in the present work. The spherical shape of microcapsules appears to be advantageous with respect to mass transport exhibiting optimal surface to volume ratio for protein and nutrient diffusion; this in turn increases cell viability in comparison to other immobilisation scaffolds which enforces oxygen and nutrient permeability (Hernandez, et al., 2010). The implantation of microcapsules containing cells in close proximity to the blood stream is enabled by their small size, which allows long-term functionality of the embedded cells due to an improved oxygen transfer into the capsules (Hernandez, et al., 2010). Additionally, microcapsules are more durable than macrocapsules and therefore more stable (Hernandez, et al., 2010).

Microcapsules can be categorised in three classes (reviewed by Hernandez, et al., 2010):

- matrix-core/shell microcapsules,
- liquid-core/shell microcapsules and
- cells-core/shell microcapsules.

Matrix-core/shell microcapsules are produced by gelling of polymer/cell droplets in a gelling solution. These microcapsules are the most studied. Many improvements of the technique have been introduced over the years. Liquid-core/shell microcapsules are manufactured by dropping a cell/gelling solution in a polymer bath. Cells-core/shell microcapsules are generated by conformal coating of cells.

Therapeutic applications of the microencapsulation technology range from therapy of acquired and inherited chronic disorders such as (reviewed by Hernandez, et al., 2010):

- cancer,
- diabetes mellitus,
- bone and cartilage defects,
- neurological disorders and
- heart diseases.

Here, the most often used applications of the microencapsulation technology will be described whereupon special attention is drawn to the application of sodium cellulose sulphate (SCS) microcapsules, which have been used in the presented study. Therefore, recent findings of the treatment of cancer and the treatment of diabetes mellitus using microencapsulation technology are described.

In the treatment of pancreatic cancer a promising approach using genetically modified cells encapsulated in biologically inert SCS was developed years ago. Cytochrom P450 overexpressing encapsulated cells, instilled near the tumour region can be used to treat cancer by subsequently systemical injection of the prodrug ifosfamide, which then will be converted into a toxic compound by the genetically modified cells to combat tumour growth (Löhr, et al., 1998). In a pioneering study Löhr and colleagues could provide proof-of-principle for this therapeutic approach in a xenograft mouse model. The use of encapsulated genetically modified feline kidney

cells producing cytochrom P450 plus the multiple injection of ifosfamide reduced tumour growth and even resulted in a complete regression of the tumour in some mice (Löhr, et. al. 1998). This result could be reproduced with genetically modified HEK293 cells by Karle and colleagues (Karle, et al., 1998). These results initiated the development of a cell therapeutic product (NovaCaps^R) for the treatment of inoperable pancreatic cancer which was produced according to GMP regulations. In a phase I/II clinical trial in 2000 genetically modified encapsulated HEK293 cells were used to treat 14 patients, which suffered from late stage pancreatic cancer (Löhr, et al., 2001, Löhr, et al., 2003). The findings of this study (reviewed by Salmons, et al., 2010) showed that the application of the encapsulated cells by an angiographic route was safe, that the encapsulated cells were well tolerated and no evidence for inflammatory or immune reactions could be found and there were no major toxicities associated with the low dose of ifosfamide that was used (Löhr, et al., 2001, Löhr et al., 2003). In addition, therapeutic efficacy (reviewed by Salmons, et al., 2010) was indicated by tumour reduction in four patients and stable disease in ten patients; moreover a improvement of the median survival as well as increased 1 year survival rates were found compared to the control group (Löhr, et al., 2001, Löhr et al., 2003). There is an eminent increase in projects investigating the cell-based treatment of cancer applying microencapsulation technology using other encapsulation matrixes. Here, one approach for treating cancer is the intratumoural implantation of encapsulated cells producing cytokines (IL-2 and TNF- α) into a mouse fibrosarcoma model (Sabel, et al., 2007). Implanted encapsulated IL-2 secreting cells result in a delay in tumour progression and prolonged survival of animals (Cirone, et al., 2002). Another approach targets the inhibition of angiogenesis for cancer treatment. Encapsulated CHO cells implanted into the peritoneal cavity and expressing endostatin result in a significant inhibition of melanoma growth in mice bearing B16 melanomas (Teng, et al., 2007). Similarly, tumour growth was suppressed to more than 90% 3 weeks after tumour induction resulting in a 100% survival compared to 100% mortality in the mock-treated control group in a project where angiostatin was expressed by encapsulated cells in a murine model for melanoma and breast cancer (Circone, et al., 2003). Additionally, a new therapeutic approach in synergistic tumour treatment was the combination of IL-2 secreting and angiostatin secreting

encapsulated cells in separate microcapsules (Circone, et al., 2005). Finally, another very promising approach is the production of cancer vaccines and hence the delivery of antibodies by immune-isolated encapsulated cells for the treatment of cancer (Orive, et al., 2001).

In general the most studied application of microencapsulation technology is its use for treating diabetes mellitus type I, but here only little has been investigated applying SCS microcapsules. The strategy aimed at the restoration of regulated insulin supply. Islets of Langerhans from a porcine source were encapsulated in SCS and employed in order to substitute insulin production. With this concept Schäffellner and colleagues could induce glucose-dependent insulin production of HIT-T15 cells in nutrient solution (Schäffellner, et al., 2005). Moreover, these encapsulated islet cell line could be frozen and thawed again (Stiegler, et al., 2006), indicating possible banking of cells for future applicability in clinical trials.

The majority of approaches to treat diabetes mellitus type I was developed using encapsulation polymers other than SCS. In these approaches, for example encapsulated porcine islets were tested in mice and monkeys; here a relieve of symptoms was observed (Elliott, et al., 2005). Evidence for improvement of glycemic control in human individuals was provided in a study of Living Cell Technologies Ltd with the Diabecell^R device, which consists of encapsulated neonatal porcine islets. Hence, no porcine viral infection could be detected and moreover, it could be demonstrated that remaining encapsulated porcine cells were still viable explanted 9.5 years after transplantation (Elliott, et al., 2007). PEGylation of islets in combination with application of low doses of cyclosporine resulted in normal blood glucose responsiveness and hormone synthesis for one year after transplantation in the rodent model (Lee, et al., 2007). A phase I/II clinical trial was started by Novocell in 2005 based on these results. Therefore, human islets allografts were implanted subcutaneously into human patients (NCT00260234 www.clinicaltrials.gov).

2.3. Magnetic nanoparticles in biomedicine

Applying nanotechnology for diagnosis, monitoring and control of biological systems has become more and more popular throughout the years. Being referred to as “nanomedicine” by the National Institute of Health, the main aim of nanomedicine is the research of rational delivery and targeting of pharmaceutical therapeutic and diagnostic agents. Devoted to manipulate structures in nanometer scale size, most of the used particles in nanotechnology are about 1-200 nm in diameter. Compared to bulk materials, the small sizes of particles can result in a dramatic change of physical and chemical properties. The majority of these particles is referred to as “magnetic nanoparticles” (MNPs), which describes the solid phases within nanometer size. In this case “magnetic” refers to temporarily magnetic material with the ability to comprise ferromagnetic, paramagnetic or superparamagnetic materials. When an external magnetic field is applied, ferromagnetic materials become magnetised and remain so for a period of time even when the magnet is removed. Paramagnetic materials have magnetic moments even in the absence of a magnetic field. However, they only exhibit magnetism when a magnetic field is applied. In the absence of an external magnetic field any magnetisation is being retained in those particles. In contrast, superparamagnetic materials only are magnetic in the presence of an external magnetic field. It reverts to a non-magnetic state as soon as the external magnet is removed. (please refer to Mostegl, 2009)

The use of MNPs can be applied to:

- Delivery of heterologous DNA by magnetotransfection (Plank et al., 2003, Plank et al. 2009)
- Concentration and targeting of chemotherapeutics to tumour cells (Alexiou, et al., 2000, Alexiou, et al., 2003)
- Heat treatment induced by MNPs through an alternating magnetic field (Ito, et al., 2003a/b/c, Ito, et al., 2004, Jordan, et al., 2006, Jordan, et al., 2009)
- In vivo imaging (Selvan et al. 2007)

Magnetotransfection is one of the most studied application for MNPs. MNPs can be associated with nucleic acids, such as viral or non-viral vectors, which can be concentrated on respective target cells by application of a permanent magnetic field which results in an enhanced uptake of nucleic acids into cells (Plank, et al., 2003, Plank, et al. 2009). For the treatment of tumours MNPs carrying chemotherapeutics are often used. By the enhanced permeation and retention effect which is mediated by leaky vasculature and decreased lymphatic transport (Alexiou, et al., 2000, Alexiou, et al., 2003) MNPs can be targeted to the tumour. MNPs can be actively directed to tumour cells by linking ligands or molecules (such as antibodies) to their surfaces. One very promising approach in the use of MNPs is the employment for hyperthermia treatment of solid tumours (Jordan, et al., 2006, Jordan, et al., 2010). Injected MNP formulations can generate heat by physical induction due to application of an alternating magnetic field which in turn reduces tumour growth (Ito, et al., 2003b, Jordan, et al., 2006). The use of so called quantum dots for in vivo imaging (Moghimi et al., 2005) is another possible application of nanoparticles. White light is being absorbed by quantum dots and re-emitted at a specific wavelength which can be tuned from blue to nearly infrared by varying size and composition of the respective nanoparticles. Quantum dots are taken up by cells and therefore can be used for live imaging as has already been shown (Selvan, et al., 2007). (please refer to Mostegl, 2009)

Without additional coating MNPs show a hydrophobic surface with a large surface to volume ratio and a strong tendency to aggregate (Lu, et al., 2007). In order to improve MNP stability, an appropriate surface coating is to be applied, which allows iron oxide MNPs to be dispersed into homogenous ferrofluids. There are several groups of coating materials that can be used to modify MNP chemistry on the surface (Shubayev, V., et al., 2009):

- organic polymers, such as dextrans, chitosan, polyethylene glycol, polysorbate and polyaniline;
- organic surfactants, such as sodium oleate and dodecylamine;
- inorganic metals, such as gold;
- bioactive molecules and structures, such as liposomes, peptides and ligands/receptors; (please refer to Mostegl, 2009)

Material for coating of nanoparticle surfaces are used on the one hand, as already mentioned, to keep nanoparticles apart from each other (Häfeli, et al., 2009), in order to avoid aggregation of nanoparticles dispersed in solution and on the other hand to functionalise nanoparticles with specific chemical or physical properties, e.g. binding to specific surfaces. The nanoparticle formulations used in this project are originally used for gene delivery by magnetotransfection. Therefore, the nanoparticles used here were coated with materials, which should enhance nanoparticle uptake into cells.

2.4. Heat generation by magnetic nanoparticles

In the presented work, MNPs should be used to generate heat within microcapsules by application of an alternating magnetic field. The strategy to generate heat using MNPs is normally applied in thermotherapy: in this application MNP-mediated hyperthermia is used to elevate temperature in a cancerous tissue. Tumour cells are more sensitive to heat compared to healthy tissue which allows selective combating of tumour growth (Jordan et al., 2007). By elevated temperatures, i.e. 43°C for approximately 30 minutes (Pankhurst, et al., 2003), tissue damage and cell death is induced. Additionally, hyperthermia also increases sensitivity of cancerous cells to ionising radiation and some cytotoxic drugs. MNP mediated hyperthermia appears to be most promising due to the high capability of MNPs to convert energy of an applied alternating magnetic field into heat. The possibility to selectively concentrate MNPs at the site of tumour growth by means of minimal invasive routes and the high transparency of the human tissue to radio-frequency magnetic fields (Bellizzi, et al., 2010) promotes MNP application.

For biologically applications such as thermotherapy, magnetite nanoparticles are often used because they appear to be minimally toxic and exhibit reduced irritation of healthy tissue; this is emphasised by the FDA approval of magnetite nanoparticles as MRI contrast agent (Häfeli, et al., 2009).

Magnetite (Fe_3O_4) belongs to the iron oxide family. It is a hard black magnetic mineral that is widespread in natural rocks. Maghemite ($\gamma\text{-Fe}_2\text{O}_3$) is a red-brown magnetic mineral, isostructural with magnetite but with cation vacancies. Their global properties are quite similar, which makes it very difficult to distinguish between them. Maghemite can result from the oxidation of magnetite (Gossuin, et al, 2009).

The magnetite particles can be either ferromagnetic or superparamagnetic at room temperature depending on their diameter. The critical diameter of magnetite becoming superparamagnetic has been calculated to be below 18.7 nm (Atsumi, et al., 2007). Exposed to an alternating magnetic field heat can be generated by both ferromagnetic and superparamagnetic particles (Mornet, et al., 2004). It has been reported that the hysteresis loss-induced heating needs larger size of magnetic multi-domain (ferromagnetic) particles. Smaller particles, consisting of a single domain structure (superparamagnetic) are inducing heat by relaxation loss in an alternating magnetic field (Mornet, et al., 2004).

2.5. Heat responsive promoters

In order to directly combine hyperthermia treatment with gene or cell-based therapy, heat-responsive promoters were developed in the past. The action of heat responsive promoters is mainly based on the binding of heat shock factor 1 (HSF1) to the heat shock elements (HSEs) present in heat-responsive promoters facilitating heat shock response (described in chapter 2.7. in more detail).

Four different types of promoters responsive to heat are known (reviewed by Walther, et al., 2009):

- HSP70B promoters,
- GADD153 promoters,
- MDR1 promoters and
- heat-responsive CMV promoters.

The HSP70B promoter is stress-inducible. It consists of an atypical TATA-box and 3 regulatory HSEs (Morgan, et al., 1993), which are responsible for heat responsiveness. This promoter was frequently used because of its low leakiness and

high inducibility in response to heat. The GADD153 promoter is also inducible by heat as well as by different other stress factors, such as reactive oxygen species, DNA damage and cytotoxic drugs (Luethy, et al., 1992). No defined mechanism for heat responsiveness has been identified so far. The MDR1 promoter revealed the stress-responsiveness of the MDR1 gene. Stressors like cytotoxic drugs, UV-irradiation, arsenite or heat are capable to activate MDR1 gene expressions. In the proximal MDR1 promoter region HSEs exist which mediate heat responsiveness (Stein, et al., 1994). The promoter of the cytomegalovirus (CMV) appeared to be inert in response external stress. However, by a still unknown mechanism also a CMV promoter can be induced by elevated temperatures (Lee, et al., 1994). However, this promoter exhibits no HSEs.

2.6. A novel promoter for gene and cell-based therapy

In the last years many studies were performed to modulate gene expression for gene therapy applications. In this context different promoter systems were established responding to environmental or physiological changes like heat, metal ions, interferons, antibiotics and steroids. Most of these systems suffer from limitations and are currently unsuitable for use in clinical gene therapy (reviewed in Goverdhana, et al., 2005) or for use in cell therapy applications.

To overcome these limitations, a novel generation of heat inducible promoters was developed in the last years. Brade and colleagues initially modified an Hsp70 promoter by including additional HSEs for improved heat-directed gene expression in tumour cells. This modification resulted in a 200- to 950-fold increase in reporter gene expression and a 1 – 2°C decrease of threshold of activation (Brade, A., et al., 2000). Based on this principle, recently a novel, artificial and bidirectional heat-inducible promoter was developed (Fig. 2.3.) by Bajoghli and colleagues (Bajoghli, et al., 2004). The artificial bidirectional heat inducible promoter consists of two minimal CMV promoters in opposite directions containing eight idealised HSEs driving the expression of two reporter genes encoding luciferase and green fluorescent protein

(GFP). This promoter was initially used in a study where reporter genes were misexpressed during fish development (Bajoghli, et al. 2004). This artificial heat-inducible promoter is characterised by a reduced background activity and increased responsiveness to heat. This promoter can be an ideal tool for biomedical applications. Heat shock promoters may be applied in tumour therapy by the combination with hyperthermia treatment and suicide gene therapy, heat-inducible polyplex gene therapy and hyperthermia, as well as cell-based therapy and hyperthermia.

The biological regulation of this novel promoter is based on the action of the endogenously expressed heat shock factor 1 (HSF1) which binds HSEs and facilitates heat shock response. Biological regulation of the heat shock response is described in the next section in more detail.



Fig. 2.3.: Heat inducible expression construct.

The artificial bidirectional heat inducible promoter consists of two minimal CMV promoters oriented in opposite directions and eight idealised HSEs in between. The artificial promoter drives the expression of two reporter genes (Bajoghli, et al. 2004). (black triangles: minimal CMV promoters; pA: polyadenylation signal; GFP: gene encoding green fluorescence protein; g.o.i.: gene of interest)

2.7. Regulation of heat shock response

The heat shock (HS) response represents an universal mechanism of protection against adverse environmental conditions, especially against the stressor heat. The HS response is one of the most evolutionarily conserved defensive mechanisms against acute exposure to environmental and pathological conditions (reviewed in Shamovsky, et al, 2008; Kubota, et al., 2009,). Although organisms have adapted to grow at temperatures from the freezing point of water to 113°C (Stetter, et al., 2006), temperatures only moderately above a certain optimum growth temperature turned out to be a challenging problem for survival of all living organisms (Richter, et al., 2010).

The biological regulation of the heat shock response is based on the action of endogenously expressed heat shock factors, especially HSF1 (Fig. 2.4. A 1). HSF1 is located in the cytoplasm as a monomer and bound to chaperones such as HSP70 or HSP90. The bound heat shock protein (HSP) inhibits DNA-binding activity of HSF1. HSF1 is released from the heat shock proteins and translocates into the nucleus (Fig. 2.4. A 2). In this case HSF1 is still hypophosphorylated. The monomers then trimerise and subsequently become hyperphosphorylated. The phosphorylation status of the trimeric HSF1 is essential for DNA binding and transcriptional activity. In the hyperphosphorylation of the trimeric HSF1 several protein kinases are involved such as MAP, JNK, protein kinase C- α , C- ζ , and GSK3- α . The phosphorylation of serine residues Ser230, Ser326 and Ser419 activates HSF1-mediated transcription, while the phosphorylation of the serine residues Ser303, Ser307, and Ser363 is associated with negative regulation of HSF1-mediated transcription. The HSF1-mediated transcription leads to an entry of HSPs into the nucleus (Fig. 2.4. A 3). Therefore, expression of HSPs is regulated by negative feedback, i.e. by binding of HSPs to HSF1 monomers (Fig. 2.4. A 4). The transcriptional activity of the HSF1 homotrimer is mediated by binding to HSEs (consensus sequence: 5'-NGAAN-3') located within heat-reactive promoters. For strong HSF1 binding at least 5 units of HSEs are required. Multiple HSEs are present in promoters of hyperthermia-inducible genes, for example the HSP70B promoter.

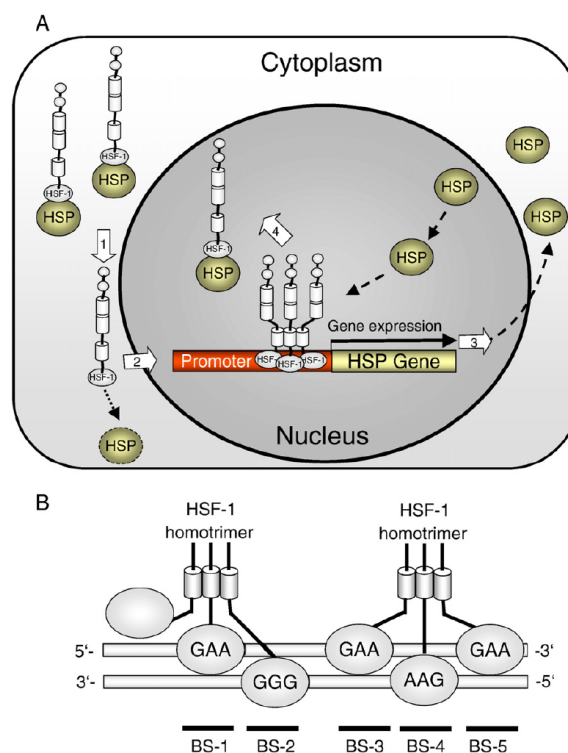


Fig. 2.4.: Regulation of the heat shock response.

A) HSF1 is monomeric, hypophosphorylated and bound to HSPs in the cytoplasm. (1) HSF1 dissociates from HSPs and (2) translocates to the nucleus still hypophosphorylated. HSF1 trimerises and becomes hyperphosphorylated. The HSF1 homotrimer binds to DNA at HSEs and gene transcription of HSP genes occurs. (3) HSPs are induced to enter the nucleus and (4) bind dissociated monomeric HSF1.

B) HSF1 binds DNA at HSEs with the consensus sequence 5'-NGAAN-3'. For strong binding a minimum of 5 units is required. (HSF1: heat shock factor; HSP: heat shock protein; BS-1 to BS-5: binding sites).

(Walther, et al., 2009)

2.8. Aim of the project

The main aim of the project is to demonstrate proof-of-principle for nanoparticle-mediated thermoregulation of reporter gene expression in encapsulated cells by applying an alternating magnetic field.

To achieve this, the main components applied for the establishment of this concept should be analysed regarding their employed properties: HEK293 cells, magnetic nanoparticles, the encapsulation process and heat inducing technology.

Genetically modified HEK293 cells harbouring an artificial heat-inducible expression construct should be investigated to determine their response to heat.

Several nanoparticle formulations should be analysed with regard to their physical properties, e.g. their heat generation capacity in an alternating magnetic field as well as their tendency to aggregate.

The co-encapsulation of cells with selected nanoparticles should be developed by optimising encapsulation parameters. Generated capsules should then be analysed regarding their physical properties such as size, membrane diffusion performance and membrane thickness.

In a next step, the encapsulated cells should be biologically characterised. Therefore, heat inducibility of encapsulated cells should be proven and biocompatibility of selected nanoparticles with encapsulated cells should be analysed.

The effects of magnetic field treatment on encapsulated cells should be described. Therefore viability, cell death (apoptosis and necrosis) as well as cell integrity in response to magnetic field treatment of encapsulated should be investigated.

Magnetic field-directed, nanoparticle-mediated heat induction of the reporter gene expression within encapsulated cells should be analysed to provide proof-of-principle *in vitro*. The above described concept should finally be evaluated in mice to provide evidence of applicability *in vivo*.

3. MATERIALS AND METHODS

3.1. Materials

3.1.1. Chemicals and reagents

Adenosine triphosphate (ATP)	Sigma-Aldrich
Agarose, electrophoresis grade	Invitrogen
AlamarBlue™	Serotec
Algenic acid (sodium salt)	Sigma-Aldrich
Amphotericin B (Fungizone)	Invitrogen
Aqua bidestillata	Mayerhofer Pharmazeutika
Bovine serum albumin	Promega
Calcein-AM	MoBiTec
Calcium chloride	Merk
Cell culture water	PAA
Deoxyribonucleotide-triphosphates (dNTPs)	Sigma-Aldrich
4',6-Diamidin-2-phenylindol (DAPI)	Sigma-Aldrich
Dimethyl-sulfoxide (DMSO)	Fluka
Dithiothreitol (DTT)	Sigma-Aldrich
Dulbecco`s modified Eagle`s medium (DMEM)	Invitrogen
DPX mounting medium (dibutyl phtalate - xylene)	Fluka
Eosin	Riedl-de Haen
Epon	Serva
Ethanol (analysis grade)	Sigma-Aldrich
Ethidium bromide	Sigma-Aldrich
Ethylen-diamine-tetraacetate (EDTA)	Sigma-Aldrich
Etoposide	Sigma-Aldrich
ExCell 293 serum free medium	Sigma-Aldrich
Fluorescein-isothiocyanate-dextran (40/70/250 kDa)	Sigma-Aldrich
Fluorescence mounting medium (Vectashield)	Vector Labs
Foetal calve serum (FCS)	Invitrogen

Formaldehyde solution 37 %	Sigma-Aldrich
Gentamycin	Invitrogen
Glutaraldehyde 25 %	Merck
Glycerine	Sigma-Aldrich
Haematoxylin	Richard-Allan Scientific
HistoGel	Richard-Allan-Scientific
Isopropanol	Sigma-Aldrich
Lead-citrate	Plano
D-Luciferin (firefly, potassium salt)	Caliper Life Sciences
D-Luciferin (firefly, sodium salt)	Sigma-Aldrich
3-(N-Morpholino)-propane sulfonic acid buffer (MOPS 20 x)	Inotech
Osmium (3 %)	Plano
Penicillin/Streptomycin	Invitrogen
Hydrogen-peroxide (H ₂ O ₂) 30 %	Sigma-Aldrich
Phosphate buffered saline (PBS)	Applichem, PAA
Poly-diallyl-dimethyl-ammonium-chloride (pDADMAC) 40 % 24 kDa	Kaptol Chemie
Potassium dihydrogen phosphate	Roth
Propidium iodide	MoBiTec
Propylene oxide	Sigma-Aldrich
Puromycin	Invitrogen
Resorufin	Sigma-Aldrich
293 SFMI serum-free medium	Invitrogen
Sodium cellulose sulphate	Fraunhofer
Sodium chloride	Merck
Sodium hydrogen phosphate	Merck
Sodium hydroxide	Merck
Toluidinblue O	Merck
Tris (tris(hydroxymethyl)aminomethane)	Sigma-Aldrich
Tris-HCl	Merck
Trypan blue	Invitrogen

Trypsin-EDTA (0.05 %)	Invitrogen
Uranyl acetate	Fluka

3.1.2. Enzymes and Kits

ApoTagRed (TUNEL assay)	Chemicon
Biotase (Protease)	Biochom
Bright Glo (luciferase assay)	Promega
Collagenase	Worthington
DNA free Turbo (DNaseI kit)	Ambion
GoTaq (DNA polymerase)	Promega
Luciferase (firefly)	Sigma-Aldrich
Proteinase K	Millipore
Restriction endonucleases	Promega

3.1.3. Cell culture materials

3.1.3.1. Tubes

1.5 ml Eppendorf tube	Eppendorf
2 ml Eppendorf tube (conical bottom)	Eppendorf
2 ml Eppendorf tube (round bottom)	Eppendorf
15 ml cell culture falcon tube	TPP, Sarstedt
50 ml cell culture falcon tube	TPP, Sarstedt
10 ml flat bottom tissue culture tubes	TPP

3.1.3.2. Cell culture flask

25 cm ² cell culture T-flask	Sarstedt
75 cm ² cell culture T-flask	Sarstedt
175 cm ² cell culture T-flask	Sarstedt
300 cm ² cell culture T-flask	TPP
Roller bottle, Cellmaster	E&K

3.1.3.3. Pipettes

20 µl filter pipette tip	Eppendorf
200 µl filter pipette tip	Eppendorf
250 µl wide orifice pipette tip	Mandel
1000 µl filter pipette tip	Eppendorf
2 ml serological pipette	Sarstedt
5 ml serological pipette	Sarstedt
10 ml serological pipette	Sarstedt
25 ml serological pipette	Sarstedt

3.1.3.4. Multi-well-plates

6-well plate (tissue culture treated)	TPP
12-well plate (tissue culture treated)	TPP
24-well plate (tissue culture treated)	TPP
96-well plate (tissue culture treated)	TPP
96-well plate (black, flat bottom)	Greiner
96-well plate (white, flat bottom)	Greiner

3.1.3.5 Syringes and accessories

Syringe 50 ml	BD Biosciences
Filter 0.2 µm	Sarstedt
Filter 0.45 µm	Sarstedt
Filter 5 µm	Sartorius

3.1.4. Laboratory devices

Automatic embedding device	Thermo Scientific
Cell culture incubator, 37°C	Memmert
Cell culture incubator, 43°C	Sanyo
Cell culture microscope, CK2	Olympus
Centrifuge, Biofuge pico	Heraeus
Centrifuge, 3 – 10	SIGMA
Confocal laser scanning microscope, LSM 510	Zeiss
Encapsulator, IE-50R	Innotech
FACS, FACScalibur	BD Biosciences
Fluorescence microscope, Axiovert 200 M	Zeiss
Homogenisator, Ultraturax, T25 basic	IKA
Incubator, 37°C	Heraeus
Incubator, GS 18-d	Memmert
Laminar airflow work bench	NuAire
Luminometer, LB9507	Berthold
Luminometer, LB953	Berthold
Magnetic field generator, custom-made	FH Campus Vienna
Magnetic stirrer, Combimag RCT	IKA
Microtome, RM 2235	Leica
Multititer-plate reader, GENios	Tecan
Photometer, Gene Quant II	Pharmacia Biotech
Shaker, Rocky	Fröbel
Sonicator, Sonoplus	Bandelin
Thermocycler, Gene Amp PCR system 9700	Applied Biosystems
Thermomixer, compact	Eppendorf
Transmission electron microscope, EM900	Zeiss
Ultratome, Ultracut S	Reichert
Viscosimeter	Bohlin
Water bath	Grant

3.1.5. Nanoparticles

13 different types of nanoparticles were kindly provided by Dr. Olga Mykhaylyk from the Institute of Experimental Oncology and Therapy Research at the Technical University in Munich. Additionally, commercially available nanoparticles from Sigma were used in this project. All nanoparticles were composed of a magnetite core. The different coatings and the crystallite mean core sizes of nanoparticles are listed below (Tab. 3.1.). Nanoparticles obtained from Sigma (Iron(II,III)oxide nanopowder 98+% Cat. No. 637106-25G) were not coated.

Tab. 3.1.: Set of employed magnetite nanoparticles.(1)

particle	coating material	core size
S1	Palmithyldextran	80 nm
S4	Palmithyldextran	8.5 nm
S5	Palmithyldextran	13 nm
S7	Palmithyldextran	30.6 nm
S8	Polyethylenimine	74.1 nm
S11	Pluronic-127 / Ammonium bis[2-(perfluoroalkyl)ethyl] phosphate	10.6 nm
S13	Palmityldextran / Lithium-3-[2-(perfluoroalkyl)ethylthio]propionate	4 nm
S16	Tween-80	10 nm
S22	Tween-60 / Lithium-3-[2-(perfluoroalkyl) ethylthio]propionate	11.7 nm
S24	1.9-Nonanedithiol	12 nm
S25	Chitosan	10 nm
S26	Dihexa-decyl-phosphate	10 nm
S34	Pluronic-127 / Lithium-3-[2-(perfluoroalkyl) ethylthio]propionate	11nm
Sigma	non-coated	30 nm

(1) Nanoparticle coating materials and core sizes are listed.

3.1.6. Cells

3.1.6.1. Cell line: HEK293

In this project, human embryonic kidney cells (HEK293) were employed, a well characterized, commercially available cell line (ATCC No. CRL-1573) which have previously met requirements for clinical use (Löhr, et al., 2001).

3.1.6.2. Single cell clone: HEK293 pSGH2lucpuro C5

For proof of principle of the proposed concept, HEK293 cells were transfected with the expression construct pSGH2lucpuro C5 (PhD thesis Viktoria Ortner, Institute of Animal Breeding and Genetics, Vetmeduni Vienna) resulting in the generation of the stable cell clone HEK293 pSGH2lucpuro C5. The expression vector carries an artificial bidirectional heat-inducible promoter, based on the human heat shock promoter Hsp70. In detail, this bidirectional promoter consists of two minimal CMV promoters, orientated in opposite directions, coupled to eight idealised heat shock elements (HSEs) harbouring the consensus sequence AGAAC (Bajoghli et al., 2004). Two reporter genes – GFP and luciferase – were driven by this artificial promoter, rendering their expression inducible by heat (see Appendix, section 7.4.). This cell clone was used in described encapsulation experiments.

3.1.6.3. Cell populations: HEK293 pCMVluc and HEK293 pCMVegfp

As a control for reporter gene expression, cell populations constitutively expressing luciferase or enhanced green fluorescent protein (EGFP; HEK293 pCMVluc and HEK293 pCMVegfp) were used. These cell populations had been generated by stable transfection of HEK293 cells with pCMVluc and pCMVegfp (Metzner, et al., 2006) and were kindly provided by the Institute of Virology at the University of Veterinary Medicine, Vienna.

3.2. Methods

3.2.1. Cell culture

3.2.1.1. Maintenance of cells

In this work an immortalised human embryonic kidney cell line (HEK293) was employed. All HEK293 cells used were cultured at 37°C, 5% CO₂ and 95% relative humidity in a cell culture incubator. All cell manipulations and handlings were performed in a laminar airflow work bench (NuAire) located in a bio-safety level 2 laboratory under aseptic conditions. The bench was sterilised by UV irradiation and disinfectant before and after usage. Cells originated from a continuous cell line, growing as monolayers. Usually they were maintained in plastic cell culture flasks with a modified inner surface allowing protein binding, facilitating attachment and proliferation of cells.

The cells were passaged according to their growth kinetics. For this purpose, the spent medium was removed and the cells were washed once with phosphate-buffered saline (PBS) solution. Afterwards the cells were submerged with trypsin solution (0.05% trypsin, 0.53 mM EDTA) and incubated until the cells detached from the bottom surface of the flask. To stop the proteolytic activity of trypsin, Dullbecco's modified eagle's medium (DMEM) supplemented with 10% foetal bovine serum (FBS) (i.e. normal medium: NM) was added. Then, the cells were resuspended by gently shaking and pipetting until a single cell suspension was generated. 20% of the single cell suspension was transferred to a new flask and the required amount of NM was added.

3.2.1.2. Storage of eukaryotic cell lines

Extended cultivation of eukaryotic cells, i.e. consecutive amplification of genomic DNA and subsequent cell division, leads to accumulation of replication errors. These mutations can alter the morphology and growth behavior (i.e. the genetic background) of the initial cell population. In order to circumvent this bias, aliquots of the generated single cell clones and cell populations were backed up at low passage numbers and frozen at -80°C. Subsequently, cells were excluded from further

experiments when they reached a passage number more than 30 and cell expansion was restarted from freshly thawed stocks (see 3.2.1.3.). For long-term storage, cells were harvested in the logarithmic growth phase and centrifuged at 260 x g (Sigma centrifuge 3 - 10) for 5 min. Then, the cell pellet was resuspended in freezing medium (DMEM + 10% FBS + 10% DMSO) and about 2×10^6 cells per ml were transferred into freezing vials (Sarstedt) kept on ice. The freezing vials were put into a pre-chilled freezing box (4°C) filled with isopropanol (Nalgene Cryo 1°C freezing container). The freezing container was incubated for 30 min at 4°C and afterwards put at -80°C. The frozen vials were shifted the next day to a storage box at -80°C.

3.2.1.3. Thawing of cells

For unfreezing, the cells were thawed rapidly by incubation in the operator's hand and immediately resuspended in pre-warmed (37°C) culture medium. The cells were centrifuged at 260 x g for 5 min and the DMSO-containing supernatant was decanted. The cell pellet was then carefully resuspended in standard culture medium and the cells were transferred into a cell culture flask filled with additional culture medium and subsequently put into the incubator for cultivation.

3.2.2. Encapsulation

3.2.2.1. Encapsulation apparatus und process principles

To realise the proposed concept of this work (nanoparticle-directed induction of expression in encapsulated cells by application of an alternating magnetic field), encapsulation of cells and co-encapsulation of cells and nanoparticles was performed. Therefore, the encapsulation apparatus IE-50R from Inotech was applied (see figure 3.1.).

The encapsulation apparatus is based on the physical principle that small beads are formed by vibration-induced breaking of a laminar jet of polymer solution under controlled conditions. Drops are collected in a gelling bath where the encapsulation material reacts with the gelling reagent to form capsules.



Fig. 3.1.: Image of used encapsulation apparatus from Inotech (IE-50R).

“The product to be encapsulated (for instance cells and/or nanoparticles) is mixed with an encapsulating polymer solution (1.8 % or 1.6 % sodium cellulose sulphate) and the mixture is put into a syringe (Fig. 3.2. (2)). The polymer-product mixture is pumped into the pulsation chamber (Fig. 3.2. (3)) by a syringe pump (Fig. 3.2. (1)). The liquid then is passed through a precisely drilled nozzle (Fig. 3.2. (4)) and is separated into equal size droplets. These droplets then pass an electrical field set up between the nozzle and the electrode (Fig. 3.2. (5)) resulting in a surface charge. Electrostatic repulsion forces disperse the beads as they drop into the gelling reagent (1.3 % pDADMAC).

Optimal parameters for bead formation are indicated by visualization of real-time bead formation in the light of a stroboscope lamp (Fig. 3.2. (8)). When optimal parameters are reached, a standing chain of droplets is clearly visible. Once established, the optimal parameters can be preset for subsequent bead production runs with the same encapsulating polymer-product mixture. Poorly formed beads, which occur at the beginning and end of production runs, are intercepted by the bead bypass collection cup (Fig. 3.2. (6)).

Depending on distinct parameters, 50 – 3000 beads can be generated per second and are collected in a hardening solution within the provided reaction vessel (Fig. 3.2. (7)) and are continuously mixed by a magnetic stir bar (Fig. 3.2. (9)) to prevent bead clumping. At the end of the production run, the gelling solution is drained off (Fig. 3.2. (waste bottle)), while the beads are retained by a filtration grid (Fig. 3.2. (10)). Washing solutions, or other reaction solutions, are added aseptically through a sterile filter. The beads can be transferred to the bead collection vessel (Fig. 3.2. (11)).”

(<http://www.encap.ch/encapsulation-technology/introduction>)

The control unit of the encapsulation apparatus was used to adjust the flow rate of the encapsulation material (polymer/cell mixture), the oscillation frequency, the oscillation amplitude, the dispersion voltage, the stirrer speed and the stroboscope light intensity. These parameters are adjustable via control panels which are located at the machine`s front panel.

After each use, the encapsulation apparatus was deconstructed and the metal pieces of the reactor top plate were cleaned with cell culture water. The nozzle was also cleaned with cell culture water, incubated in 0.5 M NaOH at least over night, cleaned

again with cell culture water and finally autoclaved for next use. Before every use, the reactor top plate was disinfected and then autoclaved. The encapsulation procedure was carried out under aseptic conditions within a laminar air work bench.

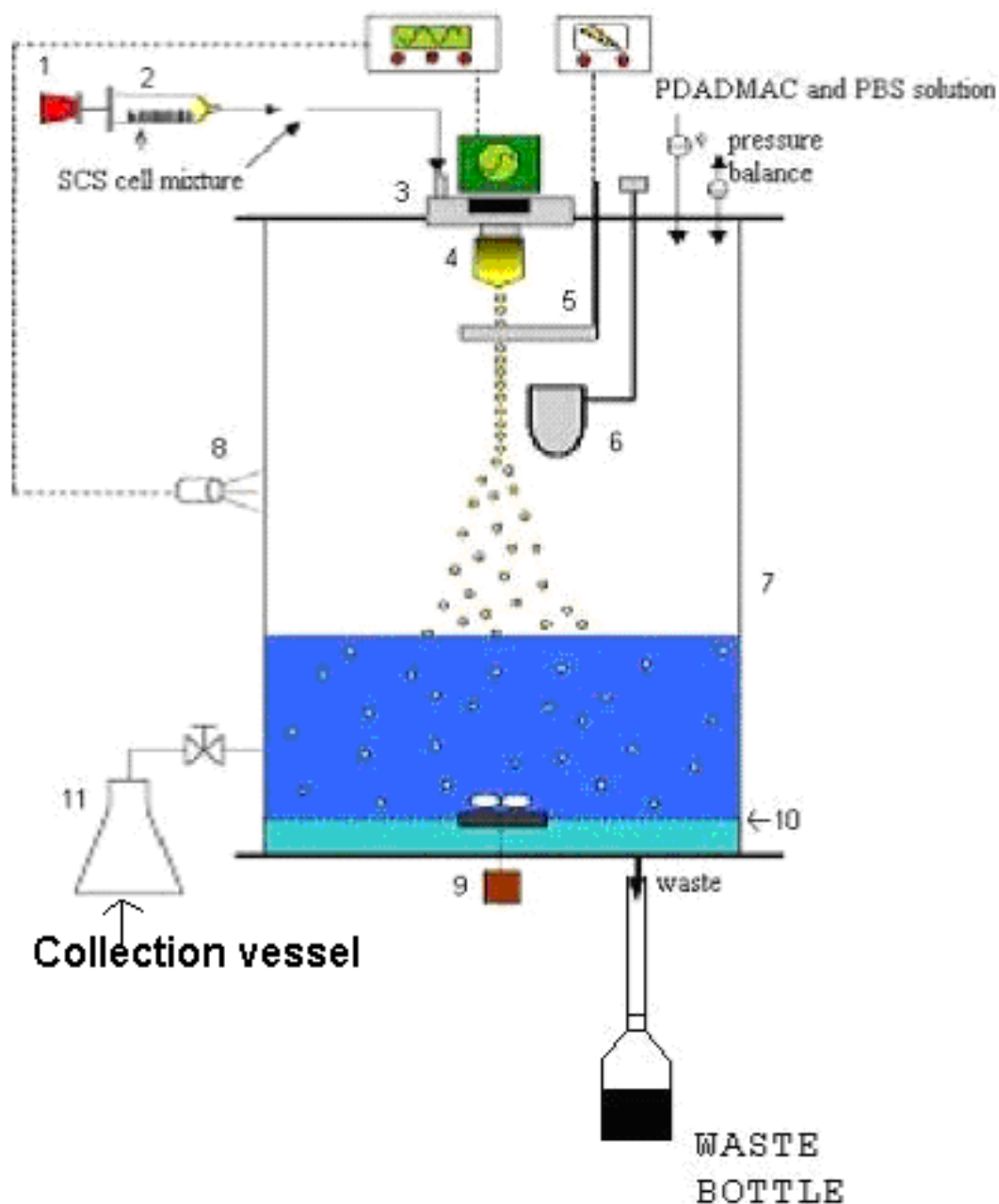


Fig. 3.2.: Schematic representation of the encapsulation process.

Components of the encapsulation apparatus: (1) syringe pump, (2) syringe, (3) pulsation chamber, (4) nozzle, (5) electrode, (6) bypass beaker, (7) reaction vessel, (8) stroboscope light, (9) magnetic stirrer, (10) filtration grid and (11) collection vessel.

(<http://www.encap.ch/encapsulation-technology/introduction>)

3.2.2.2. Encapsulation with alginate

For adjustment of encapsulation parameters alginate was used because of the lower costs of the starting material.

Therefore, 2.75 % alginate solution was used as encapsulation polymer with 1.5 % CaCl_2 as gelling reagent. The flow rate of the polymer solution, the oscillation frequency and the oscillation amplitude were adjusted, to obtain a standing chain of droplets observed in stroboscope light. Then the dispersion voltage was turned on to mediate a dispersion of the generated droplets. In the gelling bath the positively charged Ca^{2+} ions react with negative charges of alginate polymer droplets during capsule formation. Capsules were allowed to settle down and calcium buffer was decanted after gelling for 3 min. Subsequently, gelation was stopped by adding three volumes of calcium-free 1 x MOPS buffer (stock solution 20 x MOPS buffer, Inotech), followed by two additional washing steps for 5 min each. Finally, capsules were microscopically analysed with respect to size (diameters) and integrity of capsules.

3.2.2.3. Encapsulation with sodium cellulose sulphate

Sodium cellulose sulphate (SCS) / poly-diallyl dimethyl ammonium chloride (pDADMAC)-based encapsulation products (Fig. 3.3.) have demonstrated to reveal higher long-term stability and better biocompatibility (less immunogenicity) in comparison to alginate/ Ca^{2+} capsules and can be frozen and stored (Hauser, et al., 2004). Therefore, all main experiments were performed with SCS capsules.

The previously established standard encapsulation parameters (Hauser et al., 2004) for 700 μm capsules were used as a starting point for the establishment of the co-encapsulation of cells and nanoparticles in this project. Encapsulation was performed with a 1.8 % SCS solution containing 0.9 % NaCl; gelation was performed using a 1.3 % pDADMAC (MW 24 kDa) solution containing 0.9 % NaCl.

For encapsulation of cells, cells grown 80% confluent in a T175 cell culture flask were trypsinised and counted by applying a Trypan Blue assay (section 3.2.5.2). Cells were washed twice with PBS by centrifugation with 260 x g for 5 min. Subsequently, the cell number of a cell / SCS mixture was adjusted to $2 \times 10^6/\text{ml}$ viable cells by addition of SCS. For the co-encapsulation of cells and nanoparticles, the cell / SCS suspension was mixed with 1 % to 10 % nanoparticle dispersion in the

ratio of 9 parts SCS / cell suspension and 1 part nanoparticle dispersion resulting in a final SCS concentration of 1.6%.

The encapsulation parameters were defined with a flow rate of 8.5 ml/min of the nanoparticle/cell/SCS solution, an oscillation frequency of 750 Hz, an oscillation amplitude of 30 % and a dispersion voltage of 1.5 kV. Generated SCS droplets were collected in the gelling bath, where the negative charges of the poly-anion (SCS) interact with the positive charges of the poly-cation (pDADMAC) to form a hydrogel.

Immediately after gelation for 3 min, the capsules were washed with PBS once for 5 min with three times the volume of pDADMAC. Capsules were allowed to settle down and a fifth of the supernatant was decanted. Subsequently, capsules were washed three times for 5 min using PBS four times the volume of pDADMAC and followed by additional three washing steps for 5 min each with cell culture medium to completely remove the cell toxic pDADMAC.

Finally, capsules were microscopically analysed with regards to capsule size and integrity. With this procedure and a nozzle diameter of 250 μm , the resulting capsules exhibited a mean diameter of approximately 700 $\mu\text{m} \pm 50 \mu\text{m}$.

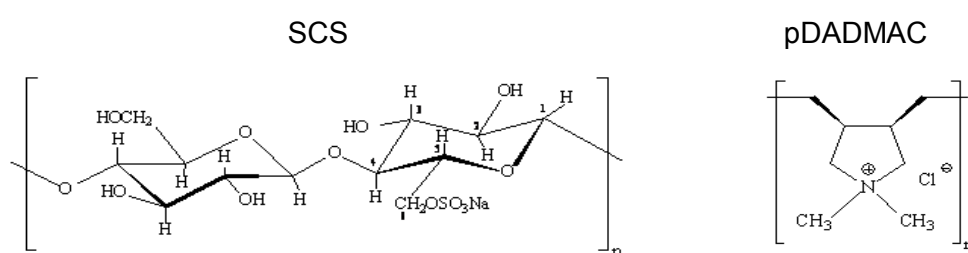


Fig. 3.3.: Chemical structure of sodium cellulose sulphate (SCS) and of poly-diallyl-dimethyl-ammonium-chloride (pDADMAC).

3.2.2.4. Maintenance of encapsulated cells

Encapsulated cells were cultivated in normal medium (NM) with 20 $\mu\text{g/ml}$ gentamycin. Approximately 15000 capsules were cultured in one T175 flask with 50 ml of cultivation medium. Twice a week, approximately 33.3 ml of the medium was exchanged to get rid of the acidic, spent medium and to feed encapsulated cells with new nutrients.

3.2.2.5. Freezing of encapsulated cells

Encapsulated cells were harvested when cells filled about 50% to 80% of the capsule volume. An aliquot of the capsule suspension being cultivated in a cell culture flask was transferred into a sterile 50 ml centrifuge tube. After capsule sedimentation, the supernatant was removed and the volume adjusted to 40 ml with fresh medium. The capsules were homogenously resuspended. 0.5 ml of this suspension was transferred into a 6-well plate and the number of capsules ($N_{0.5}$) was counted. The total amount of capsules was determined (N_{total}) by the following calculation:

$$N_{total} = N_{0.5ml} \times 80.$$

The capsule number per freezing vial (N_{freeze}) was defined. One freezing vial was dedicated to receive 1 ml freezing medium containing 200-600 capsules:

$$200 \leq N_{freeze} \leq 600$$

The supernatant was exchanged, three times with the same amount of freezing medium and finally the volume of the freezing medium (NM + 10% DMSO) was adjusted to the total freezing volume ($V_{freeze\ total}$), calculated by:

$$V_{freeze\ total} = 1ml \times N_{total} / N_{freeze}.$$

1 ml aliquots of the total amount of resuspended capsules ($V_{freeze\ total}$) were filled into freezing vials. These vials were incubated at RT for 2 to 3 h. Freezing vials were placed into a device filled with isopropanol and pre-chilled at 4°C and the freezing device was put immediately to -80°C over night to cool the vials down at a rate of -1°C per hour. Then the vials were transferred from the freezing device into a permanent storage box at -80°C.

3.2.2.6. Thawing of encapsulated cells

Thawing medium (DMEM + 50 % FBS) and cultivation medium (NM + 20 µg/ml gentamycin) were prepared. Vials containing the frozen encapsulated cells were removed from the storage location. Frozen capsules were thawed by hand warming. After disinfection with an antiseptic spray, the vials were transferred to a laminar air flow work bench and opened under sterile conditions. At least 1 ml of the thawing medium was used to resuspend and transfer the capsules from the vial to the required vessel. If necessary, the contents of different vials were pooled. The vessel was incubated at standard cell culture conditions for 1 h. The capsules were washed twice to remove cryo-preservants by swilling and removing 90% of the supernatant and finally, cultivation medium was added.

3.2.3. Determination of capsule properties

3.2.3.1. Investigation of capsule membrane thickness

To investigate capsule properties, membrane thickness of capsules manufactured with different percentages of SCS and additionally with and without nanoparticles was investigated by confocal laser scanning microscopy (CLSM). Therefore, calcufluor staining was performed. Calcufluor intercalates in β -glycosidic-linked polysaccharose. For example, calcufluor is used to stain cellulose in the cell walls of plant cells or chitin/glycan in the cell wall of fungi. Calcufluor is fluorescent under UV-light with an excitation wavelength of 365 nm and an emission wavelength of 435 nm.

Here, the cellulose sulphate capsule membrane was stained with calcufluor (3.3 mg/ml in PBS) at 22°C on a thermo-mixer (Eppendorf) with 300 rpm over night. The next day, supernatant was decanted and capsules were washed three times with PBS for 5 min. Finally, membrane thickness was visualized by CLSM using a LSM 510 microscope (Zeiss).

3.2.3.2. Determination of capsule pore size

To further investigate capsule properties, molecular cut-off limits of capsules manufactured with different percentages of SCS and with or without nanoparticles was analysed. Pore size was determined as described by Fluri, et al. 2008. Capsules were incubated with fluorescent FITC-labeled dextrans (200 µg/ml in PBS) of different molecular weight – 40 kDa, 70 kDa and 250 kDa – over night. The next day, capsules were washed twice with PBS for 5 min. Pictures were taken by a fluorescence microscope (Axiovert, Zeiss) applying identical exposure times.

3.2.4. Determination of viscosity

For the encapsulation of cells or the co-encapsulation of cells and nanoparticles, the viscosity of material to be encapsulated is a critical parameter which influences in general encapsulation capability and more over, the size of the resulting capsules. In order to investigate the viscosity of polymer-cell-nanoparticle mixtures, a coaxial-cylinder-rotation-viscosimeter was employed (Bohlin). In the coaxial-cylinder-rotation-viscosimeter a fluid to be measured is located in the space between an inner and an outer cylinder. In this case a Searle-system was used in which the inner cylinder rotated. The fluid was sheared with a proposed speed gradient. The hinge moment M_d , which is transferred by the decline between inner and outer cylinder, is directly proportional to the dynamic viscosity. The deflection is compensated by a torsion-feather and a balanced condition is electrically notated. The viscosity can be calculated as shown below:

$$\eta = \tau / dv/dy = AS / Cn$$

η : dynamic viscosity

A: shear deflection constant

τ : shear stress

S: measured variable

dv/dn : shear speed/rate

C: function of inner and outer radius

n: number of rotations

For viscosimetry, 30 ml of a given solution to be analysed was pipetted into the space between inner and outer cylinder. Viscosity was determined at 20 °C with an increasing shear rate between 1.23 s⁻¹ and 104.72 s⁻¹ and a variable shear stress. Viscosity was determined five times with continuously increasing and then continuously decreasing shear rates.

3.2.5. Analysis of cell viability

3.2.5.1. Determination of cell viability by analysis of metabolic activity (AlamarBlue assay)

To analyse the viability of cultured and encapsulated cells an AlamarBlue assay was performed which displays the metabolic activity of analysed cells. In proliferating cells specifically the ratios of NADPH/NADP, NADH/NAD, FADH₂/FAD and FMNH₂/FMN are increasing. This metabolic activity is measured in the AlamarBlue assay.

The substrate AlamarBlue is an oxidation-reduction (REDOX) indicator that undergoes a colorimetric change and yields a fluorescent signal in response to metabolic activity. Reduction causes a colour change of the oxidized form, resazurin (non-fluorescent, blue) to the reduced form, resorufin (fluorescent, red). AlamarBlue is taken up by the cell and is reduced by the metabolic intermediates; thus can be used to monitor cell proliferation by a measurable shift in colour. There are two ways to monitor AlamarBlue reduction: by measuring absorbance in a spectrophotometer or by measuring fluorescence.

Method:

Approximately 200 capsules were transferred into a 6-well plate. After medium exchange and capsule sedimentation, the supernatant was removed and cells were washed by adding fresh medium. The washing procedure was repeated a second time. In order not to damage encapsulated cells, 200 µl filter tips with wide openings were used when handling capsule suspensions. 10 capsules were pipetted in triplicate into a black 96-well plate. Cell culture medium was pipetted as sample blank in triplicate into the 96-well plate. AlamarBlueTM reagent was pipetted into all wells containing samples or blanks. 1.5 mM resorufin stock solution (which served as a

fluorescent standard, stored at -20°C) was diluted to $37.5\ \mu\text{M}$, $12.5\ \mu\text{M}$, $4.17\ \mu\text{M}$, $1.39\ \mu\text{M}$, $0.463\ \mu\text{M}$ and $0.154\ \mu\text{M}$. Each standard dilution was pipetted in triplicates onto the 96-well plate. The 96-well plate was carefully agitated and incubated at 37°C , 5% CO_2 saturation and 95% relative humidity for 4 h. In viable (encapsulated) cells resazurin is converted to resorufin. The amount of formed resorufin was analysed using the Tecan GeniosTM device. The resorufin standard enables calculation of the amount of resorufin, which is generated by cells using AlamarBlueTM as a substrate.

3.2.5.2. Determination of cell viability by analysing cell membrane integrity (TrypanBlue assay)

In order to analyse viability of cultured cells and of cells which should be encapsulated, a TrypanBlue assay was performed. In the TrypanBlue assay dead cells are stained blue and this can be analysed by using a light microscope. The dye can only enter cells via damaged or disordered membranes. Thus, based on the integrity of cell membranes, the TrypanBlue assay allows to distinguish between live and dead cells.

Method:

Cells were trypsinised. An aliquot of the cell suspension was centrifuged for 3 min at $260 \times g$. The cells were resuspended in PBS. The cell suspension was mixed carefully to avoid inhomogeneity. A sample of the cell suspension was transferred into an Eppendorf tube containing TrypanBlue reagent. Then the 1:1 mixture was incubated for 2 min at RT. An aliquot of the mixture was transferred into a Neubauer cell counting chamber. Four square areas with cells were analysed by counting the cell number of each large square separately. Additionally, the blue stained cells of each square were counted. The total cell number and the number of living cells was finally calculated.

3.2.5.3. Determination of cell viability by analysing intracellular esterase activity and membrane integrity by co-staining with calcein and propidium iodide

In order to analyse cell viability, encapsulated cells were co-stained with calcein and propidium iodide. Cells were then released from capsules and subsequently analysed by FACS. This method is utilised for simultaneous fluorescence staining of live and dead cells. Calcein-AM, which is an acetomethylester of calcein, is highly lipophilic and permeates intact cell membranes. While calcein-AM itself is not a fluorescent molecule, the calcein generated from calcein-AM by intracellular esterases emits strong green fluorescence (excitation: 490 nm, emission: 515 nm), which is the indicator for viable cells. In contrast, propidium iodide (PI) only stains dead cells. PI, a nuclei staining dye, can't pass intact membranes of viable cells. It reaches the nucleus by passing through disordered areas of the membrane of dead cells and finally, intercalates within the DNA double helix. PI emits red fluorescence (excitation: 535 nm, emission: 617 nm).

Method:

Capsules to be analysed were pipetted into a 6-well plate. Medium was removed and capsules were washed with SFMI medium twice. This medium is a serum-free medium for culturing HEK293 cells. This medium resolves SCS capsules. For lysis, capsules were incubated in SFMI medium on a horizontally shaker (~20-30 rpm) for 90 to 180 min in a cell culture incubator at 37°C. After 90 minutes, the progression of lysis was microscopically controlled and capsules were then sheared mechanically by pipetting up and down ten times with a 1000 µl pipette. After incubation, the capsules were sheared again. Depending on the density within the capsules, further separation of cell aggregates was required. Resolved capsules were transferred to an Eppendorf tube and centrifuged for 5 min with 2000 rpm. Supernatant was removed carefully to avoid destruction of the instable pellets. Pellets were resuspended in Biotase (0,0042 % protease / 0,02 % EDTA (w/v), Biochrome) or collagenase (0.5 mg/ml type 3, Worthington) and incubated for 10 min at 37°C on a thermoshaker (500 rpm). Subsequently, the process was stopped by adding two volumes of NM. Cells were centrifuged with 2000 rpm and washed twice with PBS.

For live/dead staining the single cell suspension stained with calcein and propidium iodide at a final concentration of 0.5 μM and 0.75 μM respectively. Cells were finally analysed by FACS using a FACScalibur (BD Biosciences).

3.2.6. Magnetic field treatment

To realise the proposed concept, encapsulated cells were treated in an alternating magnetic field *in vitro* as well as *in vivo*. The magnetic field treatment was performed by a custom-made magnetic field generator constructed and kindly provided by Prof. Christian Halter and Prof. Johann Walzer from the University of Applied Sciences in Vienna.

The magnetic field generating coil is driven by a current of 1 to 30 A and creates an alternating magnetic field with frequencies of 10 to 100 kHz and a magnetic field strength of up to 40000 A/m. Constituent parts are depicted in Fig. 3.3..

Constituent parts:

- power supply unit (Fig. 3.3. A 1): 0-120 V; type CPX 400A Dual, 60V 20A PSU Powerflex (TTI)
- wave form generator (Fig. 3.3. A 2): 10-100 kHz, custom-made; square wave signals with variable frequency between 10 -100 kHz were relayed by means of Timer IC 555
- transistor full bridge (Fig. 3.3. A 3): custom-made; 5 parallel transistors (typ IRFP) per full bridge part; all in all 20 transistors on a cooling plate; cooling plate is chilled by means of two aerators
- water-chilled coil (Fig. 3.3. A 4 and B): custom-made; isolated brass tubing wound on a inner diameter of approximately 25 mm, number of windings $n = 18$; chilled by distilled water
- oscilloscope (Fig. 3.3. A 5): type MO100 (GRUNDIG Electronic)
- frequency counter (Fig. 3.3. A 6): type M6612 counter/timer 80 MHz/100 ms (Phillips)

Magnetic field treatment was performed with default settings of 27 A and 60 kHz for 30 min. This equals to a magnetic field strength of 38000 A/m with the custom-made coil.

Before every experiment, a standard 1 % nanoparticle dispersion was treated in the magnetic field with the described default settings and subsequent temperature increase was measured in the dispersion. The measured maximum temperature should reach $52^{\circ}\text{C} \pm 1.5^{\circ}\text{C}$ after treatment. Additionally, magnetic field strength was measured with an exploring coil during the process, displaying a magnetic field strength of approximately 38000 A/m. Encapsulated cells were treated by application of an alternating magnetic field *in vitro* as well *in vivo* with the standard settings 27 A and 60 kHz for 30 min.

For the *in vitro* experimentations, 140 capsules were selected and pipetted into 200 μl of DMEM + 10 % FCS in a 2 ml Eppendorf tube with roundish bottom. The Eppendorf tube was placed into the middle of the coil (Fig. 3.3. B), so that the bottom of the tube was in the middle of the height of the coil where the magnetic field strength is maximal. Temperature was measured in the supernatant before and after treatment by a thermometer.

In the *in vivo* experiments, 20 capsules were implanted into the hind limbs of mice. Using default settings of magnetic field treatment the hind limb was placed in the middle of the coil and a magnetic field was applied on implanted capsules.

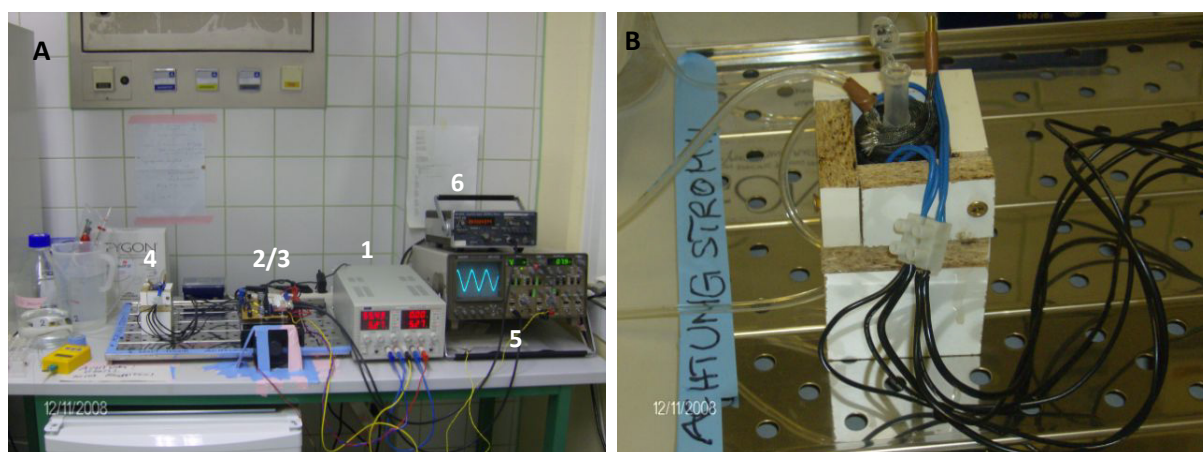


Fig. 3.4.: Custom-made magnetic field generator.

System (A) consisting of power supply (1), wave generator (2) and transistor full bridge (3), coil (4), oscilloscope (5) and frequency counter (6). Enlarged image of water-chilled coil (B) with sample vial.

3.2.7. Analysis of gene expression

3.2.7.1. Analysis of luciferase expression by luciferase assay

Both monolayer cultures of cells as well as encapsulated cells were analysed for luciferase expression. 5×10^4 cells carrying the reporter construct were seeded in 6-well plates and cultivated for two days in NM. 40 % to 80% confluent cells were shifted to a cell culture incubator adjusted to 43°C where they were kept for 1 h to 3 h. Encapsulated cells were incubated at 43°C for 45 min to 3 h or subjected to magnetic field treatment with 27 A and 60 kHz for 30 min. Luciferase expression was analysed 6 h after induction. Before analysis, medium was removed and cells were incubated with 50 μ l lysis buffer (250 mM Tris, 1% Triton X) for 20 min at RT on a shaker; capsules were mechanically destroyed with a pestle in 50 μ l lysis buffer for 5 min, vortexed and shaken for 15 min at 20°C on a thermo-shaker. Before measurement, resolved capsules were centrifuged with 1000 x g for 30 sec. 50 μ l sample volume was analysed by a measurement lasting for 10 sec. For analysis, 100 μ l each of ATP and luciferin (see below) were added. Samples were analysed using a Berthold LB9507 luminometer.

Buffers:

ATP solution

40 mM ATP

40 mM Tris pH 7.4

66.6 mM MgCl₂

Luciferin solution

50 μ M luciferin

50 mM Tris pH 7.5

3.2.7.2. Analysis of GFP expression by FACS

In order to investigate induction of GFP expression, cells were subjected to heat or magnetic field treatment, and GFP expression was analysed by FACS 24 h after induction.

For analysis of encapsulated cells, 140 capsules were pipetted into a 6-well plate. Medium was removed with a 1000 µl pipette. Capsules were first washed twice with SFMI medium. Capsules were then incubated in SFMI medium on a horizontal shaker (~20-30 rpm) in a cell culture incubator at 37°C. Capsules were resolved as described in section 3.2.5.2. According to the cell density within the capsules, separation of the cell aggregates was performed, also described in section 3.2.5.2.. Finally, cells were analysed by FACS (FACSCalibur, BD Biosciences).

3.2.8. Electron microscopy

Transmission electron microscopy (TEM) was applied to analyse localisation of nanoparticles in capsules and the impact of magnetic field treatment on the integrity of encapsulated cells.

For TEM, samples were fixed with 3% glutaraldehyde for at least 2 days to crosslink proteins. Subsequently, samples were washed three times with Soerensen buffer (pH = 7.4, ingredients are listed below, note: dilution of Soerensen buffer to 0.1 M working concentration) for 15 min to remove the fixative. Samples were put into a mixture of 3 % osmium and Soerensen buffer in a ratio of 1:3 (1% osmium) for 2 h. Samples were again washed with Soerensen buffer. Encapsulated cells were dehydrated in an ascending ethanol series, i.e. in 30% ethanol for 5 min, 50% ethanol for 5 min, 70% ethanol for 60 min, twice in 80% ethanol 15 min each, twice in 96% ethanol for 15 min each, and twice in 96% ethanol for 20 min each. Pure propylene oxide was added to the samples twice for 10 min. Propylene was sucked off. A mixture of propylene and resin in a ratio 1:1 was added for 60 min. Subsequently samples were put into a mixture of propylene and epon resin at a concentration ratio of 1:3 over night. The next day, samples were incubated in freshly prepared epon resin for 2 h. Embedding was performed in small conical tubes.

Samples were allowed to polymerise by incubation at 60°C for 3 days. Polymerised, embedded samples were cut using an ultratome (Ultracut S, Reichert) into ultra-thin (70 nm) sections which were fixed on a copper grid (Plano). Samples were stained with uranyl acetate (2% in 80% methanol) for exactly 8 min, washed three times for 10 sec in ddH₂O, incubated in lead citrate for 5.5 min and subsequently washed three times for 10 sec in ddH₂O.

Buffer:

Soerensen buffer 0.2 M

Na₂HPO₄ 22,45g

KH₂PO₄ 5,95g

Ad 2 l ddH₂O

3.2.9. Immunohistochemistry

3.2.9.1. Preparation of paraffin-embedded samples

To perform immunohistochemical staining for the investigation of effects of magnetic field treatment on cell viability and cell integrity, encapsulated cells were embedded in paraffin.

Encapsulated cells were fixed in pre-chilled (4°C) 2% formalin in PBS for 1 h at RT in a 24-well plate. Subsequently, capsules were washed twice with PBS and transferred into a 1.5 ml Eppendorf tube. PBS was removed. HistoGel (Richard-Allan Scientific) was melted in a microwave oven and subsequently cooled down to about 37°C while inverting. Capsules were moulded in warm HistoGel for sedimentation. After gelling at 4°C samples were transferred into 70% ethanol and dehydrated over night by incubation in an ascending series of ethanol using an automatic device (Thermo Scientific). The next day, samples were casted in warm and fluid paraffin and then put on a cold plate for hardening. The paraffin blocks with the embedded samples were cut into 3 µm sections using a rotation microtome (Leica). A 37°C warm water bath was used to allow unfolding of sections. The section was mounted on glass slides and allowed to dry in an incubator at 37°C over night.

3.2.9.2. Hematoxylin/Eosin staining

In order to cytologically analyse the effects magnetic field treatment paraffin-embedded, encapsulated cells were stained with hematoxylin and eosin.

Analysed samples were deparaffinised by incubation in xylol twice for 5 min each. Then samples were rehydrated by incubation in 96% ethanol twice for 5 min, 96% ethanol and 70% ethanol for 2 min each. Subsequently, slides were washed with ddH₂O for 2 min and stained with hematoxylin (Richard-Allan-Scientific) for 5 min, washed with ddH₂O for 10 min, stained with eosin (Riedl-de-Haen) for 5 min and washed again with ddH₂O for 2 min. Samples were dehydrated by incubation in 70% ethanol and three times in 96% ethanol for 2 min each. Finally, samples were put in xylol for 5 min, subsequently mounted with DPX resin and covered with a cover slip.

3.2.9.3. TUNEL assay

TUNEL assay was performed to analyse the impact of magnetic field treatment of encapsulated cells on cell viability and to determine the amount of apoptotic cells.

In the TUNEL (TdT-mediated dUTP-digoxigenin nick end labelling) assay, DNA strand breaks are detected by enzymatic labelling of free 3'-OH termini with modified nucleotides. These DNA ends are typically localised in morphologically identifiable nuclei and apoptotic bodies. The terminal deoxynucleotidyl transferase transfers digoxigenin-coupled nucleotides to free 3'-OH termini. Digoxigenin is detected by a fluorochrome (rhodamine)-labelled antibody (ApoTag^RRed *In Situ*, Chemicon).

Therefore, tissue sections were deparaffinised by incubating them three times in xylene for 5 min. Samples were rehydrated with a descending ethanol series as described above in section 3.2.8.2. Rehydrated samples were washed in PBS for 5 min. Proteinase K at a concentration of 20 µg/ml was directly added to the section on the slide and incubated for 20 min at RT. Slides were then washed twice with PBS for 2 min. As a positive control for fragmented DNA, distinct sections were treated with 10 U/ml DNaseI for 20 min at 37°C in a humidified chamber while other slides were kept in PBS. Slides were dried and equilibration buffer (ApoTag^RRed *In Situ*, Chemicon) was added for at least 10 sec. Slides were incubated with working strength TdT-enzyme (ApoTag^RRed *In Situ*, Chemicon) at 37°C for 1 h in a humidified chamber. The reaction was stopped with stop/wash buffer (ApoTag^RRed

In Situ, Chemicon) and incubated for 10 min. Slides were washed three times for 1 min in PBS, then dried and incubated with anti-digoxigenin conjugate (rhodamin, ApoTag[®]Red *In Situ*, Chemicon) in a humidified chamber in the dark. Slides were washed four times for 2 min in PBS. Samples were incubated in 1 µg/ml DAPI (in PBS) counter-stain solution for 3 min, washed in PBS, mounted with mounting medium (Vectashield, Vector Labs) to avoid bleaching of the fluorochrome and finally samples were covered with a cover slip.

3.2.9.4. Caspase 3 staining

In order to analyse the impact of magnetic field treatment on encapsulated cells, rate of apoptotic cells in paraffin-embedded sections was determined by immunohistological detection of Caspase 3.

Samples were deparaffinised and then rehydrated as described above in section 3.2.8.2. Samples were treated with 3% peroxidase blocking solution (40 ml methanol + 10 ml 15% H₂O₂) for 15 min and washed 10 times with ddH₂O. Antigen retrieval was performed by microwaving 4 x 5 min in citric acid, pH 6. Subsequently, samples were cooled down for 20 min at RT. Slides were put into cover-plates (Shandon) and washed in PBS for 5 min. Unspecific binding partners were blocked with protein blocking solution (1.5% goat serum in PBS) for 30 min. The primary antibody, rabbit anti-active-caspase 3 (R&D Systems AF835), was diluted 1:4000 in PBS and incubated with the sample over night at 4°C. The next day, samples were washed in PBS for 5 min and samples were incubated with the secondary antibody, goat anti-rabbit antiserum (Powervision), for 30 min. Slides were washed with PBS for 5 min and removed from the cover-plates. Slides were developed with diaminobenzidin (DAB, Sigma, 1 tablet /50 ml Tris-HCl pH7.4 + 500 µl 3% H₂O₂) for 10 min. Samples were washed in ddH₂O for 5 min. Staining of nuclei was performed by means of incubation with hematoxylin (Richard-Allan-Scientific) for 3 min. Samples were washed in ddH₂O for 10 min and dehydrated as described previously. Slides were treated with xylol two times for 2 min. Slides were covered with DPX and cover slips were placed on top.

3.2.10. Animal experiments

In vivo experiments were performed in order to determine induction of reporter gene expression in implanted encapsulated cells in response to heat and magnetic field treatment. All *in vivo* experiments were performed according to the regulations of the Austrian law governing animal experimentation (Animal experiment application at the Austrian Ministry for Science and Research BMWF-68.205/0213-II/10b/2009).

3.2.10.1. Maintenance of mice

Hsd. athymic Nude-*Foxn1^{nu}* mice were chosen for the *in vivo* experiments. Mice were 10 to 12 weeks old at the beginning of the experiment. In total, 24 mice were used, half female and half male. Mice were kept separately in type 2 euronorm cages. The mice were kept at daylight with a natural diurnal rhythm. Animals were fed with an autoclaved, special nutrition (V1534 R/M-H, SSNIFF) and autoclaved drinking water. Food and water took was provided ad libidum.

3.2.10.2. Anaesthesia and euthanasia

For the measurement of luminescence or fluorescence with the IVIS 50 bio-imaging-system, mice were anaesthetised by inhalation of 2 to 3 % isoflurane and for implantation as well as for heat and magnetic field treatment the mice were anaesthetised by i.p. injection of 100 mg ketamine and 4 mg xylazine per kg body weight. Euthanasia of mice was performed by cervical dislocation.

3.2.10.3. Experimental accomplishment

Aim of the experiment was to demonstrate magnetic field and heat inducible luciferase as well as EGFP expression in encapsulated cells *in vivo*.

Therefore, genetically modified HEK293 pSGH2lucpuro C5 cells harbouring the expression construct which is responsive to heat, were sterile encapsulated in biologically inert sodium cellulose sulphate (SCS). These encapsulated cells were cultivated for 3 weeks *in vitro*, till they were 75 % confluent. An aliquot of capsules (approximately 200 microcapsules) were washed three times with PBS to remove cell culture medium. Each 20 capsules were aspirated into an intravenous catheter by a

syringe. Mice were narcotised (3.2.10.3.) and subsequently, capsules were subcutaneously instilled into the thigh of the left hind limb without sewn closure. Then induction experiments started five days after administration of the microcapsules. Mice were magnetic field or heat treated once a week over a period of three weeks. Therefore, mice were narcotised (3.2.10.3.) and the hind limb was exposed either to a magnetic field (27 A, 60 kHz) for 30 min or placed on a heating plate (43°C) for 15 min. IVIS 50 (Xenogen) live bio-imaging system allowed a non-invasive measurement and quantification of luminescent and fluorescent reporter gene expression. In order to determine luciferase gene expression, mice were narcotised (3.2.10.3.) 6 h after treatment. Using luminescence *in vivo* analysis, 240 mg/kg D-Luciferin potassium salt was injected intra-peritoneally (i.p.) 15 min before anaesthesia and measurement. The luciferase measurement was performed by a measurement lasting 1 min. In order to determine EGFP gene expression, mice were analysed 24 h after treatment.

4. RESULTS

4.1. Analysis of heat-induced expression in genetically modified cells

For the presented study, i.e. analysing heat-induced reporter gene expression in encapsulated cells, a clone of HEK293 cells stably transfected with the respective expression construct was used. The selected single cell clone, HEK293 pSGH2lucpuro C5 (Materials and Methods, section 3.1.6.2.), was supplied by the Institute of Animal Breeding and Genetics (University of Veterinary Medicine, Vienna). The expression vector (Appendix, section 7.4.) carries an artificial bidirectional heat inducible promoter based on the human heat shock promoter Hsp70. In detail, this bidirectional promoter consists of two minimal CMV promoters, orientated in opposite directions, coupled to eight idealised heat shock elements harbouring the consensus sequence 5`-AGAAC-3` (Bajoghli et al., 2004). Two reporter genes – GFP and luciferase – were driven by this artificial promoter, rendering their expression inducible by heat.

Initial experiments performed by Viktoria Ortner had shown that expression levels of both genes were continuously increased when cells were incubated at elevated temperatures between 40°C and 43°C. Induction rates were shown to be maximal three log-stages, relative to promoter background activity in cells kept at 37°C. Analyses revealed that treatment of cells at 43°C resulted in an optimal promoter inducibility combined with a relatively low cell death rate (experiments performed by Viktoria Ortner from the Institute of Animal Breeding and Genetics, University of Veterinary Medicine, Vienna).

In order to characterise the transfected cells in more detail, they were exposed to 43°C for 1 – 3 h followed by analysis of reporter gene expression. Therefore, 5×10^4 cells/well were cultured in a six-well-plate for two days and then incubated at 43°C for 1 h, 2 h and 3 h. Subsequently, luciferase expression was analysed after 6 h of recovery by using a luciferase assay (Materials and Methods, section 3.2.7.1.), and in

addition, GFP expression was analysed after 24 h of recovery by quantitative FACS analysis (Materials and Methods, section 3.2.7. 2.).

Measurement of expression revealed a robust induction of reporter gene expression in response to heat treatment. Induced luciferase expression levels were increased in correlation with the heat exposure time. Values depicted in figure 4.1. are relative; the expression levels of cells kept at 37°C were set to one as a reference. In response to 1 h of heat treatment at 43°C, expression was shown to be 54-fold elevated, while a 2 h incubation at the same temperature resulted in a 667-fold elevated expression. A maximum of 944-fold increase in luciferase expression was obtained when cells were incubated for 3 h at 43°C (Fig 4.1. A).

Quantitative FACS analysis of GFP positive cells (Fig. 4.1. B) also showed induction of the respective reporter gene in response to elevated temperatures. GFP expression of cells incubated for 1 h at 43°C was found to be 1935-fold increased relative to the expression levels of cells kept at 37°C. Moreover, expression levels were found to be 4260-fold increased in response to heat treatment for 2 h at 43°C. However, the expression level decreased to 3068-fold when cells were incubated for 3 h at 43°C.

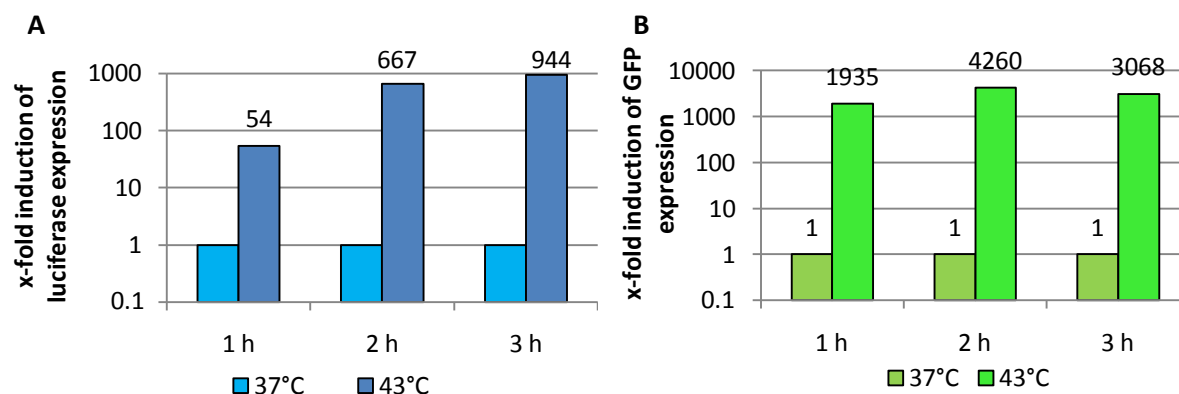


Fig. 4.1.: Heat inducibility of cultured HEK293 pSGH2lucpuro C5 cells.

Cells were analysed regarding induction of reporter gene expression (luciferase, GFP) in response to heat treatment at 43°C for 1 h, 2 h and 3 h. (A) Luciferase measurement was performed using a Berthold LB9507 luminometer. (B) Quantitative FACS analysis was performed by using FACScalibur, BD Biosciences. All values are shown as x-fold induction relative to expression in cells kept at 37°C.

Induction of gene expression in cells by heat treatment at 43°C for 1 h was also shown by UV-microscopy (Fig. 4.2). By this means, cells with a strong green fluorescence were observed in cell cultures after 24 h of recovery (Fig. 4.2. D).

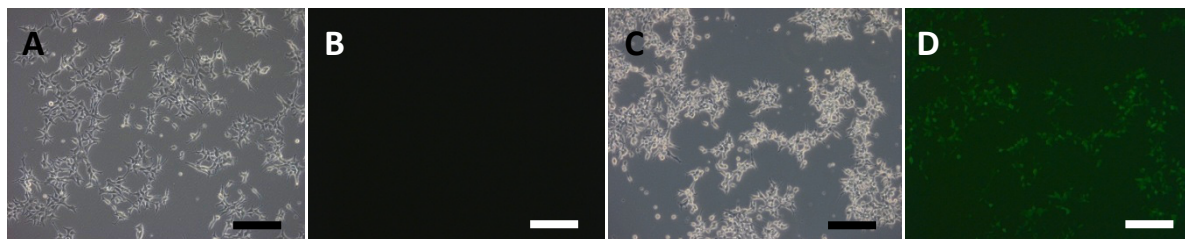


Fig. 4.2.: Induction of GFP expression in HEK293 pSGH2lucpuro C5 cells.

(A and B) Cultured cells kept at 37°C. (C and D) Cells heat-treated by incubation at 43°C for 1 h. (D) GFP expression in response to heat treatment as analysed by UV microscopy (Axiovert 200M, Zeiss; magnification 100-fold, scale bar 50 μ m; A, D: bright field analysis; B, C: UV-microscopy).

The stably transfected cells described here were used to provide the proof-of-principle for a magnetic nanoparticle-mediated thermoregulation of gene expression in encapsulated cells in response to treatment with an alternating magnetic field. To follow this aim, in a next step different magnetic nanoparticles were analysed with respect to their applicability in this concept.

4.2. Characterisation of magnetic nanoparticles with respect to physical properties, heat generation capacity and tendency to aggregate

In this project magnetic nanoparticles should be used within microcapsules to generate heat by exposing them to an alternating magnetic field. For this specific application, magnetic nanoparticles which should be used had to fulfil specific characteristics. Besides others, the most important criteria were that these particles had to generate substantial heat in an alternating magnetic field and, additionally, that they were encapsulate-able. Therefore, a set of 14 different nanoparticles was analysed for the specific needs of this project. 13 of these nanoparticles were generated and kindly provided by Dr. Olga Mykhaylyk from the Institute of Experimental Oncology and Therapy Research from the Technical University in Munich. These nanoparticles were regularly produced for magneto-transfection (Plank, et al., 2003). In addition, a commercially available magnetic nanoparticle formulation from Sigma (product number 637106) was used. The distinct physiochemical characteristics of the particles used are given in table 4.1.

Tab. 4.1.: Physicochemical characterisation of different nanoparticles.(1)

Sample	S1	S4	S5	S7	S8	S11	S13	S16	S22	S24	S25	S26	S34	Sigma
Shell (surface composition)	Palmityl-dextran	Palmityl-dextran	Palmityl-dextran	Palmityl-dextran	Polyethylenimine	Pluronic-127/FSE	Palmityl-dextran/FSA	Tween-80	Tween 60/FSA	1.9-Nonandithiol	Chitosan-OSL	Dihexadecyl phosphate	Pluronic127/FSA	Poly-vinyl pyrrolidone
Core density [g/cm ³]	5.21	5.21	5.21	5.21	5.21	5.21	5.21	5.21	5.21	5.21	5.21	5.21	5.21	-
Mean core size (crystallite size) d (nm)	80	8.5	13	30.6	74.1	10.6	4	10	11.7	12	10	10	11	30
Mean hydrated particle diameter (nm)	215 ± 102	55 ± 10	380 ± 200*	103 ± 60*	409 ± 190*	106 ± 40*	55 ± 11	53 ± 27		68 ± 30	1200*	nd	100 ± 49	n.d.
Electrokinetic potential or x-potential (mV)**	Nd	-15.6 ± 1.6	-16.3 ± 1.6	-16.6 ± 1.6	+ 50 ± 2	-13.3 ± 1.6	- 31.4 ± 0.9	+27.8 ± 4	-1.4 ± 1.6	-14.6 ± 0.7	+21.5 ± 0.5	-39 ± 6.3	-18.3 ± 0.2	-
Concentration [mg dry nano-material/ml]	7.4	19.0	18.7	25.0	23.2	24.4	17.6	33.1	34.9					-
Iron concentration [mg Fe/ml]	5	10	10	15	15	10	8,9	13,9	15	10	5	5	9	-
Iron content (g Fe /g dry weight)	0.675	0.526	0.534	0.601	0.646	0.41	0.507	0.42	0.43	0.5	0.52	0.44	0.21	-
Coating content (g coating material/g dry weight)	0.07	0.27	0.26	0.17	0.11	0.43	0.30	0.42	0.41	0.31	0.28	0.39	0.71	-
Average core weight per particle (g/particle)	1.4E-15	1.7E-18	6.0E-18	7.8E-17	1.1E-15	3.2E-18	1.7E-19	2.7E-18	4.4E-18	4.7E-18	2.7E-18	2.7E-18	3.6E-18	-
Average iron weight per particle (g Fe/particle)	1.0E-15	1.2E-18	4.3E-18	5.7E-17	8.0E-16	2.4E-18	1.3E-19	2.0E-18	3.2E-18	3.4E-18	2.0E-18	2.0E-18	2.6E-18	-
Particle per unit iron weight [particle/g Fe]	9.9E+14	8.2E+17	2.3E+17	1.8E+16	1.2E+15	4.3E+17	7.9E+18	5.1E+17	3.2E+17	2.9E+17	5.1E+17	5.1E+17	3.8E+17	-
Particles per unit volume [particle/μl]	4.9E+09	8.2E+12	2.3E+12	2.7E+11	1.9E+10	4.3E+12	7.0E+13	7.0E+12	4.7E+12	2.9E+12	2.5E+12	2.5E+12	3.4E+12	powder

(1) According to analyses provided by the Institute of Experimental Oncology and Therapy Research, Technical University Munich.

For the intended application, the provided set of nanoparticles was investigated with regard to their capacity for heat generation. Therefore, dispersions containing 1% (w/v) nanoparticles in PBS were treated with an alternating magnetic field (27 A, 60 kHz) for 30 min. Temperature was measured in the dispersions with a thermometer before and after treatment with the alternating magnetic field. In figure 4.3. temperature increases are shown in relation to the temperature increase obtained with PBS lacking nanoparticles.

The custom-made S8 and S24 nanoparticles as well as the commercially available nanoparticles from Sigma were shown to yield the highest temperature increase (Fig. 4.3.). According to these results, the S8, the S24 and the Sigma nanoparticles were further used in the following experiments.

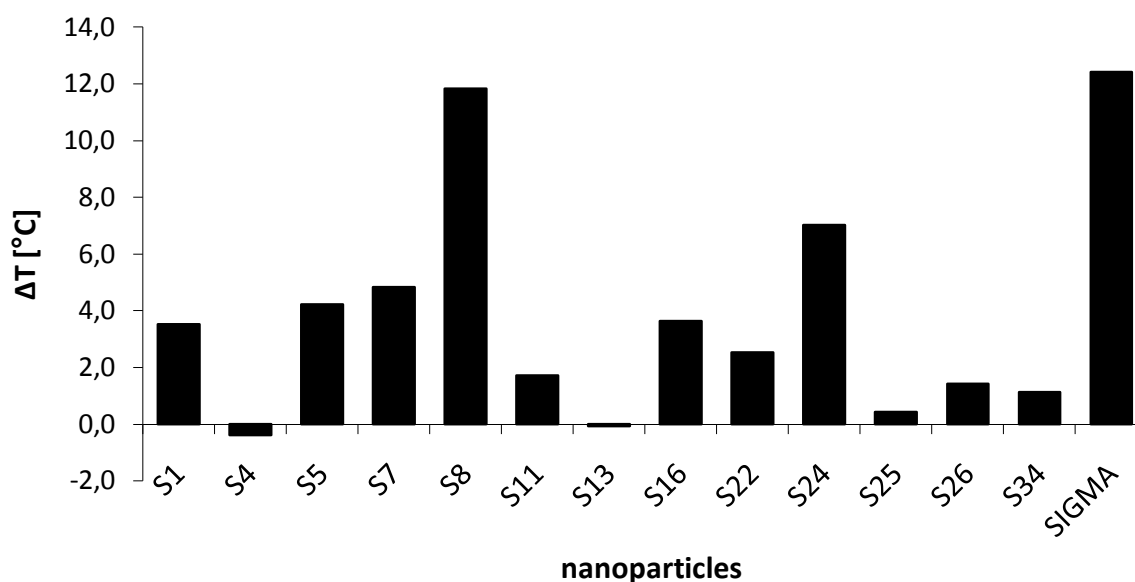


Fig. 4.3.: Heat generation capacity of a set of different magnetic nanoparticles.

Nanoparticle dispersions (1% w/w) were subjected to an alternating magnetic field with 38 kA/m and 60 kHz for 30 min (experiment performed by Viktoria Ortner from the Institute of Animal Breeding and Genetics, University of Veterinary Medicine, Vienna).

Magnetic nanoparticles provided by Sigma consisted of 100% magnetite and are stabilised by polyvinylpyrrolidone. They had a diameter of 30 nm. In contrast to the Sigma nanoparticles, the S8 nanoparticles had a core of 100% magnetite with a diameter of 74.1 nm (Table 4.1.). The coating material was polyethylenimine. The

S24 nanoparticles also contained a core of 100% magnetite with a diameter of 12 nm and were coated with 1,9-nonane-dithiol.

As already mentioned, the second important criterion was the ability of nanoparticles to be encapsulated. In order to investigate this characteristic, first the tendency for aggregation of nanoparticles S8, S24 and “Sigma” was analysed. This was important because high concentrations of aggregated particles would cause a blockage of the nozzle during the encapsulation process. All particles analysed, showed a tendency to aggregate. As a result of aggregation, particles could be investigated by applying a light microscope. Nanoparticle formulations were diluted to a concentration of 0.01% (w/w) and treated with ultrasound for 15 sec on dry ice. Light microscopically analysis was performed after 30 sec of incubation at RT.

The analysis revealed that the S24 nanoparticles aggregate to a lower extent (Fig. 4.4. B), when compared to S8 and Sigma nanoparticles. The S8 nanoparticles formed netlike structures (Fig. 4.4. A), whereas Sigma nanoparticles had already aggregated into large clumps with a diameter up to approximately 100 μm (Fig. 4.4. C). Consequently, these particles despite their high heat inducing capacity could not be used for co-encapsulation with HEK293 cells.

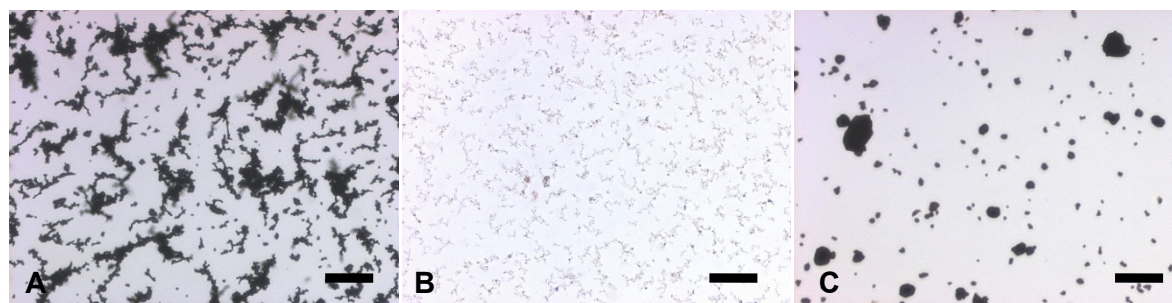


Fig. 4.4.: Nanoparticle aggregation.

Light microscopic analysis of nanoparticle aggregation was performed (magnification 400-fold, scale bar 200 μm). Pictures show nanoparticle aggregation of A) S8 nanoparticles, B) S24 nanoparticles and C) Sigma nanoparticles.

4.3. Co-encapsulation of cells and nanoparticles

In the following section the establishment of the co-encapsulation of nanoparticles and cells and the subsequent effect on the physical properties will be described. In the previous section (4.2.) it has been shown that the nanoparticles from Sigma are not encapsulatable because they formed large aggregates of up to 100 μm in size. Therefore, encapsulation with nanoparticles was established for S8 and S24 nanoparticles which showed a lower aggregation tendency.

Encapsulation parameters have been established previously for the encapsulation of cells (Hauser, et al., 2004) with 1.8 % sodium cellulose sulphate (SCS). For co-encapsulation of cells and nanoparticles, the concentration was reduced to 1.6 % SCS because of the increased viscosity of the encapsulation material containing 0.5% nanoparticles. Other parameters were kept constant: a flow rate of 8.5 ml/min, an oscillation-frequency of 730 Hz, an oscillation-amplitude of 30 % and a dispersion voltage of 1.5 kV were applied. This resulted in formation of microcapsules with a diameter of approximately 700 μm . In figure 4.5. different generated capsules are depicted. Capsules manufactured using a SCS concentration of 1.8 % containing cells (Fig. 4.5. A), whereas capsules generated using SCS concentration of 1.6 %, containing co-encapsulated cells and S8 (Fig. 4.5. B) or S24 (Fig. 4.5. C) magnetic nanoparticles shown in figure respectively.

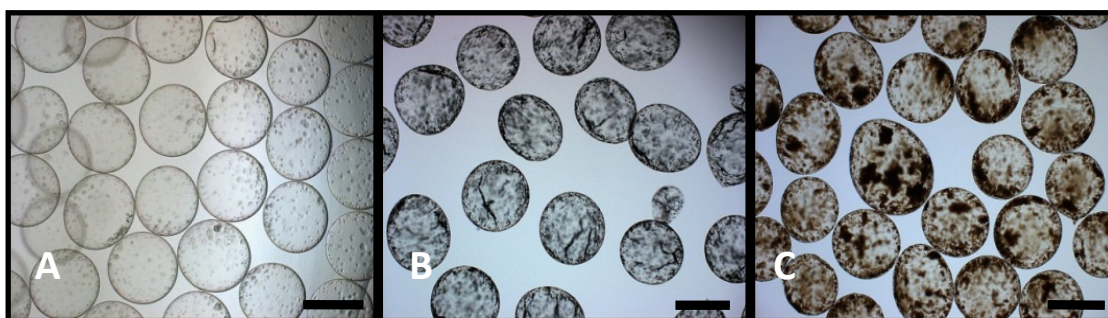


Fig. 4.5.: SCS capsules containing HEK293 pSGH2lucpuro C5 cells with and without nanoparticles.

Images show 1.8% SCS capsules and 1.6 % SCS capsules. Cells only were encapsulated in 1.8% SCS (A). Cells and 0.5% nanoparticles were encapsulated in 1.6% SCS: (B) co-encapsulated S8 nanoparticles and (C) co-encapsulated S24 nanoparticles. Light microscopic analysis was performed with an Axiovert 200M (Zeiss). Scale bar is 700 μm and magnification is 40-fold.

4.3.1. Characterisation of physicochemical properties of capsules with and without nanoparticles

Having modified the encapsulation process according to the enhanced viscosity of SCS containing nanoparticles, it was investigated if the physicochemical characteristics of generated capsules still complied with the intended application. Therefore, it was investigated if the physical capsule properties differ in comparison to the standard capsules manufactured with 1.8 % SCS.

The microcapsule diameter is an important parameter because it is defining the diffusion-limited supply of encapsulated cells with nutrients. Moreover, it is determining the space cells can occupy within the microcapsule and thus it is defining the biological power per microcapsule in terms of a cell-based therapy.

Manufactured capsules were microscopically analysed using the microscope Axiovert 200 M (Zeiss). Diameters were determined using the software AxioVision (Zeiss) by calibrating the taken picture according to the used objective and by employing the measurement tool. 180 diameters of capsules were defined analysing nine independent encapsulation experiments. The encapsulation of different combinations of cells and nanoparticles, namely HEK293 pSGH2lucpuro C5 cells alone, cells co-encapsulated with S8 nanoparticles and cells co-encapsulated with S24 nanoparticles, resulted in capsule diameters which were varying in a range between 530 μm and 753 μm (Fig. 4.6.). The median of the frequency distribution of measured capsule diameters was 646 μm for capsules containing HEK293 pSGH2lucpuro C5 only. The median of the frequency distribution of measured capsule diameters was 620 μm for capsules containing HEK293 pSGH2lucpuro C5 and S8 nanoparticles. The median of the frequency distribution of measured capsule diameters was 625 μm for capsules harbouring HEK293 pSGH2lucpuro C5 and S24 nanoparticles (Fig. 4.6.). The different percentages of SCS used in the distinct encapsulation processes appeared not to have a strong impact on capsule diameters as no significant difference in capsule diameters was observed comparing capsules containing cells and nanoparticles to 1.8 % SCS capsules containing cells only. In conclusion, co-encapsulation of nanoparticles and following reduction of SCS concentration to 1.6% did not affect capsule diameters.

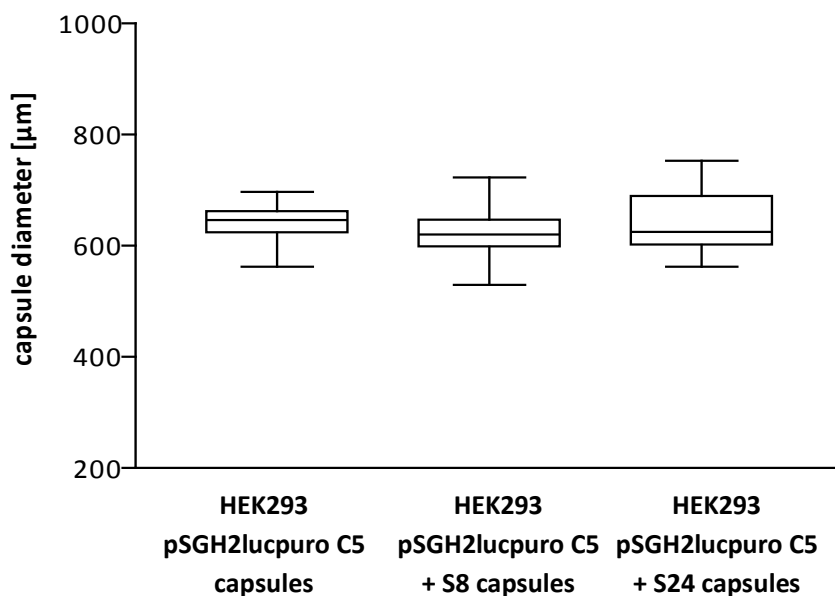


Fig. 4.6.: Capsule diameters of capsules with cells and with co-encapsulated nanoparticles.

Capsule diameters of nine independent encapsulations ($n = 180$) determined by microscopical analysis and software assisted measurement (AxioVision, Zeiss). Box- and Whiskers-blot is depicted for diameters of encapsulated HEK293 pSGH2lucpuro C5 cells without nanoparticles, encapsulated HEK293 pSGH2lucpuro C5 cells with S8 nanoparticles and encapsulated HEK293 pSGH2lucpuro C5 cells with S24 nanoparticles.

The calculated mean value of capsule diameters was 680 μm considering all performed 64 encapsulation experiments. The mean diameters defined by analysing 20 capsules each varied in a narrow range between 605 μm and 800 μm (Fig. 4.7.). The 64 encapsulations were performed within a period of 2 years. This reflects the reproducibility of the encapsulation process regarding capsule diameters.

In order to further analyse the influence of co-encapsulation of nanoparticles and reduced SCS concentration on capsule formation process, the different capsules were investigated with respect to their diffusion properties.

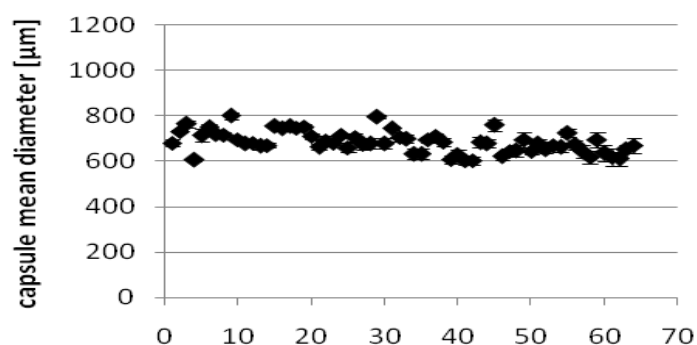


Fig. 4.7.: Capsule diameters.

Experimental variance of mean capsule diameters determined by analysing diameters of 20 capsules in each of the 64 performed encapsulations within two years.

Diffusion properties of microcapsules are of great interest because they define the supply of encapsulated cells with nutrients and determine the disposal of metabolites as well as the dispensing of therapeutic substances into the surrounding tissue in terms of a cell-based therapy.

Diffusion properties of capsule membranes were analysed using capsules with encapsulated nanoparticles manufactured with 1.6% SCS, a reduced concentration of SCS in comparison to standard 1.8 % SCS capsules. Capsule diffusion properties were determined by size exclusion of FITC-labelled dextrans of different molecular weight. FITC-dextrans of 40 kDa, 70 kDa and 250 kDa were used. Therefore, capsules lacking and containing S8 or S24 nanoparticles were incubated in medium containing different FITC-dextrans over night. The next day, capsules were washed twice with PBS and UV-microscopy was performed immediately using Axiovert 200 M (Zeiss) (Materials and Methods 3.2.3.2.). The molecular cut-off limit was between 70 kDa and 250 kDa for all used capsules (Fig. 4.8.). In conclusion, the encapsulated nanoparticles S8 and S24 and a reduced concentration of 1.6% SCS did not result in differences regarding the molecular cut off limit of capsule membranes compared to standard 1.8% SCS capsules.

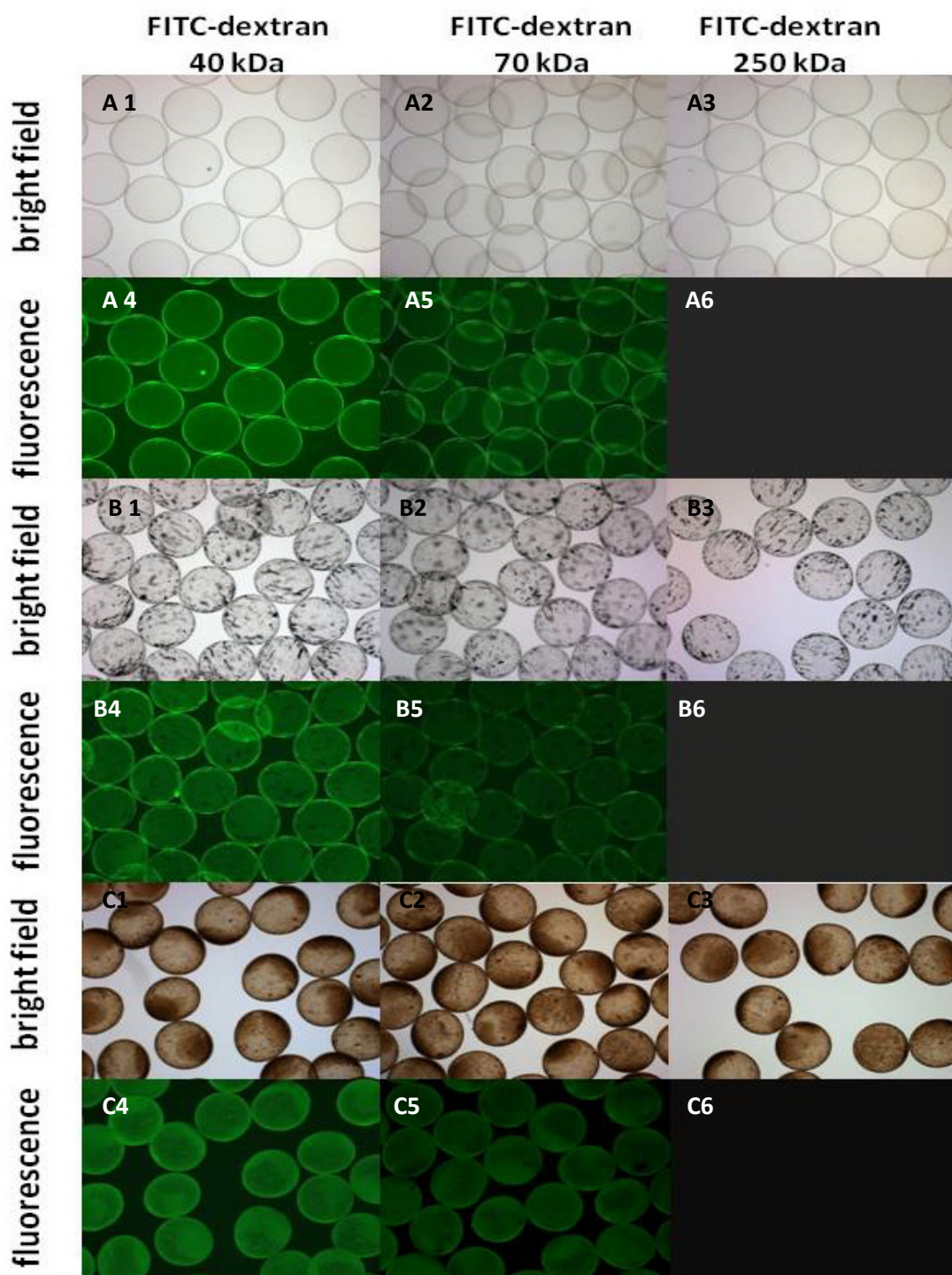


Fig. 4.8.: Analysis of size exclusion of FITC-dextrans by capsule membranes manufactured with different SCS concentrations.

Determination of size exclusion of FITC-dextrans by membranes of 1.8% SCS capsules without nanoparticles (A1 – 6) as well as of 1.6% SCS capsules with S8 (B1 – 6) or S24 (C1 – 6) nanoparticles. Fluorescence microscopical analysis was performed with microscope Axiovert 200M (Zeiss).

To further define capsule properties, the influence of the different concentrations of SCS used for encapsulation and the influence of the following co-encapsulation of nanoparticles was analysed by investigation of membrane thickness. Membrane thickness determines diffusion speed of nutrients and metabolites and hence is important parameter for viability of encapsulated cells.

Membrane thickness was analysed by calcofluor staining. Calcofluor intercalates in β -glycosidic-linked poly-saccharose. For example, calcofluor is used to stain cellulose in the cell walls of plant cells or chitin/glycan in the cell wall of fungi. Calcofluor has an excitation wavelength of 365 nm and an emission wavelength of 435 nm.

After incubating capsules in 3.3 mg/ml calcofluor in PBS for 12 h, capsules were washed twice with PBS and subsequently, fluorescence was analysed by fluorescence confocal laser scanning microscopy (CLSM) (Material and Methods 3.2.3.1.) using a 420 nm wavelengths filter. Original images were analysed using the software LSM Image browser (Zeiss) and membrane thickness was determined by the included measurement tool.

Analysis of the thickness of the capsule membranes revealed that the membranes had diameters of approximately 35 μm . 1.8 % SCS capsules had a diameter of 35.5 $\mu\text{m} \pm 8.7 \mu\text{m}$ (Fig. 4.9. A), while 1.6 % SCS capsules containing S8 nanoparticles had a diameter of 35.9 $\mu\text{m} \pm 10.3 \mu\text{m}$ (Fig. 4.9. B) and 1.6% SCS capsules carrying S24 nanoparticles revealed a diameter of 35.2 $\mu\text{m} \pm 9.4 \mu\text{m}$ (Fig. 4.9. C). Encapsulation using different concentrations of SCS as well as the co-encapsulation of nanoparticles appeared not to have an impact on membrane thickness.

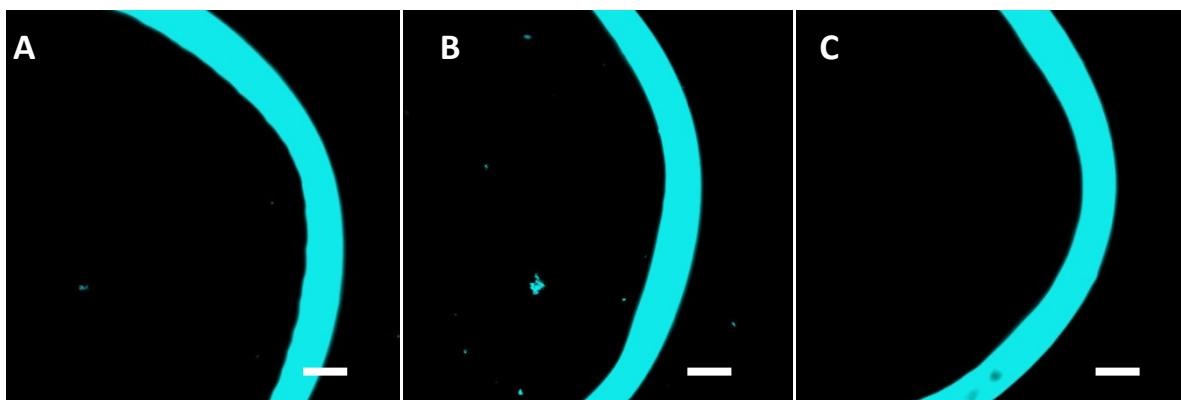


Fig. 4.9.: Determination of capsule membrane thickness.

Calcofluor-stained cellulose membrane of a 1.8 % SCS capsule without nanoparticles (A), of a 1.6% SCS capsule with S8 nanoparticles (B), and of a 1.6% SCS capsule with S24 nanoparticles (C) analysed by CLSM using a LSM 510 microscope (Zeiss, scale bar 30 μm) by $\lambda = 405 \text{ nm}$.

In the previous sections genetically modified HEK293 pSGH2lucpuro C5 cells were characterised regarding inducibility of gene expression in response to heat. Expression analysis of heat-treated cells revealed robust induction of luciferase and EGFP expression. Furthermore, a set of different nanoparticles was characterised with respect to parameters relevant in this project: their heat generation capacity in an alternating magnetic field and their ability to be encapsulated. According to these criteria, S8 and S24 nanoparticles were selected for further experiments. Microcapsules generated by co-encapsulation of cells and nanoparticles were analysed with respect to important physical capsule parameters such as size, diffusion properties and membrane thickness. In summary, the reduced SCS concentrations applied for co-encapsulation of cells and nanoparticles had no influence on the capsule diameters, capsule diffusion properties and membrane thickness, three characteristics important for viability of encapsulated cells.

In a next step, encapsulated cells shall be investigated with regard to nanoparticle localisation within microcapsules, inducibility of gene expression in response to heat treatment and cell viability in response to heat treatment; in addition, biocompatibility of nanoparticles and heat inducibility of expression in encapsulated cells are being investigated during long-term cultivation and after multiple heat inductions.

4.4. Characterisation of encapsulated cells

After the physical parameters of microcapsules were investigated, the biological characteristics of encapsulated cells should be analysed. In particular, localisation of nanoparticles within microcapsules, their biocompatibility with respect to encapsulated cells and heat responsive expression within encapsulated cells should be investigated.

4.4.1. Characterisation of encapsulated cells with respect to nanoparticle localisation

The nanoparticles provided for the presented work originally were made predominantly for gene delivery (Plank, et al. 2003 and Plank, et al. 2009). The selected S8 and S24 nanoparticles exhibited a magnetite core. They were either coated with polyethylenimine (PEI, S8, Fig. 4.10. A) or with 1,9-nonanedithiol (1,9-NDT, S24, Fig. 4.10. B).

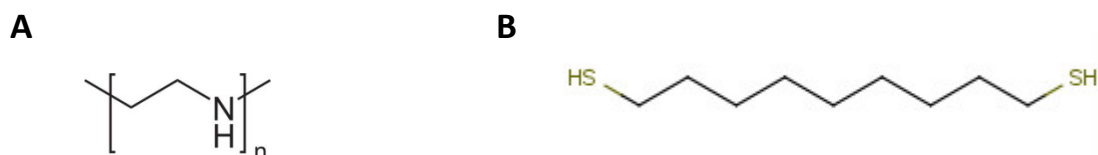


Fig. 4.10.: Coating material of selected nanoparticle formulations.

Both selected nanoparticles had a magnetite core. S8 nanoparticles were coated with polyethylenimine (A) and S24 nanoparticles with 1,9-nonanedithiol (B).

PEI is usually used as a transfection reagent for gene delivery applications (Arsianti, et al, 2010; Rudolph, et al. 2000; Wirth, et al., 2011). It is involved in nucleic acid binding via interaction of its positive charges with negative charges of phosphate groups in the nucleic acids at physiological pH. Cellular uptake is directed by the interaction with negatively charged plasma membranes (Akinc, et al. 2005).

1,9-NDT was also intended to use for gene delivery. It was reported that free thiol groups are essential for infectivity of viruses (Mirazimi, et al., 1999). By mimicking

viral particles it was speculated that free thiol groups at the surface of nanoparticles enhance association with cell membranes and thus enforce internalisation of nanoparticles.

Because of the distinct intended use, nanoparticles in the present project were analysed with respect to their intra-capsular localisation. In order to analyse localisation of nanoparticles within generated microcapsules, capsules containing HEK293 pSGH2lucpuro C5 cells with or without co-encapsulated S8 and S24 nanoparticles were analysed by transmission electron microscopy (TEM). Encapsulated cells with and without S8 or S24 nanoparticles were prepared for electron microscopy in the second week of cultivation (please refer to chapter 4.4.3. Fig. 4.13.). Samples were fixed with glutaraldehyde, 100 nm sections were prepared and contrasted with uranyl acetate and lead citrate (Material and Methods 3.2.8.).

In capsules containing cells and S8 nanoparticles (0.5 % w/w), the nanoparticles were detected within the capsule membrane (Fig. 4.11. H) , inside the capsule (Fig. 4.11. G) and also within cells (Fig. 4.11. E and F). Apparently, the S8 nanoparticles which were coated with PEI were spontaneously taken up into cells. In capsules containing HEK293 pSGH2lucpuro C5 cells and 1.9- NDT-coated S24 nanoparticles (0.5 % w/w), nanoparticles were detected within the capsule membrane (Fig. 4.11. L), within cell cytoplasm (Fig. 4.11. I, J and K) and also to a certain extent within the nucleus (Fig. 4.11. J). Thus, according to their intended use, S8 and S24 were both taken up by encapsulated cells. In the next chapter, it should be analysed if cellular nanoparticle uptake influences cell viability. Although, magnetite containing nanoparticles have been shown to be biologically tolerable (reviewed by Hafeli, et al., 2009), the applied coating material which not only mediates cellular uptake but also reduces agglomeration and keeps particles dispersed (reviewed by Hafeli, et al., 2009), might reveal cytotoxic characteristics.

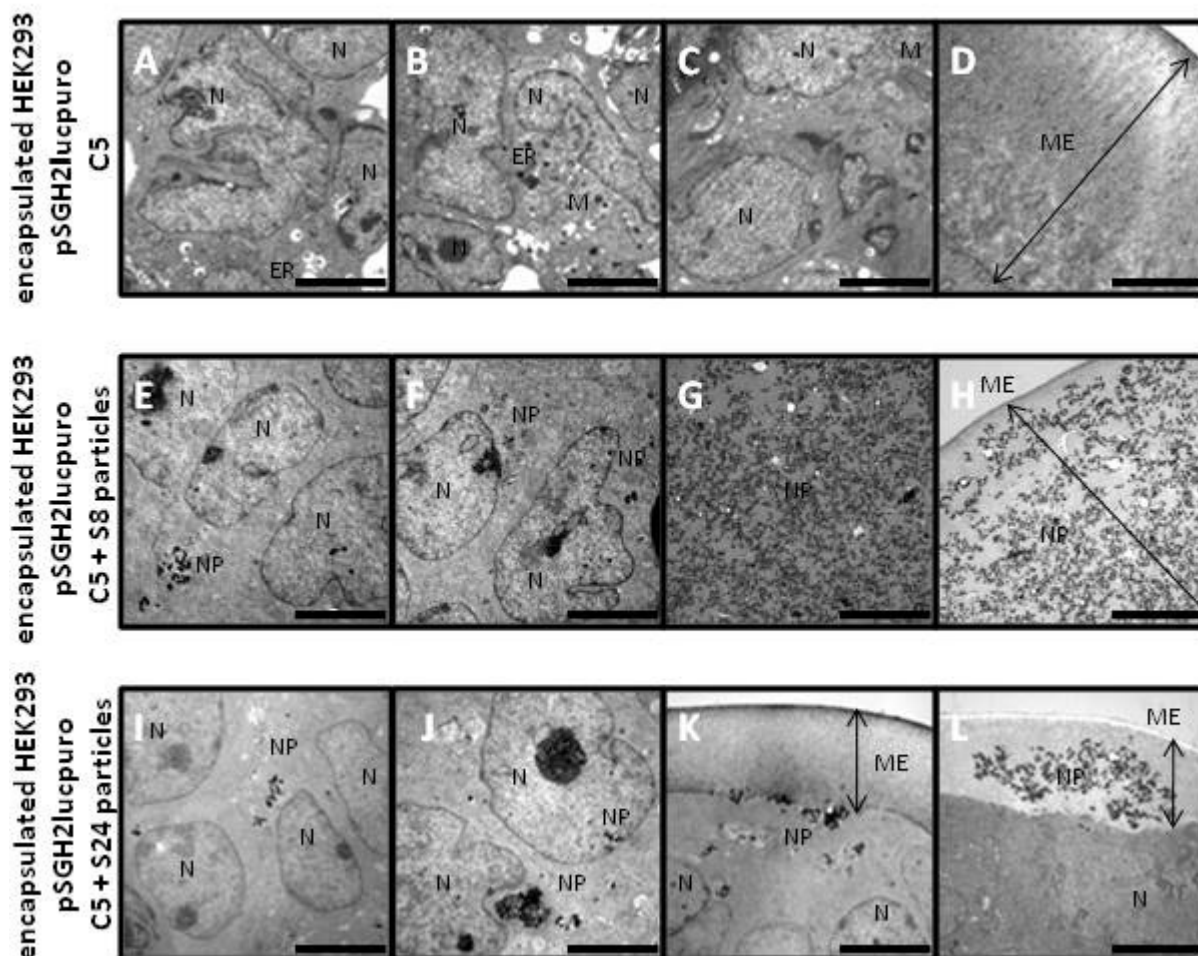


Fig. 4.11.: Nanoparticle localisation.

TEM analysis of SCS microcapsules containing HEK293 pSGH2lucpuro C5 cells only (A – D), cells co-encapsulated with S8 nanoparticles (E – H) or with S24 nanoparticles (I – L). Microscopy was performed using the EM900 transmission electron microscope from Zeiss (magnification 3000-fold and scale bar 5 μ m; N = nucleus; ER = endoplasmatic reticulum; NP = nanoparticles; ME = membrane of capsule).

4.4.2. Characterisation of encapsulated cells concerning biocompatibility of nanoparticles

In order to investigate the biocompatibility of this specifically coated magnetite nanoparticles, viability of encapsulated cells was determined by calcein-AM staining followed by FACS analysis. Living cells are characterised by the ubiquitous presence of intracellular esterase activity, which is determined by the enzymatic conversion of the virtually non-fluorescent calcein-AM into the intensively fluorescent calcein.

Cells co-encapsulated with S8 and S24 nanoparticles were cultivated for four weeks. Encapsulated cells were prepared for analysis on day seven, on day 15, on day 21 and on day 28 post encapsulation. Therefore, cells were released from capsules and viable cells were stained with calcein-AM (Materials and Methods 3.2.4.3.). Subsequently, FACS analysis was performed.

In general, FACS analysis revealed 59.2 to 86.7% viable cells (Fig. 4.12.). During the encapsulation process cells are exposed to different stress factors affecting viability. This is reflected by the number of living cells determined seven days after encapsulation (Fig. 4.12.). Capsules with HEK293 pSGH2lucpuro C5 cells contained only 79.3% viable cells (Fig. 4.12., black dot, 7 days after encapsulation), whereas capsules with cells and S8 nanoparticles contained 80.8% viable cells (Fig. 4.12., gray square, 7 days after encapsulation) and the highest percentage with 86.7% of viable cells was found in capsules containing cells and co-encapsulated S24 nanoparticles (Fig. 4.12., bright gray triangle, 7 days after encapsulation). On day 15 after encapsulation, in capsules containing cells only the percentage of viable cells had further decreased to 64.8% (Fig. 4.12., black dot, 15 days after encapsulation) in comparison to capsules containing cells and S8 or S24 nanoparticles, where the percentages of viable cells was found to be 68.2% (Fig. 4.12., gray square, 15 days after encapsulation) and 67.8% (Fig. 4.12., bright gray triangle, 15 days after encapsulation), respectively. From here on the percentage of viable cells increased on day 22 post encapsulation to 79.1% viable cells in capsules with cells lacking nanoparticles (Fig. 4.12., black dot, 22 days after encapsulation). In capsules with co-encapsulated S8 nanoparticles, 81.0% viable cells were detected (Fig. 4.12., gray square, 22 days after encapsulation) and in capsules with co-encapsulated S24

nanoparticles 79.1% viable cells were identified (Fig. 4.12., bright gray triangles, 22 days after encapsulation). In contrast, on day 28 post encapsulation, the percentage of viable cells decreased again. Encapsulated cells lacking nanoparticles revealed 65.7% of living cells (Fig. 4.12., black dots, 28 days after encapsulation), whereas co-encapsulated cells with S8 nanoparticles showed 80.9% viable cells (Fig. 4.12., gray square, 28 days after encapsulation). In capsules containing cells and S24 nanoparticles, 72.7% viable cells were detected (Fig. 4.12., bright gray triangles, 28 days after encapsulation). At day 28 in all capsules cells had grown to their highest density, which means that due to limited space and nutrient levels cell death rates increased. In summary, the percentage of viable cells determined in capsules lacking nanoparticles was found to be similar that of capsules containing cells and co-encapsulated nanoparticles. Thus it can be stated that co-encapsulation of nanoparticles did not have a negative influence on cell viability of encapsulated cells.

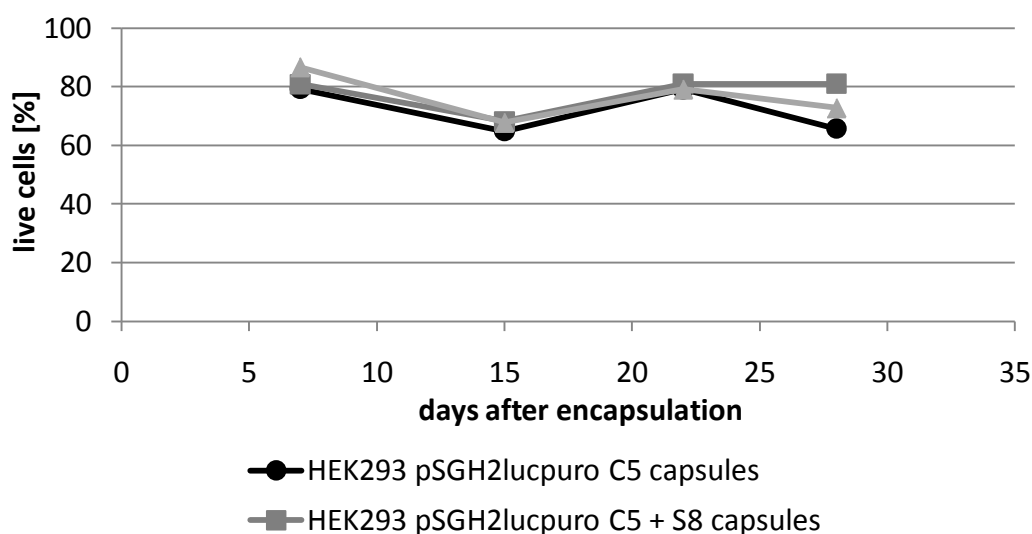


Fig. 4.12.: Viability of encapsulated cells during long-term cultivation.

Encapsulated cells were cultivated for four weeks. Cells were released from capsules on day seven, day 15, day 22, day 28 post encapsulation. Subsequently, calcein-AM staining was performed. Finally, fluorescent cells were analysed by quantitative FACS analysis using a FACScalibur (Becton Dickinson Biosciences).

To compare the growth of encapsulated cells, encapsulated HEK293 pSGH2lucpuro C5 cells with or without S8 and S24 nanoparticles were cultivated for 32 days.

Metabolic activity was determined by AlamarBlue™ assays. Then growth curves were determined (Fig. 4.13). The doubling time of encapsulated HEK293 cells during the exponential growth phase varied between 48 h (co-encapsulated S24 nanoparticles) and 72 h (co-encapsulated S8 nanoparticles or without nanoparticles). Metabolic activity increased continuously for a period of 28 days. Highest metabolic activities were measured in encapsulated HEK293 pSGH2lucpuro C5 cells without particles and in encapsulated HEK293 pSGH2lucpuro C5 cells with S8 particles. No statistically significant difference could be detected between growth curves of encapsulated HEK293 pSGH2lucpuro C5 cells lacking the particles and of encapsulated HEK293 pSGH2lucpuro C5 cells with S8 particles. In contrast, growth curve of encapsulated HEK293 pSGH2lucpuro cells with co-encapsulated S24 particles was significantly different; encapsulated cells entered a stationary phase already after 13 days.

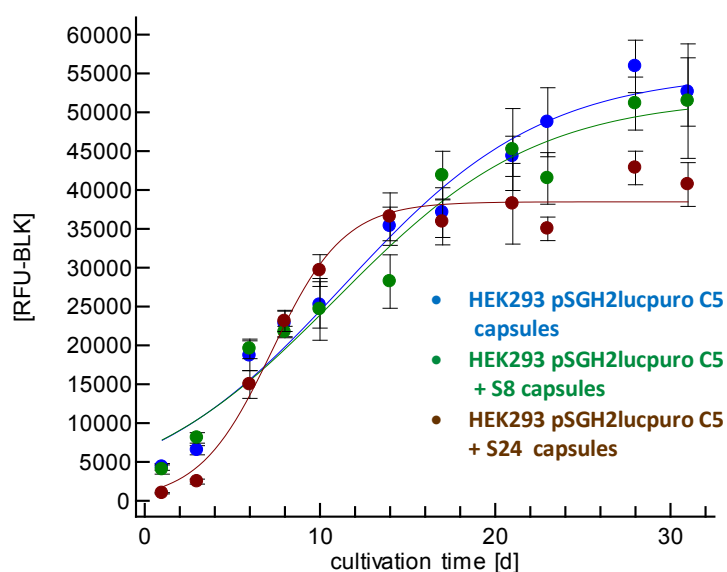


Fig. 4.13.: Metabolic activity of encapsulated cells during long-term cultivation with or without nanoparticles.

Encapsulated HEK293 pSGH2lucpuro C5 cells without nanoparticles (blue dots and blue curve) and with S8 nanoparticles (green dots and green curve) or with S24 nanoparticles (brown dots and brown curve) were cultivated for 32 days. Metabolic activity was determined by fluorometric AlamarBlue assays using multiwell formats measured by plate reader Tecan Genios.

Growth of encapsulated HEK293 pSGH2lucpuro C5 cells with and without S8 or S24 nanoparticles was microscopically documented. In the encapsulation process 2×10^6

cells/ml were used. This corresponded to a cell density of 600 cells per capsule on the day of encapsulation. One day after encapsulation few cells clumps are visible in the microcapsules (Fig. 4.14. A, B and C). As shown in figure 4.14. encapsulated cells with and without nanoparticles exhibited equal cell densities 14 days after encapsulation (Fig. 4.14. D, E and F). 28 days after encapsulation microcapsules were completely filled with cells (Fig. 4.14. G,H and I). This corresponded to a calculated cell number of 10^4 cells per capsule. The presence of nanoparticles in microcapsules appeared to result in no differences in the growth of encapsulated cells. Proliferation of encapsulated cells seemed not to be inhibited.

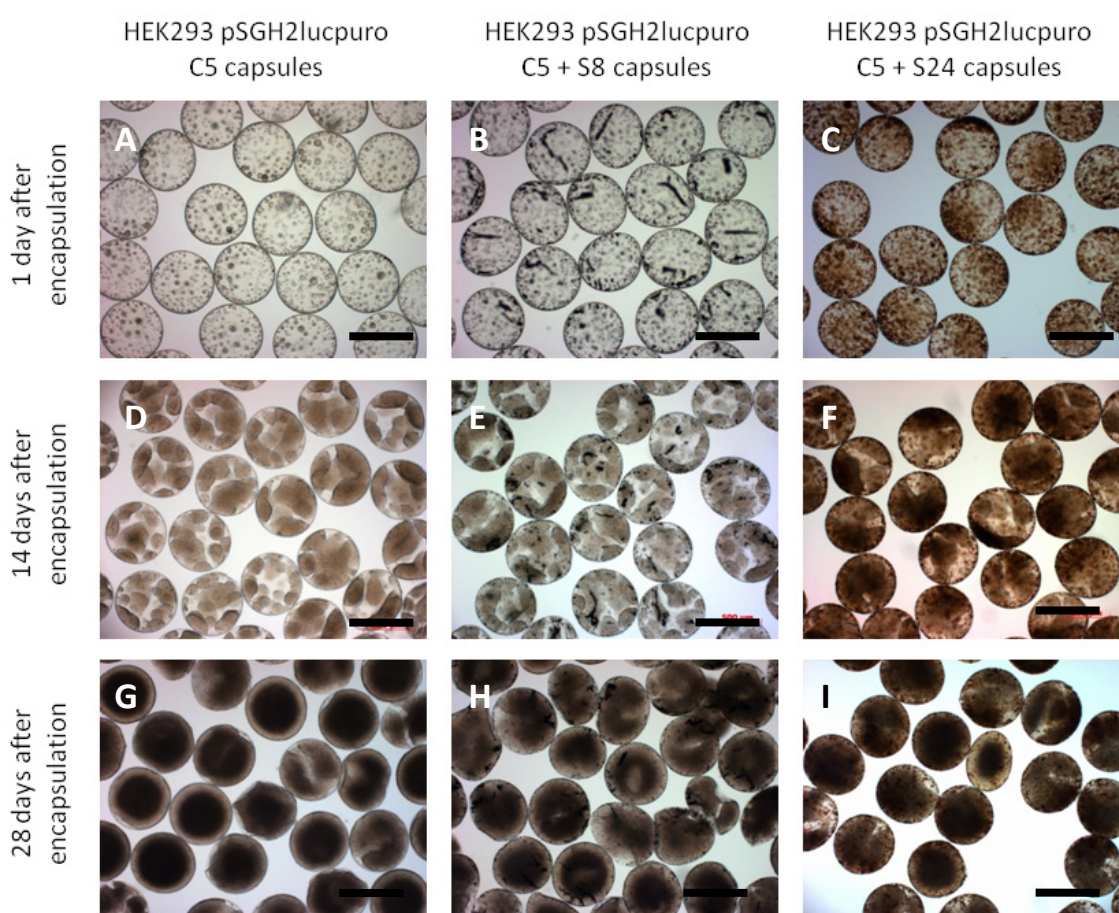


Fig. 4.14.: Growth of encapsulated cells with or without nanoparticles.

Encapsulated HEK293 pSGH2lucpuro C5 cells without nanoparticles (A, D, G) and with S8 nanoparticles (B, E, H) or with S24 nanoparticles (C, F, I) were cultivated for 28 days. Growth of encapsulated cells was microscopically documented one day, 14 days and 28 days after encapsulation using microscope Axiovert 200M (Zeiss, magnification 40-fold, scale bar 700 μm).

4.4.3. Characterisation of encapsulated cells with respect to heat inducibility

In this project heat-mediated induction of reporter gene expression in HEK293 cells co-encapsulated with two different types of nanoparticles should be demonstrated by means of incubation in an alternating magnetic field. In a first step, induction of reporter gene expression in encapsulated HEK293 pSGH2lucpuro C5 cells by heat treatment should be investigated.

Therefore, encapsulated cells were cultured for 21 days, which has been shown previously to be the optimal time point with respect to cell density and viability. The encapsulated cells were then heat-treated by incubation at 43°C for 1 h, 2 h and 3 h, respectively. Luciferase expression was measured after 6 h of recovery. Induction of luciferase was calculated as the ratio of luciferase expression in encapsulated cells in response to heat treatment compared to luciferase expression of encapsulated cells kept at 37°C. Expression levels of cells kept at 37°C were set to one and expression values were given relative to that (Fig.4.15. A). The level of luciferase expression in cells kept for 1 h at 43°C was found to be increased 397-fold, and up to 1586-fold in response to heat treatment for 2 h. A maximum of 1588-fold expression increase resulted from 3 h of heat treatment (Fig. 4.15. A). Thus, extending heat-treatment from 1 h to 2 h resulted in a further 4-fold increase of expression, whereas 3 h treatment in comparison to 2 h at 43°C did not further enhance luciferase expression. In addition to measurement of luciferase expression, EGFP expression in response to activation of the dual promoter was analysed. Therefore, encapsulated cells were incubated at 43°C for 1 h and subsequently microscopically investigated after 24 h of recovery. Fluorescence microscopic analysis revealed induction of EGFP expression in heat-treated cells within inspected microcapsules (4.15. E). No fluorescence was detected in encapsulated cells kept at 37°C (4.15. C).

Metabolic activity of encapsulated cells kept at 37°C before starting the heat treatment was set to 100% (Fig. 4.16.). The results demonstrated that metabolic activity of cells kept at 37°C was marginally changing during a period of four days. Two days after the heat treatment metabolic activity of encapsulated cells kept at 37°C was found to be decreased by 20% and then stayed stable over four days. In detail, the metabolic activity of encapsulated cells kept at 37°C was 83% of the initial activity two days after heat treatment and 81% of the initial activity four days after heat treatment. The metabolic activity of encapsulated cells incubated at 43°C for 1 h was found to be 87% two days after treatment. Then metabolic activity slightly decreased to 85% four days after heat treatment. The metabolic activity in encapsulated cells treated with 43°C for 2 h decreased to 76% of the initial activity two days after treatment. Then the metabolic activity increased to 98% four days after treatment. Analysis of metabolic activity revealed that incubation at 43°C for 3 h resulted in a strong decrease of metabolic activity down to 45 % two days after treatment. Furthermore, metabolic activity was found to be further decreased to 5 % of the initial metabolic activity four days after treatment (Fig. 4.16.). The decreasing metabolic activity was most probably due to cell death in response to the extended heat treatment. Thus 1 h and 2 h incubation at 43°C appeared to be well tolerated by encapsulated cells while 3 h incubation at this elevated temperature affected cell viability severely.

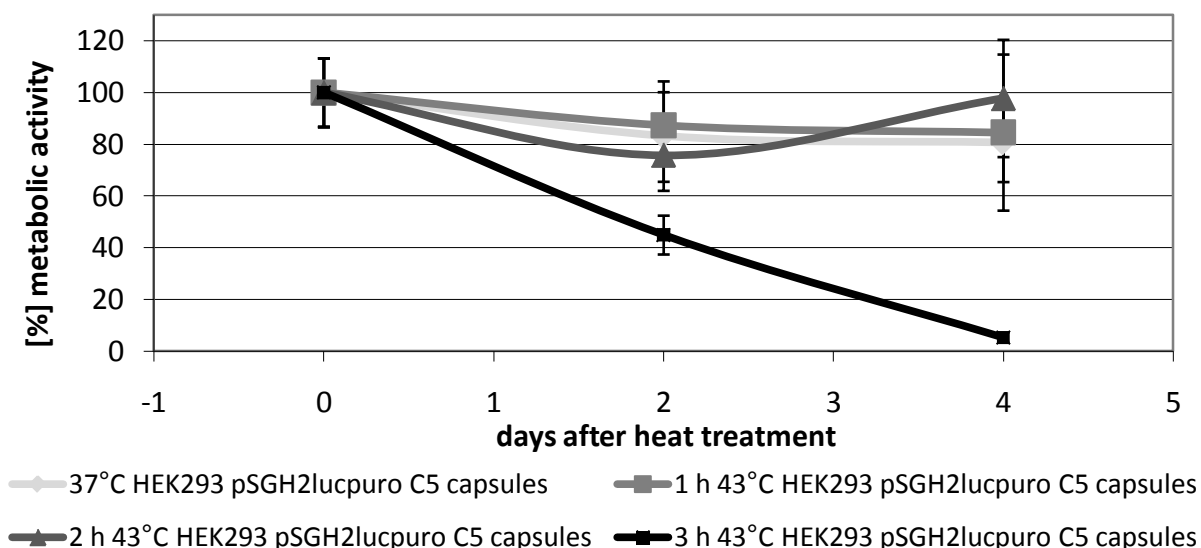


Fig. 4.16.: Effect of heat treatment on metabolic activity of encapsulated cells.

Encapsulated cells were either kept at 37°C or incubated at 43°C for 1 h, 2 h, and 3 h. Metabolic activity was measured by an AlamarBlue assay before, two days and four days after the different treatments. Assays were performed in 96-well formats and analysed using a Tecan Genios fluorometer.

In order to further determine inducibility of gene expression in encapsulated cells in response to heat treatment during long-term cultivation, encapsulated cells were cultured for four weeks and each week subjected to heat treatment followed by analysis of reporter gene expression. Therefore, encapsulated cells were heat-treated by incubation at 43°C for 1 h once a week and reporter gene expression was analysed by luciferase assay after 6 h of recovery also once a week. Again the luciferase expression level of cells kept at 37°C was set to one and hence the increase of luciferase expression in response to heat treatment for 1 h at 43°C is shown relative to this as x-fold induction.

The level of luciferase expression in encapsulated cells was decreased with an increasing time of cultivation (Fig. 4.17. A). Thus luciferase expression in treated cells was found to be 3021-fold increased in comparison to the expression levels of cells kept at 37°C in the first week of cultivation. In the second week, expression levels had already decreased to 2419-fold. Moreover, in the third week the expression levels of treated cells were further decreased to 408-fold and finally only an 18-fold induction was obtained in the fourth week of cultivation.

Looking at absolute measurements it was noticed that expression levels in cells kept at 37°C for the time of cultivation were raised above average in the last week of the experiment (4.17. C). This 160-fold increase of the basic level expression is most probably due to a stress response of the synthetic promoter resulting from hypoxia, because heat shock promoters can be induced by hypoxia (Taylor, et. al, 2010). Thus in consequence the relative induction values of heat-treated cells at this time point were also diminished (Fig. 4.17., A, 28 days post encapsulation). Because of this finding further induction experiments were performed at the end of the first week till the beginning of the third week of cultivation to ensure good responsiveness of expression of encapsulated cells upon heat treatment.

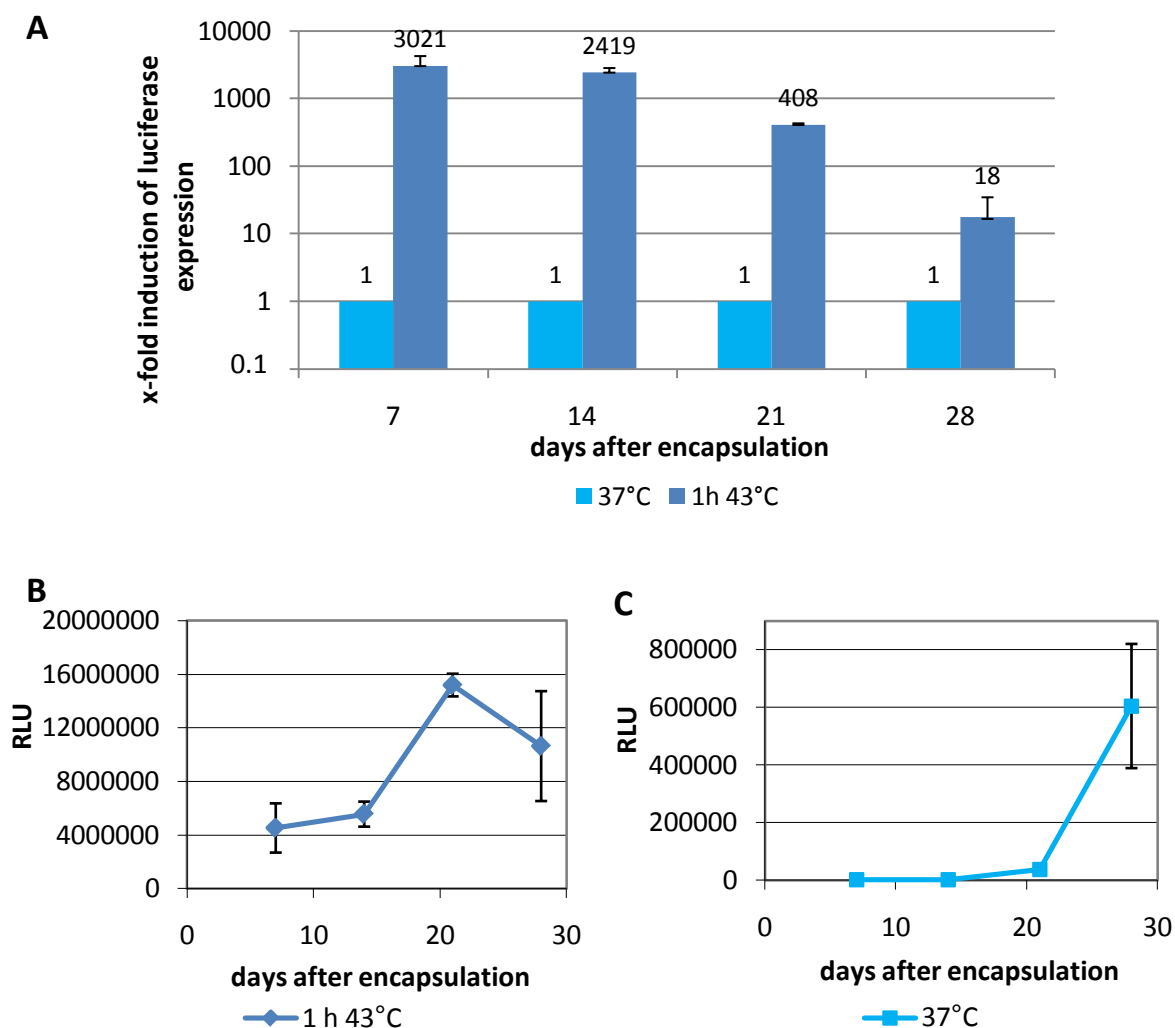


Fig. 4.17.: Induction of luciferase expression during long-term cultivation.

Encapsulated HEK293 pSGH2lucpuro C5 cells were incubated at 43°C for 1 h and luciferase expression was analysed after 6 h of recovery in cell lysates. Subsequently, measurement was performed with a luminometer (Berthold, LB9507). This experiment was performed during long-term cultivation of encapsulated cells for four weeks. Picture (A) shows x-fold induction of luciferase expression in response to heat treatment. Expression levels are given relative to expression levels of cells kept at 37°C. Absolute measurement values are given in relative luminescence values (RLU) in (B) and (C). Picture (B) shows induced expression in response to heat treatment. Picture (C) shows basic promoter expression of encapsulated cells cultivated at 37°C.

In order to investigate the possibility of repeated induction of gene expression in response to heat treatment, encapsulated cells were cultured and subjected to elevated temperatures several times. Therefore, encapsulated HEK293 pSGH2lucpuro C5 cells were treated by incubation at 43°C for 1 h in the first week of cultivation. One aliquot of capsules was taken for analysis of luciferase expression

and subsequently cell lysates were analysed after 6 h of recovery. In the following two weeks, same batch of capsules were treated equally and luciferase expression was analysed. Another batch of capsules was heat treated for the first time in the second week of cultivation and subsequently treated a second time in the third week of cultivation. Finally the third batch of capsules was treated by incubation at an elevated temperature in the third week of cultivation. The luciferase expression levels of cells kept at 37°C were set to one and hence the increase of luciferase expression in response to heat treatment for 1 h at 43°C is shown relative to this as x-fold induction.

In detail, a batch of encapsulated HEK293 pSGH2lucpuro C5 cells was treated by elevated temperature in the first week of cultivation and analysis of luciferase expression revealed an induction luciferase expression of 1464-fold (Fig. 4.18. dark blue bars). The same batch was treated with heat and analysed with respect to luciferase expression in the following two weeks. Luciferase expression level decreased to 406-fold (Fig. 4.18. dark blue bars) in response to heat treatment for the second time in the second week of cultivation. Furthermore, the luciferase expression level further decreased to 296-fold (Fig. 4.18. dark blue bars) in response to heat treatment for the third time in the third week of cultivation. Another batch of encapsulated cells was heat treated the first time in the second week of cultivation. Here, the analysis of luciferase expression level in encapsulated cells revealed an induction of 350-fold (Fig. 4.18. bright blue bars). Furthermore, luciferase expression level decreased to 152-fold (Fig. 4.16. bright blue bars) in the third week of cultivation in response to heat treatment for the second time. The last batch of encapsulated cells was subjected to elevated temperature in the third week of cultivation only. The expression level in response was 56-fold (Fig. 4.18. brightest blue bars) only in response to heat treatment for the first time in the third week of cultivation.

In summary, it can be stated that after multiple heat shock maximal luciferase expression decreases with increasing time of cultivation; induction at early time points after encapsulation results in higher expression levels compared to induction of longer cultivated encapsulated cells (Fig. 4.18.).

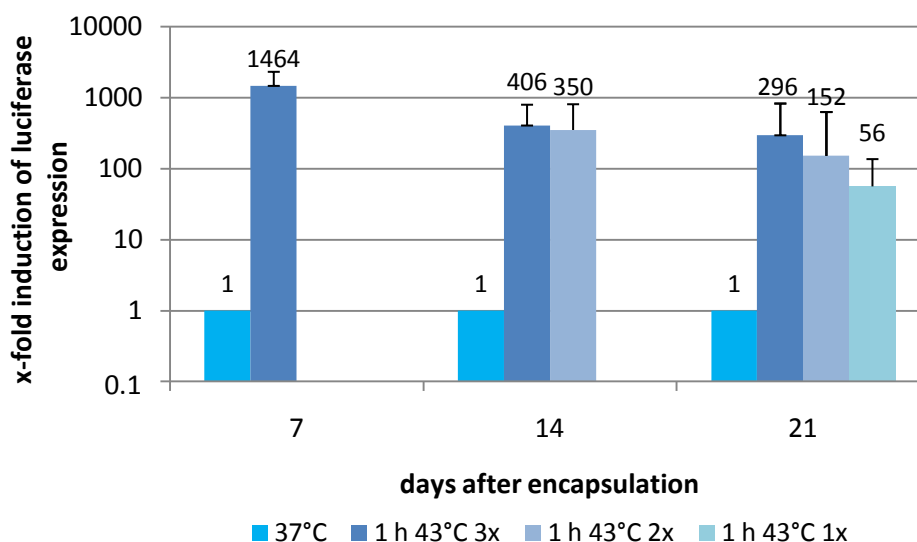


Fig. 4.18.: Multiple heat treatment during long-term cultivation of encapsulated cells.

Encapsulated HEK293 pSGH2lucpuro C5 cells were incubated at 43°C for 1 h. Luciferase expression was analysed after 6 h of recovery in cell lysates. Subsequently, measurement was performed with a luminometer (Berthold, LB9507). Encapsulated cells were repeatedly treated with 43°C for 1 h: either encapsulated cells were heat-treated in the first week and additionally in the following two weeks of cultivation (dark blue bars) or encapsulated cells were heat-treated in the second week and in the following week of cultivation (bright blue bars) or they were heat treated only once in the third week of cultivation (brightest blue bars).

To briefly sum up, with respect to localisation of nanoparticles it was shown that S8 nanoparticles are found in the capsules membrane, within the capsule lumen and moreover, can be taken up by the cell into the cytoplasm. The same was demonstrated for the S24 nanoparticles with the exception that these were also found to a certain extent in the nucleus. Furthermore, co-encapsulation of nanoparticles appeared to have no negative influence on cell viability. The analysis of reporter gene expression in encapsulated cells in response to heat treatment for up to 2 h revealed robust promoter activity. After heat treatment for two hours and more, gene expression levels were no longer increased. Heat treatment for 3 h caused almost a complete loss of metabolic activity within four days after heat induction most likely due to cell death. In addition, it could be shown that the inducibility of gene expression within encapsulated cells was decreased with increasing time of cultivation. This descent was maybe due to an increased basis level activity of the promoter at 37°C. Increasing time of cultivation most likely leads to hypoxic

conditions within the microcapsule caused by an increased cell density. This hypoxic stress might contribute to activation of the synthetic heat shock promoter (Taylor, et al., 2010). Furthermore, it could be shown that after multiple heat shock maximal luciferase expression decreases with increasing cultivation times and induction at early time points of cultivation results in higher expression levels compared to induction of encapsulated cells cultivated for longer periods. After this detailed characterisation encapsulated cells, it should now be further analysed the effects of magnetic field treatment with respect to cell integrity and cell viability.

4.5. Effects of magnetic field treatment on cell integrity and cell viability of encapsulated cells

According to the present knowledge, it is assumed that similar to tumour cells which are particularly sensitive to heat treatment (Jordan, A., et al., 2010), heat generation by means of magnetic nanoparticles exposed to an alternating magnetic field has also negative impact on cell integrity and cell viability of co-encapsulated HEK293 cells.

Here, electron microscopy was performed with encapsulated cells in order to investigate the effects of magnetic field treatment on cell integrity. Therefore, SCS microcapsules containing HEK293 pSGH2lucpuro C5 cells and co-encapsulated S8 or S24 nanoparticles were treated for 30 min in an alternating magnetic field with 60 kHz and 38 kA/m (Materials and Methods 3.2.6.). Samples were taken before and five days after magnetic field treatment, prepared for electron microscopy and microscopically analysed (Material and Methods 3.2.8.).

In magnetic field-treated microcapsules containing cells and S24 nanoparticles, most cells were found to be structurally intact and appeared to be viable five days after the treatment (Fig. 4.19. B). Analysis of electronmicrographs of capsules containing cells and S8 nanoparticles cultured five days after magnetic field treatment revealed areas with disrupted cells (Fig. 4.19. D, black arrows).

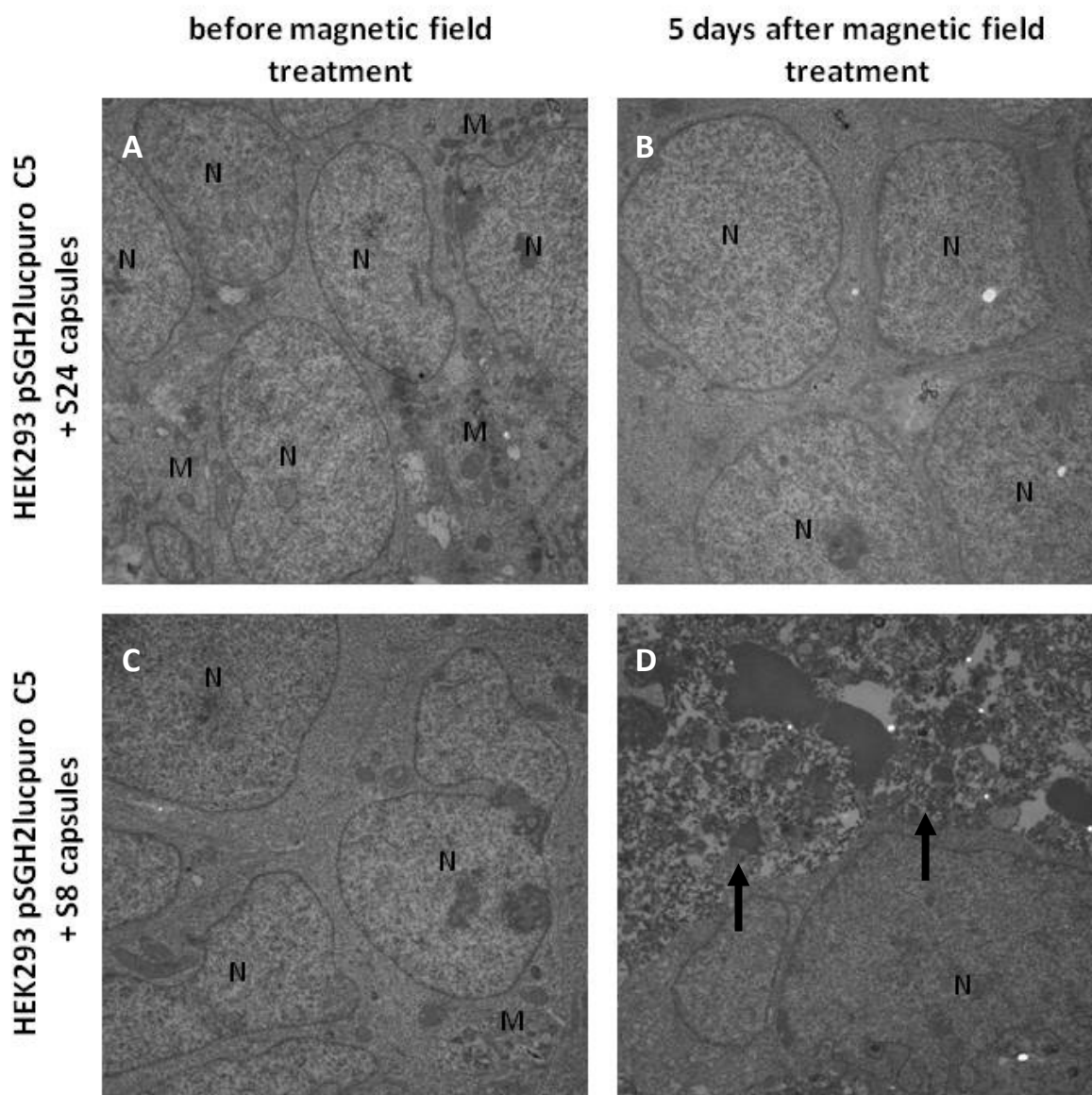


Fig. 4.19.: Effects of magnetic field treatment on integrity of encapsulated cells.

Encapsulated HEK293 pSGH2lucpuro C5 cells with S8 or S24 nanoparticles were exposed to a magnetic field with 38 kA/m and 60 kHz. Electron microscopic investigation of cell integrity was performed before and five days after magnetic field treatment using a EM900 transmission electron microscope (Zeiss). Picture A and B show electronmicrographs of encapsulated HEK293 pSGH2lucpuro C5 cells co-encapsulated with S8 nanoparticles. Picture C and D show electronmicrographs of encapsulated HEK293 pSGH2lucpuro C5 cells co-encapsulated with S24 nanoparticles. Pictures A and C show images before magnetic field treatment and pictures B and D show images five days after the treatment (magnification 3000-fold); (N = nucleus, M = mitochondrium, arrows = disrupted cells).

In order to further investigate effects of magnetic field treatment on nuclear integrity and cell viability, HEK293 cells co-encapsulated with nanoparticles were

histochemically analysed. Therefore, encapsulated HEK293 pSGH2lucpuro C5 cells with co-encapsulated S8 or S24 nanoparticles were treated by applying an alternating magnetic field with 60 kHz and 38 kA/m for 30 min. Samples were taken before magnetic field treatment and two days, five days and eight days after magnetic field treatment. Subsequently, samples were fixed with 2% formalin, embedded in paraffin and prepared for haematoxylin/eosin staining (Material and Methods 3.2.9).

Analysis revealed only few aberrant nuclei (Fig. 4.20. black arrows). No increase of aberrant nuclei of magnetic field-treated HEK293 pSGH2lucpuro C5 cells co-encapsulated with S8 (Fig. 4.20. A – D) or S24 nanoparticles (Fig. 4.20. E – H) could be detected compared to also magnetic field-treated encapsulated cell lacking the nanoparticles (Fig. 4.20. I – L). In samples with co-encapsulated S24 nanoparticles brownish aggregates of nanoparticles are visible (Fig. 4.20, G and H, red arrows).

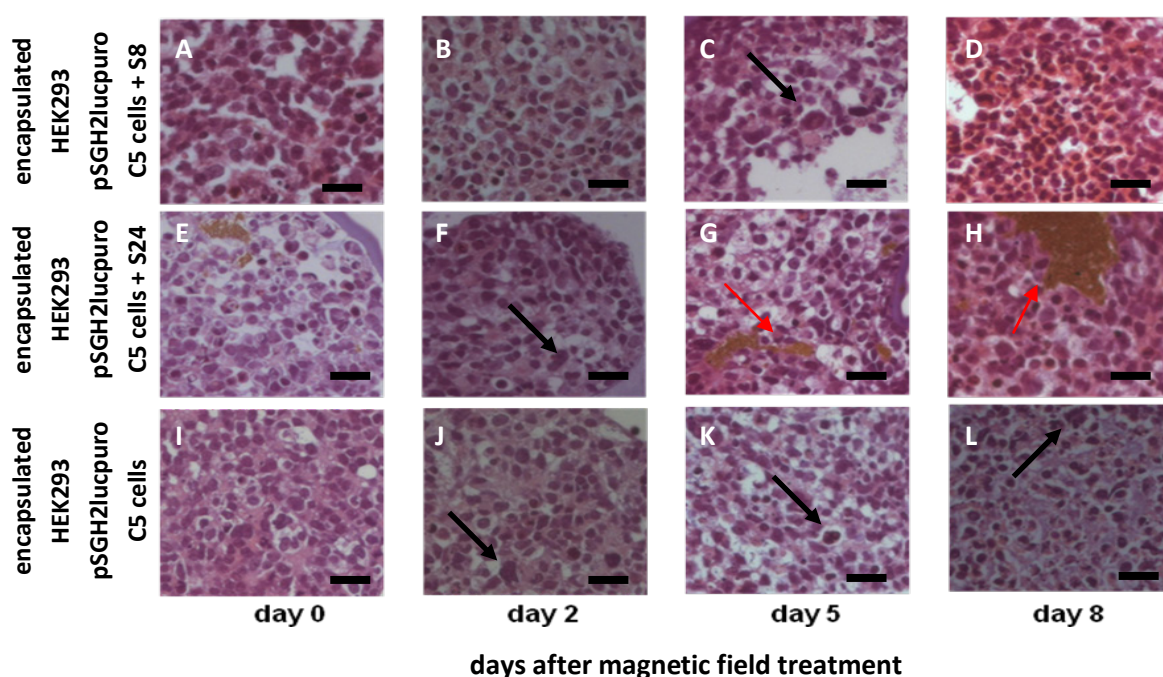


Fig. 4.20.: Effects of magnetic field treatment on nuclear integrity and cell viability. Histochemical analysis of encapsulated HEK293 pSGH2lucpuro C5 cells without (I – L) and with co-encapsulated S8 (A – D) and S24 (E – H) nanoparticles. Samples were taken before, two days, five days and eight days after incubation in an alternating magnetic field (38kA/m, 60 kHz, 30 min). Microscopic analysis was performed by 400-fold magnification with Axiovert 200M (Zeiss); (black arrows = aberrant nuclei, red arrows = nanoparticle agglomerations, scale bar 25 μ m).

In order to further investigate viability of encapsulated cells in response to magnetic field treatment, levels of apoptotic cell death were determined. Heat is generated by applying an alternating magnetic field to capsules containing HEK293 cells and co-encapsulated nanoparticles. At 42°C – 45°C apoptosis occurs (Dyson et al. 1986, Barry et al. 1990) and at temperatures above 45°C cells die by necrosis (Harmo et al. 1990). As recently published, apoptosis in response to heat treatment results from two mechanisms: either a fast process in which activation of MAP-kinases is involved, or a slow process in which the accumulation of aggregated proteins is involved (Bellmann, et al., 2010). In this study, HEK293 cells were heat-treated by incubation at an elevated temperature of 44°C for 120 min resulting in characteristic deformation (crumbled and crenated) nuclei indicating cytotoxic protein aggregation (Bellmann, et al., 2010).

Both pathways result in the activation of effector caspases as a late event in apoptosis. In the presented work, activation of the caspase 3 was investigated in response to magnetic field treatment. Therefore, to analyse effects on magnetic field-treated cells, encapsulated cells with and without nanoparticles were subjected to an alternating magnetic field with 38 kA/m and 60 kHz for 30 min. Magnetic field-treated encapsulated cells were fixed by incubation in formalin and embedded in paraffin before, two days, five days and eight days after magnetic field treatment. Finally, sections of 3 µm were prepared and immunohistochemically stained for activated caspase 3 using a specific monoclonal antibody. Staining was microscopically analysed, and the total number of cells as well as the number of caspase 3 positive cells was determined in three different regions of 3 µm sections (20000 µm²). Subsequently, the percentage of apoptotic cells was the calculated relative to total cell numbers.

In encapsulated HEK293 pSGH2lucpuro C5 cells lacking nanoparticles, 20.1% of cells were found to be positive for activated caspase 3 before treatment, 22.6% two days after treatment, 24.7% five days after treatment and 30.1 % eight days after treatment (Fig. 4.21 A, black bars). In encapsulated HEK293 pSGH2lucpuro C5 cells with S8 nanoparticles, 18.9% of cells were found to be positive for activated caspase 3 already before magnetic field treatment. Two days after magnetic field treatment, 19.1% of cells were shown to be apoptotic, five days after treatment 23.8% were

apoptotic and eight days after treatment 25.7% of cells were apoptotic (Fig. 4.21 A, gray bars). In capsules containing HEK293 pSGH2lucpuro C5 cells and S24 nanoparticles, 22.2% of cells were positive for activated caspase 3 before magnetic field treatment, 32.3 % of cells were positive for caspase 3 two days after treatment and 27.6% and 34% were shown to be apoptotic five days and eight days after magnetic field treatment (Fig. 4.21. A, dark grey bars).

In summary, more and more cells became apoptotic with increasing time of cultivation. Regarding the magnetic field treatment, only the difference between encapsulated cells lacking nanoparticles and encapsulated cells with S24 nanoparticles two days after treatment was statistically significant (Student's T-test with $p \leq 0.05$ Fig. 4.19 A).

In figure 4.21. B – G photographs of the analysed samples stained for caspase 3 are given. Encapsulated HEK293 pSGH2lucpuro C5 cells stained for caspase 3 showed only a slight increase in cells positive for activated caspase 3 comparing staining before magnetic field treatment (brown cells, Fig. 4.21. B) and staining two days after treatment (brown cells, Fig. 4.21. C). Cells co-encapsulated with S8 nanoparticles showed no increase of brown cells stained for activated caspase 3 when comparing samples taken before magnetic field treatment (Fig. 4.21. D) and samples taken two days after magnetic field treatment (Fig. 4.21. E). Encapsulated cells containing S24 nanoparticles were found to be increasingly stained for activated caspase 3 comparing the status before magnetic field treatment (brown cells, Fig. 4.21. F) and the status two days after magnetic field-treatment (Fig. 4.21. G).

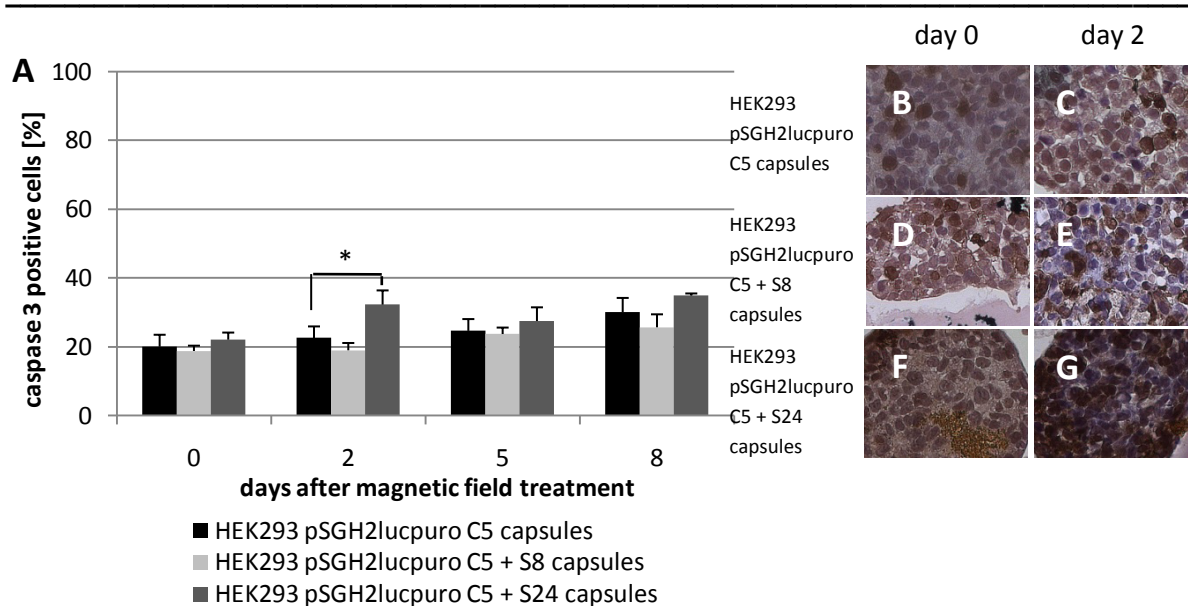


Fig. 4.21.: Apoptosis of encapsulated cells in response to magnetic field treatment.

Apoptosis was determined in sections prepared from SCS capsules containing HEK293 pSGH2lucpuro C5 cells co-encapsulated with S8 or S24 nanoparticles by immunohistological staining of activated caspase 3. Capsules containing cells only were used as a control. Samples were prepared before, two days, five days and eight days after their incubation in an alternating magnetic field with 38 kA/m and 60 kHz for 30 min. Stained cells were counted and percentage of apoptotic cells was calculated relative to total cell number. (A) Analysed percentages of apoptotic cells are depicted. (B and C) Stained for activated caspase 3 and microscopically analysed samples of encapsulated cells lacking nanoparticles before and two days after magnetic field treatment are given. Samples of cells co-encapsulated with S8 (D and E) or S24 nanoparticles (F and G) and stained for caspase 3 from day zero and two days after magnetic field treatment are shown.

In addition to determining the level of apoptosis by immunohistological staining of caspase 3, sections were analysed for the presence of fragmented DNA which is also an indication of late-stage apoptosis.

Encapsulated HEK293 pSGH2lucpuro C5 cells with and without S8 or S24 nanoparticles were subjected to a magnetic field with 38 kA/m and 60 kHz for 30 min (Fig. 4.22. A1 – L2). Then encapsulated cells were fixed with formalin before treatment, two days, five days and eight days after magnetic field treatment. Subsequently, encapsulated cells were embedded in paraffin and sectioned. Finally, TUNEL assay was performed (Materials and Methods 3.2.9.3.).

The TUNEL assay revealed some sporadic appearing nuclei positive for fragmented DNA (Fig. 4.22.). With the exception of the DNaseI treated positive control (Fig. 4.20. M2) a very low number of nuclei were stained for fragmented DNA was found in other

samples (Fig. 4.22. A2 – L2) The control, which was stained omitting digoxigenin-labelled dNTPs did not show any unspecific reactions (Fig. 4.22. N2). All pictures were taken with the same exposure time (2 sec) using a fluorescence microscope. This experiment may suffer from limitations of sensitivity of the performed TUNEL assay. Resulting from the low sensitivity of this assay, the number of nuclei positive for fragmented DNA could not be quantified.

After the investigation of the effects of magnetic field treatment on cell integrity and cell viability of encapsulated cells, the regulation of reporter gene expression in encapsulated cells *in vitro* by means of magnetic field and heat treatment should be analysed.

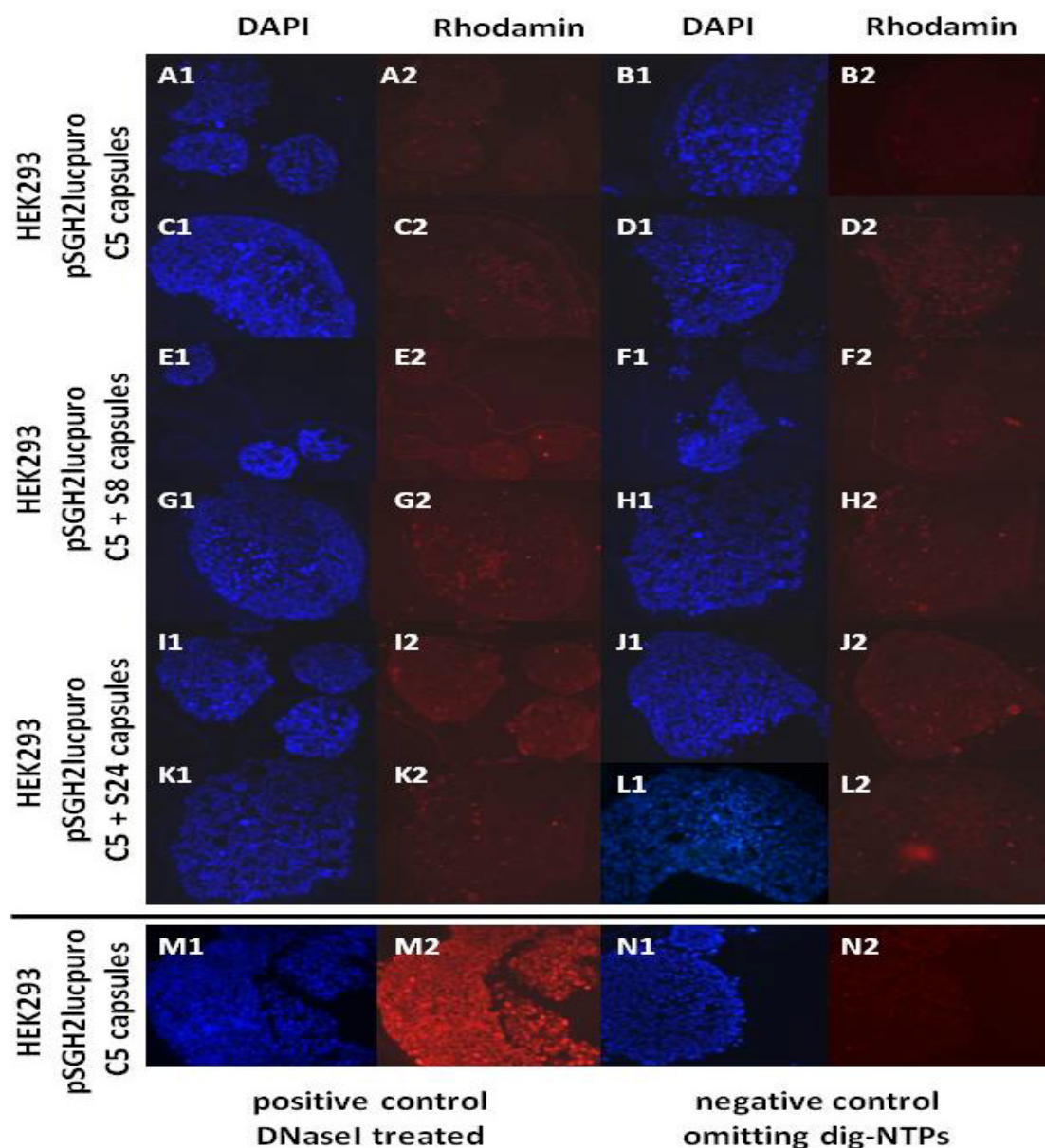


Fig. 4.22.: Apoptosis in response to magnetic field treatment in encapsulated cells.

Encapsulated HEK293 pSGH2lucpuro C5 cells with and without S24 and S8 nanoparticles were treated by incubation in an alternating magnetic field with 38 kA/m and 60 kHz for 30 min. Encapsulated cells with and without nanoparticles were fixed at day zero (A, E and I), day two (B, F and J), day five (C, G and K) and day eight (D, H and L) post magnetic field treatment. (A1 – D2) Co-encapsulated cells and S8 nanoparticles are depicted. (E1 – H2) Capsules carrying cells and S24 nanoparticles. (I1 – L2) Encapsulated cells without nanoparticles. (M1 and M2) Encapsulated cells DNaseI-treated as a positive control for fragmented DNA. (N1 and N2) Encapsulated cells stained omitting digoxigenin-labelled dNTPs as a negative control for background reactions. Microscopic analysis was performed with the fluorescence microscope Axiovert, 200M (Zeiss).

4.6. Magnetic field-induced nanoparticle-mediated gene expression in encapsulated cells

In order to proof the concept of this project – to proof the possibility of regulation of reporter gene expression by nanoparticle-mediated, magnetic field-directed heat induction – capsules containing genetically modified cells and respective magnetic nanoparticles were exposed to an alternating magnetic field.

For proof-of-principle experiments S8 nanoparticles were chosen only because they revealed the higher temperature increase in an alternating magnetic field compared to S24 nanoparticles (Fig. 4.3.). S8 nanoparticles appeared to exhibit a better biocompatibility as compared to S24 nanoparticles (Fig. 4.13). Additionally, they appeared to affect cell viability to a lower extent when subjected to an alternating magnetic field as compared to S24 nanoparticles (Fig. 4.21.).

Induction of luciferase expression in encapsulated HEK293 pSGH2lucpuro C5 cells in response to magnetic field treatment, i.e. 38 kA/m, 60 kHz and/or in response to heat treatment, i.e. incubation at 43°C, was analysed by luciferase assays.

Four independent experiments were performed with SCS microcapsules containing HEK293 cells which harboured the heat-inducible expression construct (HEK293 pSGH2lucpuro C5) either alone, or co-encapsulated with S8 nanoparticles (0.5 % w/w). As a control, HEK293 cells constitutively expressing luciferase were also analysed. The capsules were treated in three different ways: exposure to an alternating magnetic field with 38 kA/m, 60 kHz for 30 min or heat treatment by incubation at 43°C for 45 min or incubation at 37°C.

The increase of reporter gene expression in response to the different treatments was determined relative to the expression level of cells kept at 37°C. Therefore, expression of cells kept at 37°C was set to one and all other expression levels were given relative to this (Fig. 4.23.). Heat treatment resulted in a robust induction of luciferase expression in encapsulated cells, in the absence as well as in the presence of co-encapsulated nanoparticles (Fig. 4.23. dark blue bars). By contrast, the magnetic field treatment led to a strong induction of luciferase expression only when cells had been co-encapsulated with S8 nanoparticles (Fig. 4.23. red bars). In detail, incubation of encapsulated cells at 43°C for 45 min resulted in a 4539-fold increase

of luciferase expression in cells co-encapsulated with S8 nanoparticles and in a 4577-fold increase in cells encapsulated without nanoparticles. This finding demonstrated a robust heat inducibility of luciferase expression in the encapsulated cells. Application of an alternating magnetic field resulted in a 1758-fold increase in cells co-encapsulated with S8 nanoparticles. While, magnetic field treatment of encapsulated cells without nanoparticles only resulted in a 26-fold induction. This difference in the gene expression levels in encapsulated cells with and without S8 nanoparticles is highly significant (p-value of 0.029, Mann-Whitney-Test). In contrast, constitutive luciferase expression of HEK293 pCMVluc cells was not influenced, neither by magnetic field induction nor by incubation at 43°C (Fig. 4.23.).

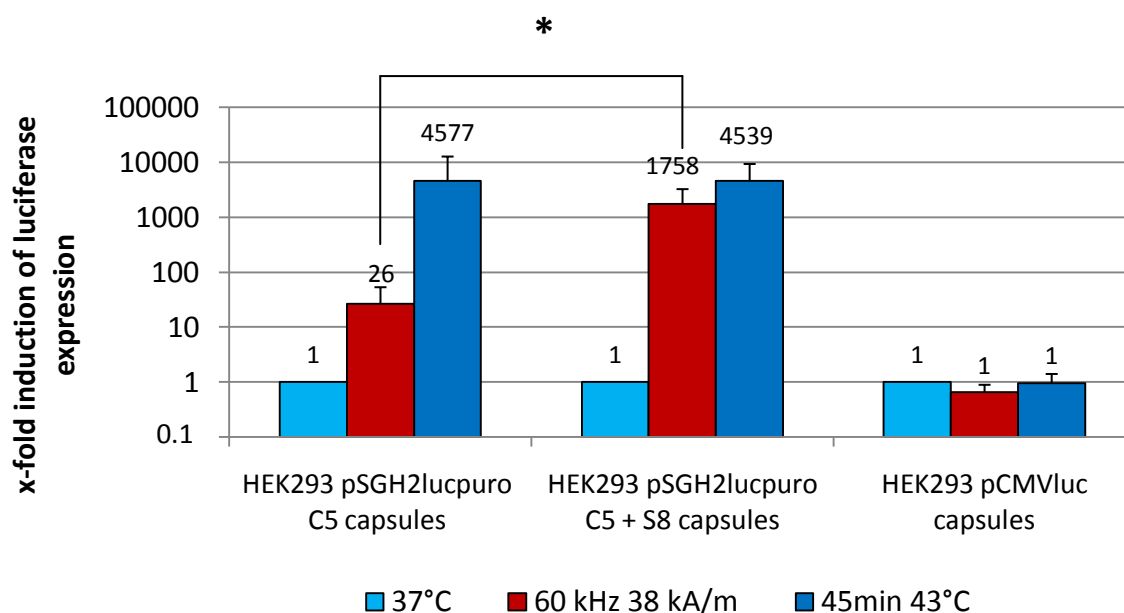


Fig. 4.23.: Magnetic field-directed, nanoparticle-mediated, thermoregulation of luciferase expression in encapsulated cells.

Encapsulated HEK293 pSGH2lucpuro C5 cells +/- S8 nanoparticles and HEK293 pCMVluc cells were either exposed to an alternating magnetic field with 38 kA/m and 60 kHz or incubated in a cell culture incubator at 43°C for 45 min or kept at 37°C. All luciferase expression values are given relative to the expression levels of cells kept at 37°C.

These data provided evidence that luciferase expression driven by the artificial heat shock promoter can be regulated by nanoparticle-mediated, magnetic field-directed heat induction within encapsulated cells. As previously mentioned, the used artificial

promoter is bidirectional and regulates the expression of two reporter genes. Here the regulation of the second reporter gene GFP should be investigated using an alternating magnetic field. Therefore, also induction of expression of GFP in encapsulated cells in response to magnetic field and/or heat treatment was determined by quantitative FACS analysis.

Again, capsules containing HEK293 pSGH2lucpuro C5 cells either alone or with co-encapsulated S8 nanoparticles (0.5 % w/w) were used in this experiment. As controls, encapsulated HEK293 pCMVluc cells constitutively expressing luciferase and encapsulated HEK293 pCMVegfp cells constitutively expressing EGFP were also analysed by FACS. As described before, the capsules were treated in three different ways: magnetic field treatment with 38 kA/m 60 kHz for 30 min or heat treatment at 43°C for 45 min or incubation at 37°C. For FACS analysis the cells were released from the microcapsules (Materials and Methods 3.2.7.2.).

As shown in figure 4.24., strong GFP expression was detected in cells released from capsules that had been incubated at 43°C for 45 min in comparison to cells kept at 37°C. Here, only little differences were observed when capsules containing cells and nanoparticles (17.69% GFP positive cells, table 4.2.) were compared to capsules harbouring cells only (17% GFP positive cells, table 4.2). In contrast, magnetic field treatment resulted in a high percentage of GFP positive cells (37.12% GFP positive cells, table 4.2.) in capsules containing cells and nanoparticles while encapsulated cells lacking nanoparticles revealed only a very low number of GFP expressing cells (0.40% GFP expressing cells, table 4.2.). Hence, capsules with nanoparticles showed a high expression of GFP in response to magnetic field treatment in contrast to capsules lacking nanoparticles. A high percentage of EGFP expressing cells (99.29% EGFP positive cells, table 4.2.) was detected in the positive control which consisted of constitutively EGFP expressing HEK293 cells. In contrast, no fluorescent (Table 4.2.) cells were detected in the negative control consisting of cells constitutively expressing luciferase.

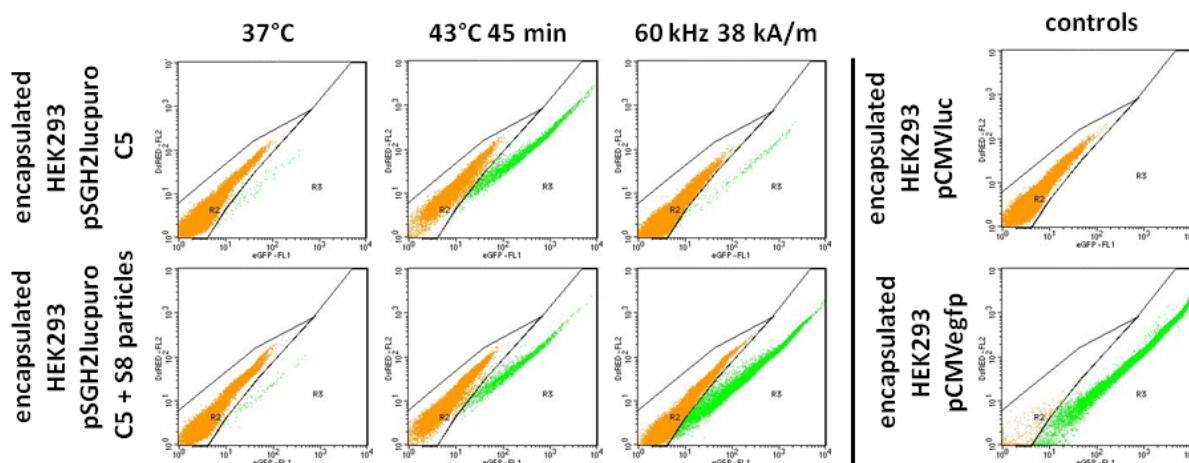


Fig. 4.24.: Magnetic field-directed, nanoparticle-mediated, thermoregulation of GFP expression in encapsulated cells.

Encapsulated cells were either incubated in an alternating magnetic field with 38 kA/m, 60 kHz for 30 min or incubated in a cell culture incubator at 43°C for 45 min or kept at 37°C. As controls were used encapsulated cells constitutively expressing EGFP and luciferase. Flowcytometry was performed using FACScalibure BD.

In table 4.2. raw data of the FACS analysis (percentage positive cells and mean fluorescence intensity (MFI)) is given. Expression levels were calculated by MFI multiplied with the percentage of positive cells. X-fold induction values are relative; the expression levels of cells kept at 37°C were set to one as a reference. Analysing induction levels differences were observed when capsules containing cells and nanoparticles (332-fold, table 4.2.) were compared to capsules harbouring cells only (956-fold, table 4.2). Magnetic field treatment resulted in high expression levels of GFP (805-fold, table 4.2.) in capsules containing cells and nanoparticles while encapsulated cells lacking nanoparticles revealed only a very low expression level of GFP (13-fold, table 4.2.).

Tab. 4.2: Magnetic field-directed, nanoparticle-mediated thermoregulation of GFP expression in encapsulated cells. (1)

Cells	treatment	number of positive cells [%]	MFI	MFI x number of positive cells [%]	x-fold induction
<i>HEK292 pSGH2lucpruro C5 capsules</i>	37°C	0.15	67.51	10	1
<i>HEK292 pSGH2lucpruro C5 capsules</i>	38 kA/m, 60 kHz	0.40	318.07	127	13
<i>HEK292 pSGH2lucpruro C5 capsules</i>	43°C	17.00	569.36	9679	956
<i>HEK292 pSGH2lucpruro C5 + S8 capsules</i>	37°C	0.27	72.01	19	1
<i>HEK292 pSGH2lucpruro C5 + S8 capsules</i>	38 kA/m, 60 kHz	37.12	421.61	15650	805
<i>HEK292 pSGH2lucpruro C5 + S8 capsules</i>	43°C	17.69	365.37	6463	332
<i>HEK293 pCMVegfp</i>	37°C	99.29	2359.54	234279	-
<i>HEK293 pCMVluc</i>	37°C	0.00	0.00	0	-

(1) Encapsulated cells +/- S8 nanoparticles were either incubated in an alternating magnetic field (AMF) with 38 kA/m and 60 kHz or incubated in a cell culture incubator at 43°C for 45 min or kept at 37°C. As controls, encapsulated HEK293 pCMVluc cells constitutively expressing luciferase and encapsulated HEK293 pCMVegfp cells constitutively, expressing EGFP were also analysed. FACS analysis performed with FACScalibur BD. (MFI = mean fluorescence intensity)

In summary, these data suggest that reporter gene – luciferase as well as GFP – expression in encapsulated cells can be switched on by nanoparticle-mediated heat induction using an alternating magnetic field. In an application of this concept the *de novo* production of a therapeutic protein can be switched on in encapsulated cells by the use of co-encapsulated nanoparticles and by applying of an alternating magnetic field. In the next chapter the potential application for an *in vivo* use was investigated by implanting encapsulated cells in the hind limb of mice.

4.7. Heat inducible expression in encapsulated cells

in vivo

After the described proof-of-principle of the proposed concept *in vitro*, inducibility of the reporter gene expression *in vivo* should be investigated by means of heat treatment of encapsulated cells implanted into mice. Aim of the experiment was to demonstrate luciferase as well as GFP expression in encapsulated cells implanted into the hind limb of mice in response to magnetic field treatment or in response to an increase in temperature.

In the *in vivo* experiment Hsd. athymic Nude-*Foxn1^{nu}* mice were used. 20 microcapsules of HEK293 pSGH2lucpuro C5 co-encapsulated with S8 nanoparticles (0.5% w/w) were implanted into the left hind limb. Mice were either subjected to a magnetic field with 38 kA/m and 60 kHz for 30 min or heat-treated by placing the leg on a 43°C warm heating plate for 15 min. For magnetic field treatment the left hind limb was placed within the coil whereas the remaining body was outside. For the induction experiments the mice were narcotised as described in Materials and Methods 3.2.10.2. Luciferase expression was measured 6 h after treatment and GFP expression was measured 24 h after treatment again by narcotising mice. Luciferase and GFP expression was visualised using a bio-imaging system IVIS 50 from Xenogen. For luciferase measurement 240 mg/kg D-Luciferin potassium salt was injected i.p. 15 min before anaesthesia and measurement. The luciferase measurement was performed by applying an integration time of 3 min. Fluorescence as a result of GFP expression was also measured. The induction experiments were performed once a week (Material and Methods 3.2.10.3).

Measured luminescence values are given in table 4.3. Image data analysis was performed with LivingImage (Igor Pro 4.09A) software. Values were acquired by measuring a standardised region of interest. Subsequently, normalised luminescence values were calculated by subtracting background luminescence values of a non-treated mouse (Table 4.3.). Moreover, relative expression levels in x-fold induction of expression were calculated by dividing measured luminescence values obtained from a heat-treated mouse by measured luminescence values of a non-treated mouse (Table 4.3.).

The experiment revealed luciferase expression in response to heat treatment in two out of six mice. In these two mice luciferase expression was inducible once a week over a period of three weeks (Fig. 4.25.). In detail, the mouse E10 which had been exposed to 43°C for 15 min, revealed an expression level of 3.05E+05 photons/sec indicating heat-induced luciferase expression of implanted encapsulated cells in the first week of investigation. One week later, the implanted and again heat-treated encapsulated cells of this mouse resulted in an increase in the emitted luminescence to 5.41E+05 photons/sec. Another week later, the luminescence of implanted encapsulated cells in the mouse E10 was decreased to 3.08E+05 photons/sec (Fig. 4.25. A and Table 4.3.). In the mouse C3 which had also been treated with 43°C for 15 min, the implanted encapsulated cells emitted 7.37E+04 photons/sec indicating luciferase expression in response to heat treatment in the first week. In the second week of investigation, the luminescence of implanted heat-treated encapsulated cells was increased to 1.46E+05 photons/sec. The luminescence of the implanted and heat-treated encapsulated cells was further increased to 6.77E+05 photons/sec in the third week of investigation (Fig. 4.25. B and Table 4.3.).

Tab. 4.3.: *In vivo* thermoregulation of luciferase expression in encapsulated cells implanted into mice. (1)

mouse (id no.)	week	treatment	Measured photons/sec	normalized photons/sec	x-fold induction
E10 male	1	43°C 15 min	3.78E+05	3.05E+05	5.2
E10 male	2	43°C 15 min	6.34E+05	5.41E+05	6.8
E10 male	3	43°C 15 min	3.74E+05	3.08E+05	5.6
C3 female	1	43°C 15 min	1.47E+05	7.37E+04	2.0
C3 female	2	43°C 15 min	2.39E+05	1.46E+05	2.5
C3 female	3	43°C 15 min	7.44E+05	6.77E+05	11.2
C5 male	1	non treated	7.33E+04	0	1
C5 male	2	non treated	9.31E+04	0	1
C5 male	3	non treated	6.62E+04	0	1

(1) Left hind limb with implanted encapsulated cells was treated with 43°C for 15 min on a heating plate. Luminescence data was acquired by bio-imaging system IVIS50 (Xenogen).

Thus heat-inducible luciferase expression in encapsulated cells could be demonstrated *in vivo*. However, no GFP expression could be detected because of the lower sensitivity of the fluorescence measurement. Moreover, no reporter gene expression could be induced by applying an alternating magnetic field. This may

result from to fast temperature exchange with the surrounding tissue in contrast to the situation set for the *in vitro* proof-of-principle.

Nevertheless, in summary these data provided evidence that the reporter gene expression in encapsulated cells can be switched on by heat *in vivo*. All *in vivo* experiments were performed according to the regulations of the Austrian law governing animal experimentation (Animal experiment application at the Austrian Ministry for Science and Research BMWF-68.205/0213-II/10b/2009).

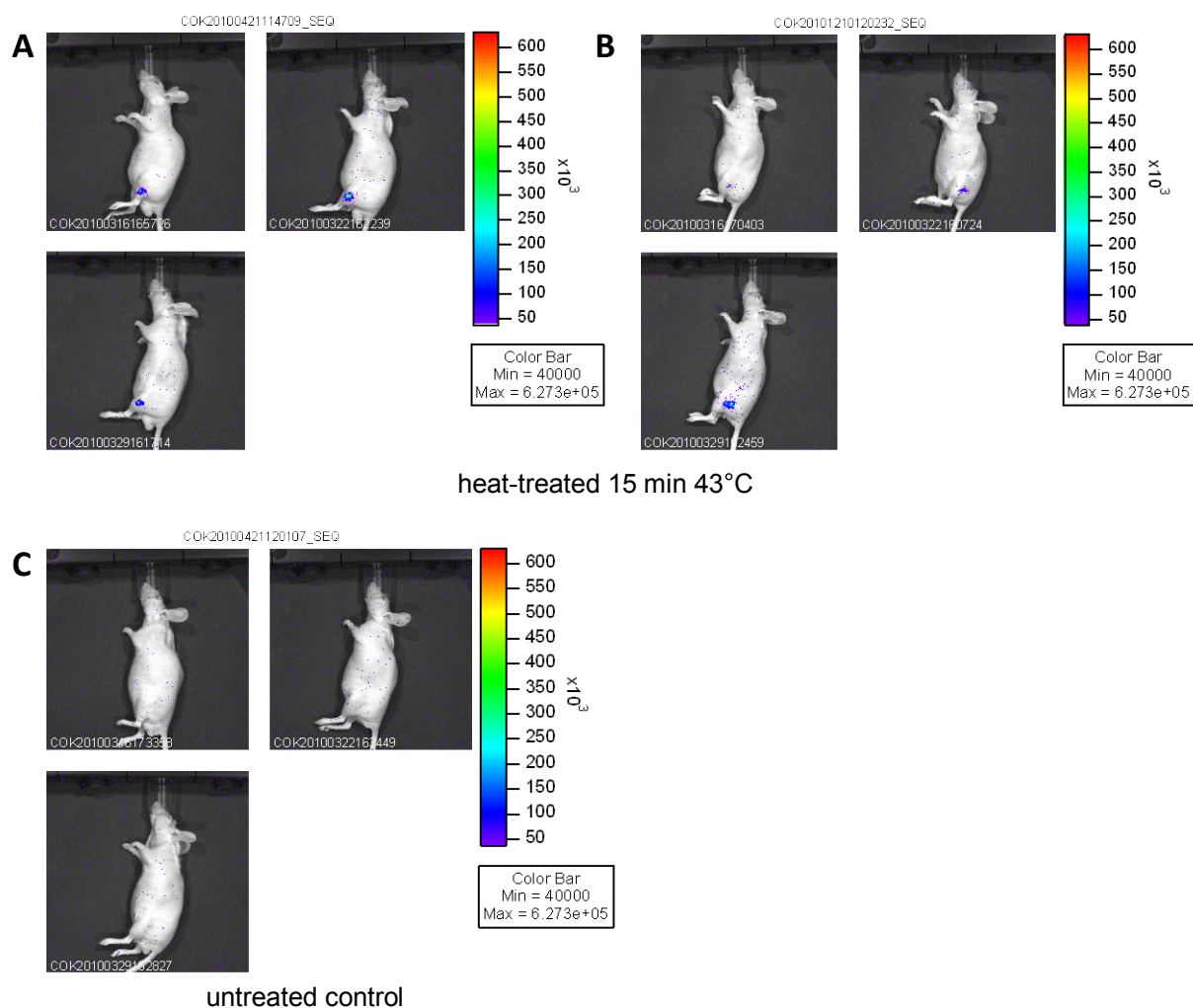


Fig. 4.25.: *In vivo* imaging of luciferase expression in implanted encapsulated cells.

20 capsules containing HEK293 pSGH2lucpuro C5 cells and S8 nanoparticles were implanted into the left hind limb of Hsd. athymic Nude-*Foxn1*^{nu} mice. Magnetic field treatment was performed with 38 kA/m and 60 kHz for 30 min and heat treatment was performed by placing the limb on a heating plate at 43°C for 15 min. Luciferase expression was measured 6 h after recovery. Using an IVIS 50 (Xenogen) bio-imaging device, measurement of luciferase expression was performed once a week during a period of three weeks. Pictures in A and B show bio-imaging results of luciferase expression in response to heat treatment in two mice. Pictures in C show one of the untreated control mice.

4.8. Summary of the results

In this project genetically modified HEK293 pSGH2lucpuro C5 cells were characterised regarding inducibility of expression in response to heat. Expression analysis of heat-treated cells revealed robust induction of luciferase as well as EGFP expression.

Furthermore, a set of different nanoparticles was characterised with respect to parameters relevant in this project: their heat generation capacity in an alternating magnetic field and their ability to be encapsulated. According to these criteria, S8 and S24 nanoparticles were selected for further experiments.

Microcapsules generated by co-encapsulation of cells and S8 or S24 nanoparticles were analysed with respect to important physical capsule parameters such as size, diffusion properties and membrane thickness. The different SCS concentrations applied for co-encapsulation of cells and nanoparticles had no influence on the capsule diameters, capsule diffusion properties and membrane thickness, three characteristics important for viability of encapsulated cells.

Furthermore, biological characteristics of encapsulated cells were analysed. Nanoparticle localisation with respect to encapsulated cells was investigated, taking the original use of the nanoparticles into considerations, which have been designed for magnetotransfection. Electron microscopic analysis revealed that nanoparticles were taken up by cells into the cytoplasm (S8 and S24 nanoparticles) and also to a certain extent into the nucleus (S24 nanoparticles). Encapsulated cells were further characterised regarding biocompatibility of nanoparticle formulations as well as heat inducibility. Analysis of biocompatibility revealed acceptable tolerability of nanoparticles. Viability of encapsulated cells is most likely more influenced by growth conditions within capsules. Proliferation of encapsulated cells was not affected by the presence of nanoparticles. However, metabolic activity of encapsulated cells was diminished by the presence of S24 nanoparticles during long-term cultivation. Investigation of heat inducibility of reporter gene expression in encapsulated cells revealed continuous inducibility for four weeks of cultivation as well as the possibility of multiple induction of expression during three weeks of cultivation. The survival of encapsulated cells after magnetic field treatment was investigated. The analysis

revealed that apoptosis in response to magnetic field treatment was transiently increased two days after treatment only in samples harbouring S24 nanoparticles. Analysis of necrosis in response to magnetic field treatment showed no increase of aberrant nuclei in capsules containing nanoparticles. Proof-of-principle for the proposed novel cell therapy concept could be provided *in vitro* by magnetic field-directed, nanoparticle-mediated heat induction of reporter gene expression in encapsulated cells. Additionally, preliminary *in vivo* experiments confirmed repeated heat-inducible expression of encapsulated cells implanted into mice, a relevant result for future therapeutic approaches.

5. DISCUSSION

Many acquired and inherited human diseases are mediated by absence or deregulation of gene products. Cell therapy offers a simple replacement strategy for the respective gene products. For the treatment of most diseases however, regulated gene expression is needed. Here, externally controlled expression levels of therapeutic genes would be of advantage.

The aim of the presented study was to develop a novel cell therapy concept in which gene expression of encapsulated cells should be thermo-regulated by means of co-encapsulated nanoparticles generating heat in response to an external induction, i.e. an alternating magnetic field. This concept should be evaluated *in vitro* as well as *in vivo*.

This interdisciplinary study targets aspects of molecular biology, biotechnology and nanotechnology. To realise the proposed concept, the different components used needed to be characterised with respect to their applicability. The main components were:

- genetically modified cells,
- nanoparticles,
- encapsulation technology,
- inducibility of gene expression and
- magnetic field generation.

By characterising and further combining these components, a novel cell therapeutic concept can be realised enabling a cell-based therapy with spatial and temporal regulateable gene expression, facilitating treatment of diseases in which the amount and time point of expression of a therapeutic substance is critical. In the following section the different components and their combination will be discussed with regard to a potential future cell therapy approach.

Genetically modified cells

A heat-inducible synthetic and bidirectional promoter which had been developed based on the human HSP70 promoter by Bajoghli and colleagues in 2004 (Bajoghli, et al., 2004) was initially used in order to regulate gene expression during fish development.

In the presented study, this bidirectional promoter was inserted between two reporter genes, GFP and luciferase, facilitating distinct analysis of gene expression. This construct (pSGH2lucpuro) was transfected into HEK293 cells and a stable cell clone was selected.

The expression levels of luciferase and GFP in response to heat treatment were analysed in the cultured cell clone. Measurement of expression revealed a robust induction of reporter gene expression (Fig. 4.1. A). Moreover, induced luciferase expression levels were increased in correlation with the heat treatment. Quantitative FACS analysis of GFP positive cells also showed induction of the respective reporter gene in response to elevated temperatures (Fig. 4.1. B). Here the expression levels were increased from 1 h to 2 h of heat treatment and then the expression level was decreased in response to heat treatment for 3 h most likely due to cell death 24 h after induction as shown for encapsulated cells in Fig. 4.16. that heat treatment of 3 h decreases viability.

In summary it can be stated that two different genes regulated from the same bidirectional promoter can differ in their expression kinetics because of different transcription and translation efficacy due to different processing, stability and degradation. The luciferase protein is less stable whereas the GFP protein is more stable and hence accumulates.

The synthetic bidirectional promoter applied here can be used for a spatial and temporal regulation of potential therapeutic genes to accomplish a novel cell-based therapy concept: magnetic field-directed, nanoparticle-mediated thermoregulation of gene expression within encapsulated cells. This will be evaluated by means of reporter genes *in vitro* as well *in vivo* to provide evidence for a potential future cell-based therapy approach.

Nanoparticles

In order to generate heat within microcapsules by applying an alternating magnetic field, a set of 13 magnetite-based nanoparticles was evaluated in this study. These particles were analysed with respect to their heat generation capacity in an alternating magnetic field. According to these results (Fig. 4.3), two ferromagnetic particles and one superparamagnetic particle were selected for further investigations. S8 nanoparticles with a diameter of 74.1 nm and Sigma nanoparticles with a diameter of 30 nm were ferromagnetic and S24 nanoparticles with a diameter of 12 nm were superparamagnetic. The calculated size of a single domain magnetite particle is 18.7 nm (Atsumi, et al, 2007). Heat is generated by both ferromagnetic and superparamagnetic particles in an alternating magnetic field, even though the physical mechanisms of heat generation are different. It has been reported that the hysteresis loss-induced heating depends on the larger magnetic multi-domain (ferromagnetic) particles while smaller (superparamagnetic) particles consisting of a single domain structure are inducing heat by relaxation loss (Mornet, et al., 2004).

In figure 5.1. temperature increase of the applied set of nanoparticles subjected to an alternating magnetic field is depicted in correlation to their core diameter. According to these results particles with a core size of 50 nm would provide the maximum heat generation capacities. This is in accordance with the results of Ma and colleagues showing that the specific absorption rate (SAR) is highest in particles around 50 nm (Ma, et al., 2004). However, to predict the heat generation capacity of a nanoparticle formulation in an alternating magnetic field, also the specific surface area (SSA) of the particle has to be taken into account (Motoyama, et al., 2008).

In dispersions of 1% the S8 nanoparticles exhibited a temperature increase of 27.8°C, the S24 nanoparticles showed a temperature increase of 23°C and the nanoparticles from Sigma yielded a temperature increase of 28.4°C. In matters of their application in this concept all selected particles were sufficient to cause an absolute temperature increase above 43°C and therefore met requirements for heat-induced gene expression within the generated genetically modified cells.

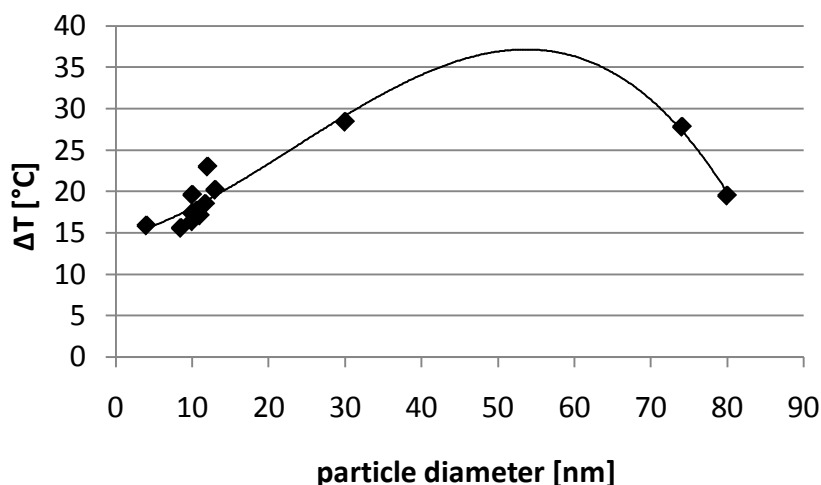


Fig. 5.1.: Heat generation capacity of a set of nanoparticles with different core sizes. Nanoparticle dispersions (1% w/w) in PBS were subjected to an alternating magnetic field with 38 kA/m and 60 kHz for 30 min and temperature increases were determined.

Encapsulation technology

By employing described HEK293 pSGH2lucpuro C5 cells and selected nanoparticle formulations, co-encapsulation was developed. Therefore, the three selected nanoparticles were analysed with respect to their aggregation tendency. The particles from Sigma could not be encapsulated even at low concentrations because of their high aggregation tendency. They formed particle-clusters up to 100 μm in size (Fig. 4.4). Subsequently they blocked the nozzle of the used encapsulation device. In contrast to this, coated S8 and S24 particles could be encapsulated in concentrations up to 0.5% (w/w). The co-encapsulation of S8 and S24 nanoparticles and cells was successfully established by modifying already existing encapsulation parameters previously established in our laboratory (Hauser, et al., 2004). Due to higher viscosity of nanoparticles in SCS, encapsulation parameters were adjusted to 1.6 % SCS instead of 1.8 % SCS. This modification of encapsulation parameters for the co-encapsulation of cells and nanoparticles had no impact on capsule diameter, capsule membrane diffusion properties, and membrane thickness of the capsules (Chapter 4.3.1. Fig. 4.6 – Fig. 4.9.).

These parameters are particularly important for the potential biological application of such a cell-based therapy system. In implanted encapsulated cells therapeutic peptides and proteins are produced *de novo* at the site of therapeutic relevance without the rejection of cells by the host's immune system. The capsule diameter is important since it determines the space cells can occupy within the microcapsule and it hence defines the biological power of implanted capsules. The addition of cells and nanoparticles resulted in higher viscosity of the SCS/cell/nanoparticle mixtures. Hence SCS concentration was reduced for the co-encapsulation of cells and nanoparticles. This in turn resulted in equal diameters of capsules of containing cells and nanoparticles compared to standard 1.8 % SCS 700 μm capsules lacking nanoparticles. The standard capsules have been previously shown to be effective for the treatment of xenograft tumours in the mouse model (Löhr, et al., 2001). In this therapy concept cytochrom P450 derived from encapsulated genetically modified cells converts Ifosfamide into a cytotoxic drug. The cytotoxic drug is reaching the tumour by diffusion via the capsule membrane. Here, the pore size of the hydrogel membrane is a critical parameter. It determines the diffusion of the therapeutic substance, the exclusion of the detrimental influx of host immune cells, and free diffusion of nutrients as well as export of metabolic waste. In alginate-based hydrogels the pore size of capsule membranes can vary over a huge range between 5 to 200 nm (Schmidt, et al., 2008). However, using SCS capsules we determined the molecular cut-off limit between 70 kDa and 250 kDa equating a pore size of 11 to 45 nm. No differences in FITC-dextran diffusion could be detected in the different capsules manufactured with different percentages of SCS as well as with and without S8 and S24 nanoparticles. This result indicates that therapeutic peptides and proteins as well as nutrients with a molecular weight up to 70 kDa can pass the membrane, whereas larger molecules such as antibodies (e.g. IgG = 150 kDa) might be excluded from entering the capsule. In order to define more precisely the upper limit of exclusion a better resolution would be needed.

Moreover, the membrane thickness was demonstrated to be 35 μm irrespective of the SCS concentration and the co-encapsulation of S8 or S24 nanoparticles, meaning that diffusion speed also appears to be equally effective.

In general, the requirements microcapsule technology (reviewed in Rabanel, et al., 2009) has to meet are:

- material biocompatibility: material should be totally biocompatible, not influencing homeostasis of encapsulated cells and of surrounding tissue and not causing an immune response of the host;
- mechanical stability: microcapsules should resist physical and osmotic stress;
- microcapsule permeability: microcapsules should have a defined permeability in terms of entry and exit of molecules;
- microcapsule membrane size: the thinner the membrane is, the faster the nutrients and waste can diffuse;
- a gentle encapsulation technique: aqueous medium without no reactive components or organic solvents should be used;
- durable microcapsules material: material degradation should be avoided to enable long-term *in vivo* use;

Considered requirements were achieved by reproducible microencapsulation technology using biologically inert SCS as demonstrated by a successful utilisation in a phase I/II clinical trial in 2000 (Vienna, Austria) for the treatment of inoperable pancreatic cancer (reviewed by Salmons, et al., 2010). In the clinical trial 14 patients which suffered from pancreatic cancer were treated (Löhr, et al., 2001, Löhr, et al., 2003). The findings of this study (reviewed by Salmons, et al., 2010) were that the application of the encapsulated cells by an angiographic route was safe, that the encapsulated cells were well tolerated and no evidence for inflammatory or immune reactions could be found. No major toxicities were associated with the low dose of ifosfamide that was used (Löhr, et al., 2001, Löhr et al., 2003). The benefit of this clinical trial (reviewed by Salmons, et al., 2010) was that quality of life was improved for most patients. Tumour reduction was seen in four patients and ten patients showed stable disease. Overall a 100 % improvement of the median survival time was found compared to the control group and 1 year survival rates were shown to be two times higher as documented for the treatment with the gold standard, gemcitabine (Löhr, et al., 2001, Löhr et al., 2003).

Further, the biological characterisation of the here used encapsulated cells should be discussed. The above described parameters – capsule diameter, membrane thickness and molecular cut-off limit of the capsule membrane – influence in general the viability of encapsulated cells. Hence, the viability of encapsulated cells during long-term cultivation in the presence of co-encapsulated nanoparticles was investigated within the current work. In figure 4.12. the viability of cells co-encapsulated with magnetic nanoparticles is shown for the period of four weeks. Encapsulated cells with and without S8 and S24 nanoparticles did not differ in their viability. This finding is in agreement with previous studies stating that magnetite is minimally toxic (reviewed by Häfeli, U., et al., 2009). This is also emphasised by the FDA approval of magnetite particles as an MRI (magnet resonance imaging) contrast agent (Häfeli, U., et al, 2009). Moreover, as reported by Häfeli and colleagues magnetic nanoparticle concentrations of 5 mg/ml ($\approx 0.5\%$), which were also used for the evaluated microcapsules, did not disturb cell proliferation of endothelial, epithelial and tumour cells (Häfeli, et al. 2009). During long-term cultivation, viability of encapsulated cells appeared to be more influenced by the capsule microenvironment: In the first days post encapsulation, cell viability was decreasing most probably because cells suffered during the encapsulation process and had to get used to grow in a 3D network within the microcapsule. Two weeks after encapsulation, cells started to recover and viability was increasing till the fourth week of cultivation. Then cell viability stagnated or decreased again because of the limited space within the microcapsule. Finally, a balance of cell death and cell division is established within the microcapsule. Therefore, from the obtained result may be concluded that co-encapsulation of magnetite nanoparticles appears to have no negative influence on cell viability during long-term cultivation. As shown in figure 4.14., proliferation of encapsulated cells was not disturbed by the presence of 0.5% magnetic nanoparticles during a period of cultivation for four weeks, as predicted by Häfeli and colleagues (see above). Furthermore, metabolic activity of cells co-encapsulated with magnetic nanoparticles S8 and S24 was analysed and growth curves were determined (Fig. 4.13). The doubling time of encapsulated HEK293 cells during exponential growth phase varied between 48 h (co-encapsulated S24 nanoparticles) and 72 h (co-encapsulated S8 nanoparticles or without nanoparticles).

Encapsulated HEK293 pSGH2lucpuro C5 cells lacking the particles and encapsulated HEK293 pSGH2lucpuro C5 cells with S8 particles showed similar metabolic kinetics. In contrast to this, the curve determined with metabolic activity of encapsulated HEK293 pSGH2lucpuro cells with co-encapsulated S24 particles was different. Metabolic activity of HEK293 pSGH2lucpuro C5 cells might be influenced by the presence of 0.5 % S24 nanoparticles. In summary, viability and proliferation appeared not to be influenced by the presence of 0.5% nanoparticles. In contrast metabolic activity appeared to be diminished by the presence of 0.5% S24 nanoparticles. The reason for this difference could be different tolerability towards the coating materials used for the different nanoparticle formulations.

With respect to biocompatibility of nanoparticles, it was reported by Schwalbe and colleagues that magnetic nanoparticles are incorporated into cells by endocytosis into phagosomes which then eventually fuse with lysosomes for degradation (Schwalbe, et al., 2005). TEM analysis within the presented study revealed that in capsules containing cells and S8 nanoparticles, nanoparticles could be detected within the capsule membrane, inside the capsule, and also within cells (Fig. 4.9. E – H). In capsules containing cells and S24 nanoparticles, nanoparticles were detected within the capsule, within the capsule lumen, within the cytoplasm and also to a certain extent within the nucleus (Fig. 4.9. I – L). Hence S24 nanoparticles appear to have a stronger tendency to be taken up by cells. This is in agreement with the original intended use of the applied nanoparticles. Both nanoparticle formulations were originally designed and coated to be used for magnetotransfection. The coating material is either polyethylenimine (S8) or 1.9-nonanedithiol (S24). Both materials have been previously used to enhance uptake of nanoparticles into cells (Arsianti, et al, 2010; Mirazimi, et al., 1999).

Inducibility of gene expression

In a next step, in order to further characterise generated encapsulated cells for realising the proposed concept, magnetic field-directed, nanoparticle-mediated, heat induction of reporter gene expression within encapsulated cells, inducibility of reporter gene expression in response to heat treatment in general was analysed. Analysis revealed that reporter gene expression was responsive to heat also in encapsulated cells (Fig. 4.15.). However, heat inducibility of reporter gene expression in encapsulated cells decreased during long-term cultivation for four weeks (Fig. 4.13. A). This decrease in induction levels resulted from an increase in basal level promoter activity at 37°C which was only observed with an increasing time of cultivation. This effect was most likely due to generation of hypoxic conditions within microcapsules (Fig. 4.17. C). Heat shock promoters can be activated by hypoxia (Taylor, et al., 2010). Nevertheless, it was possible to repeatedly induce reporter gene expression within encapsulated cells in intervals of one week (Fig. 4.18). Induced expression levels were higher in capsules where cell had grown to low densities compared to capsules grown confluent with cells. In addition, also expression levels were higher in encapsulated cells induced at early time points. The reason for this effect could be that heat treatment leads to a transient inhibition of proliferation resulting in lower hypoxic conditions whereas encapsulated cells heat-treated the first time in the second or third week of cultivation suffer more from hypoxia due to higher cell densities. Thus enforced hypoxic conditions and could result in an enhanced background promoter activity at 37°C. In order to circumvent the problem of hypoxia, encapsulated cells could be cultured for a short time and treated by Mitomycin C to arrest cell proliferation at low cell densities within capsules. Moreover, the problem of hypoxia could be avoided by generating microcapsules with a smaller diameter. Thereby encapsulated cells would be better supplied with oxygen because of the smaller diffusion distance. In terms of a cell-based therapy, multiple heat induction is possible at least in intervals of one week without refraction effects.

With respect to inducible gene expression systems in SCS microcapsules, an antibiotic responsive gene expression, was recently published (Fluri, et al., 2008). In this project a mixture of genetically modified cell lines were co-encapsulated; one cell

line harboured a doxycycline or erythromycin responsive expression construct driving the expression of a bacterial gene encoding cellulase and another cell line which produced a potential therapeutic protein (Fluri, et al., 2008). Induction of gene expression by addition of the respective antibiotic resulted in SCS capsule rupture, which was accomplished in order to set free the therapeutic cell line (Fluri, et al., 2008). In contrast to the here presented concept, the gene expression was switched on only once in order to unload the therapeutic cargo. However, to fulfil requirements of a potential therapeutic regime multiple inducibility of potential therapeutic gene expression would be of advantage. That this is possible has been demonstrated with the respective genetically modified encapsulated cells used here.

Encapsulated cells could be heat treated for 1 h to 2 h without relevant decrease in metabolic activity during the next four days (Fig. 4.16). Heat treatment for 3 h, however, led to almost complete loss in metabolic activity four days after heat treatment. This loss was most likely due to cell death in response to heat treatment. Considering potential therapeutic applications, this suggests that induction durations up to 2 h are tolerated.

For long-term remaining of implanted microcapsules containing cells in the human body a security mechanism can be employed in order to avoid uncontrolled escape of cells. Cells could be further genetically modified with a potential self-killing mechanism. Therefore, the gene for thymidin kinase from herpes simplex could be transferred into a therapeutic cell line. By injection of Gancyclovir or Acyclovir (Jiang, et al., 2011) remaining encapsulated cells could be completely eliminated from a human body at the end of a therapy. Despite regulate-able gene expression systems also constitutively expression systems could be used for such a security mechanism.

Magnetic field generation

The combination of the genetically modified HEK293 cells and magnetic nanoparticles for encapsulation leads to establishment of microcapsules containing cells and nanoparticles. These microcapsules were further used in realising the proposed concept: nanoparticle-mediated, magnetic field-directed thermoregulation of gene expression within encapsulated cells.

Within the presented work, the effect of an alternating magnetic field on cell integrity and cell viability within microcapsules was investigated. In magnetic field-treated samples, cells were shown to be intact and seem to be viable with the exception of capsules containing nanoparticles S8 cultured for five days after magnetic field treatment. Here, an increased number of areas with disrupted cells were detected when analysing electronmicrographs (Fig. 4.19.). In addition, necrosis and apoptosis in encapsulated cells in response to magnetic field treatment was analysed. The effect on necrosis of encapsulated cells was minor (Fig. 4.20.). It appears that necrosis in encapsulated cells was more dependent from extended periods of cultivation. The effect of apoptosis on encapsulated cells was also minor (Fig. 4.21. and Fig. 4.22.). Here, the quantified rate of apoptosis (20 – 30 %) in encapsulated cells lacking nanoparticles was increasing with the time of cultivation. The only significant increase in apoptosis was shown with encapsulated cells and S24 nanoparticles as compared to standard capsules lacking the nanoparticles on day two after magnetic field treatment. In summary, it appears that the utilised HEK293 cell line is a robust cell line showing little sensitivity to transiently elevated temperatures.

For proof-of-principle experiments only cells co-encapsulated with S8 nanoparticles were selected. S8 nanoparticles exhibited higher heat generation capacity in an alternating magnetic field, a better tolerability as revealed by the investigation of their biocompatibility during long-term cultivation, and a lower effect of apoptosis on cells when subjected to an alternating magnetic field.

Proof-of-principle of the proposed concept could be provided *in vitro* (Fig. 4.23. and Fig 4.24.). It was possible to switch on reporter gene expression within encapsulated cells by applying an alternating magnetic field. The magnetic field treatment led to a strong induction of luciferase expression only when cells had been co-encapsulated with S8 nanoparticles. The difference in gene expression levels in encapsulated cells with and without S8 nanoparticles was shown to be highly significant (p-value of 0.029, Mann-Whitney-Test).

However, the experimental setup suffers from some limitations. The calculated induction rates of luciferase expression in differing experiments are highly variable resulting in large standard deviations. High standard deviations were observed in four independently performed experiments with the same parameters (Fig. 4.23.) indicating most likely a variability in the cell densities of the used microcapsules containing cells and/or nanoparticles. For proof-of-principle experiments, encapsulated cells cultured for two weeks post encapsulation were used. These encapsulated cells differ in their induction capabilities most probably due to increasing hypoxic conditions within the microcapsules. Hence, induction levels in the four independent experiments considerably differ resulting in high standard deviations.

Additionally, variations in the performance of the magnetic field generator have been a problem, even though the temperature increase of a 1% standard nanoparticle dispersion was measured before every use as well as the magnetic field which was measured with an exploring coil. Wave generator and power amplifier were commercially available as pre-made units; the coil had to be constructed according to the required dimensions and field strength of the magnetic field. The Helmholtz coil was custom-made prepared and driven with frequencies up to 80 kHz and amplitudes up to 40 kA/m. In a final experimental version of the arrangement it would be helpful to have a bigger coil in which a mouse could fit in. For exact calculation of the applied magnetic field it would be desirable to have a symmetrically wound coil. It would be beneficial to have a water-cooled coil thereby avoiding direct heat transfer to the sample. Furthermore, it would be favourably to have a temperature adjustable water jacket between coil and sample vial to simulate body temperature. Several of these

requirements are fulfilled by an experimental high-performance magnetic field generator available by the company MFH Hyperthermiesystem GmbH, Berlin, Germany. These devices are already used in clinical trials for the treatment of solid tumours by magnetic fluid hyperthermia and are therefore used by the companies Magforce Nanotechnologies AG, Berlin, Germany and Sirtex Medical Ltd, Sydney, Australia.

For the treatment of deep-seated solid tumours by nanoparticle-mediated thermotherapy, Bellizzi and Bucci stated that 10 mg/ml ($\approx 1\%$) particle concentrations are sufficient to reach temperatures above 43°C. Moreover, they calculated that 3 mg/ml ($\approx 0.3\%$) is sufficient when particles are distributed monodispersely in moderately perfused tissues. (Bellizzi et Bucci, 2010) In the presented work, the capsules used contain only 5 mg/ml ($\approx 0.5\%$) nanoparticles which were shown to form aggregates (Fig. 4.4). 5 mg/ml ($\approx 0.5\%$) was the maximal encapsulate-able concentration for magnetic nanoparticles S8 and S24. However, the parameters are calculated for moderately perfused tissues suggesting that the used concentrations are just sufficient for heat generation *in vitro* in a non-perfused sample, as shown in the result of the *in vitro* proof-of-principle experiments.

Proof-of-principle for an *in vivo* heat-induced reporter gene expression in encapsulated cells could be provided in the mouse model (Fig. 4.25.). Luciferase expression could be multiply induced in two mice. There, expression was detected three times in intervals of one week in mice. However, no reporter gene expression could be demonstrated in response to magnetic field treatment. As already mentioned, for non-monodispers nanoparticles the nanoparticle concentration has to be at least 10 mg/ml (Bellizzi et Bucci, 2010). In conclusion, it appears that the maximal encapsulate-able nanoparticle concentration of 0.5% (≈ 5 mg/ml) is too low to generate a lasting temperature increase for induction of gene expression in perfused tissue by application of an alternating magnetic field. Thus the encapsulation process has to be further optimised to allow the encapsulation of higher nanoparticle concentrations. Moreover, nanoparticle formulations have to be further optimised to prevent their aggregation without using cell toxic reagents or substances disturbing the encapsulation process.

Conclusion and applications of the proposed cell therapy concept

In summary, proof-of-principle for the novel cell therapy concept could be provided *in vitro* by magnetic field-directed nanoparticle-mediated heat induction of reporter gene expression in encapsulated cells. Additionally, preliminary *in vivo* experiments have demonstrated multiple heat-inducible reporter gene expression in encapsulated cells implanted into mice. This generally indicates applicability of this novel cell therapeutic concept, even though further optimisations of the modulateable concept are needed. In cell-based therapy the transplanted cells can basically produce all kinds of proteins and peptides. Both, simple replacement strategies which seek to compensate for gene deficiencies and also fine-tuned interference with genetic and biochemical pathways are potential applications for cell therapy. Examples for a not critical dosage is blood coagulation (Garcia-Martin, et al. 2002), whereas critical regulatory constraints apply to hormones and growth factors like insulin, growth hormone for treatment of dwarfism (Al-Hendy, et al., 1996), nerve growth factor and ciliary neurotrophic factor for neurological disorders (Bloch, et al. 2004) and erythropoietin for β -thalasemia (Dalle, et al., 1999). Immunostimulatory proteins like interferons are yet another example for dose-dependent factors. Real-time regulation by the patient would ideally be required for the expression of the pain alleviating proopiomelanocortin gene (Saito et al., 1995). (please refer to Czerny, et al., 2006) In this project we provide a new concept for cell-based therapy in which the expression of the therapeutic peptide or protein can be externally fine-tuned, dependent to the requirements of the therapy.

6. REFERENCES

- Akinc, A., Thomas, M., Klibanov, A.M., Langer, R., 2005, Exploring polyethylenimine-mediated DNA transfection and the proton sponge hypothesis. *J Gene Med* 7, 657-663.
- Al-Hendy, A., Hortelano, G., Tannenbaum, G.S., Chang, P.L., 1996, Growth retardation--an unexpected outcome from growth hormone gene therapy in normal mice with microencapsulated myoblasts. *Hum Gene Ther* 7, 61-70.
- Alexiou, C., Arnold, W., Klein, R.J., Parak, F.G., Hulin, P., Bergemann, C., Erhardt, W., Wagenpfeil, S., Lubbe, A.S., 2000, Locoregional cancer treatment with magnetic drug targeting. *Cancer Res* 60, 6641-6648.
- Alexiou, C., Jurgons, R., Schmid, R.J., Bergemann, C., Henke, J., Erhardt, W., Huenges, E., Parak, F., 2003, Magnetic drug targeting--biodistribution of the magnetic carrier and the chemotherapeutic agent mitoxantrone after locoregional cancer treatment. *J Drug Target* 11, 139-149.
- Arsianti, M., Lim, M., Marquis, C.P., Amal, R., 2010, Assembly of polyethylenimine-based magnetic iron oxide vectors: insights into gene delivery. *Langmuir* 26, 7314-7326.
- Atsumi, T., Jeyadevan, B., Satob, Y., Tohji, K., 2007, Heating efficiency of magnetite particles exposed to AC magnetic field. *Journal of Magnetism and Magnetic Materials* 2007, 2841 - 2843.
- Bajoghli, B., Aghaallaei, N., Heimbucher, T., Czerny, T., 2004, An artificial promoter construct for heat-inducible misexpression during fish embryogenesis. *Dev Biol* 271, 416-430.
- Bellizzi, G., Bucci, O.M., 2010, On the optimal choice of the exposure conditions and the nanoparticle features in magnetic nanoparticle hyperthermia. *Int J Hyperthermia* 26, 389-403.
- Bloch, J., Bachoud-Levi, A.C., Deglon, N., Lefaucheur, J.P., Winkel, L., Palfi, S., Nguyen, J.P., Bourdet, C., Gaura, V., Remy, P., Brugieres, P., Boisse, M.F., Baudic, S., Cesaro, P., Hantraye, P., Aebischer, P., Peschanski, M., 2004, Neuroprotective gene therapy for Huntington's disease, using polymer-encapsulated cells engineered to secrete human ciliary neurotrophic factor: results of a phase I study. *Hum Gene Ther* 15, 968-975.

-
- Brade, A.M., Ngo, D., Szmitko, P., Li, P.X., Liu, F.F., Klamut, H.J., 2000, Heat-directed gene targeting of adenoviral vectors to tumor cells. *Cancer Gene Ther* 7, 1566-1574.
- Chang, T.M., 2005, The role of artificial cells in cell and organ transplantation in regenerative medicine. *Panminerva Med* 47, 1-9.
- Cherukuri, P., Glazer, E.S., Curley, S.A., 2010, Targeted hyperthermia using metal nanoparticles. *Adv Drug Deliv Rev* 62, 339-345.
- Cirone, P., Bourgeois, J.M., Austin, R.C., Chang, P.L., 2002, A novel approach to tumor suppression with microencapsulated recombinant cells. *Hum Gene Ther* 13, 1157-1166.
- Cirone, P., Bourgeois, J.M., Chang, P.L., 2003, Antiangiogenic cancer therapy with microencapsulated cells. *Hum Gene Ther* 14, 1065-1077.
- Cirone, P., Shen, F., Chang, P.L., 2005, A multiprong approach to cancer gene therapy by coencapsulated cells. *Cancer Gene Ther* 12, 369-380.
- Czerny, T., Günzburg, W.H., Walzer, J. 2006. Regulated gene expression in encapsulated cells. FWF grant P19936-B11, 2-3
- Dalle, B., Payen, E., Regulier, E., Deglon, N., Rouyer-Fessard, P., Beuzard, Y., Aebischer, P., 1999, Improvement of mouse beta-thalassemia upon erythropoietin delivery by encapsulated myoblasts. *Gene Ther* 6, 157-161.
- Elliot, R.B., Escobar, L., Calafiore, R., Basta, G., Garkavenko, O.; Vasconcellos, A., Bambra, C., 2005, Transplantation of micro- and macroencapsulated piglet islets into mice and monkeys, *Transplant. Proc* 37, 466–469.
- Elliott, R.B., Escobar, L., Tan, P.L., Muzina, M., Zwine, S., Buchanan, C., 2007, Live encapsulated porcine islets from a type 1 diabetic patient 9.5 yr after xenotransplantation, *Xenotransplantation* 14, 157–161.
- Ferry, N., Pichard, V., Aubert, D., Bony, S., Nguyen, T.H., 2011, Retroviral Vector-Mediated Gene Therapy for Metabolic Diseases: An Update. *Curr Pharm Des.* Jul 21. [Epub ahead of print]
- Fluri, D.A., Kemmer, C., Daoud-El Baba, M., Fussenegger, M., 2008, A novel system for trigger-controlled drug release from polymer capsules. *J Control Release* 131, 211-219.

-
- Garcia-Martin, C., Chuah, M.K., Van Damme, A., Robinson, K.E., Vanzielegem, B., Saint-Remy, J.M., Gallardo, D., Ofori, F.A., Vandendriessche, T., Hortelano, G., 2002, Therapeutic levels of human factor VIII in mice implanted with encapsulated cells: potential for gene therapy of haemophilia A. *J Gene Med* 4, 215-223.
- Gossuin, Y., Gillis, P., Hocq, A., Vuong, Q.L., Roch, A., 2009, Magnetic resonance relaxation properties of superparamagnetic particles. *Wiley Interdiscip Rev Nanomed Nanobiotechnol* 1, 299-310.
- Goverdhan, S., Puntel, M., Xiong, W., Zirger, J.M., Barcia, C., Curtin, J.F., Soffer, E.B., Mondkar, S., King, G.D., Hu, J., Sciascia, S.A., Candolfi, M., Greengold, D.S., Lowenstein, P.R., Castro, M.G., 2005, Regulatable gene expression systems for gene therapy applications: progress and future challenges. *Mol Ther* 12, 189-211.
- Günzburg, W.H., 2004, A milestone year for gene therapy goes unnoticed. *Curr Opin Mol Ther* 6, 358-359.
- Hacein-Bey-Abina, S., Von Kalle, C., Schmidt, M., McCormack, M.P., Wulffraat, N., Leboulch, P., Lim, A., Osborne, C.S., Pawliuk, R., Morillon, E., Sorensen, R., Forster, A., Fraser, P., Cohen, J.I., de Saint Basile, G., Alexander, I., Wintergerst, U., Frebourg, T., Aurias, A., Stoppa-Lyonnet, D., Romana, S., Radford-Weiss, I., Gross, F., Valensi, F., Delabesse, E., Macintyre, E., Sigaux, F., Soulier, J., Leiva, L.E., Wissler, M., Prinz, C., Rabbitts, T.H., Le Deist, F., Fischer, A., Cavazzana-Calvo, M., 2003, LMO2-associated clonal T cell proliferation in two patients after gene therapy for SCID-X1. *Science* 302, 415-419.
- Häfeli, U.O., Riffle, J.S., Harris-Shekhawat, L., Carmichael-Baranauskas, A., Mark, F., Dailey, J.P., Bardenstein, D., 2009, Cell uptake and in vitro toxicity of magnetic nanoparticles suitable for drug delivery. *Mol Pharm* 6, 1417-1428.
- Hauser, O., Prieschl-Grassauer, E., Salmons, B., 2004, Encapsulated, genetically modified cells producing in vivo therapeutics. *Curr Opin Mol Ther* 6, 412-420.
- Hernandez, R.M., Orive, G., Murua, A., Pedraz, J.L., 2010, Microcapsules and microcarriers for in situ cell delivery. *Adv Drug Deliv Rev* 62, 711-730.
- Hunt, N.C., Grover, L.M., 2010, Cell encapsulation using biopolymer gels for regenerative medicine. *Biotechnol. Lett.* 32, 733-742.

-
- Ito, A., Matsuoka, F., Honda, H., Kobayashi, T., 2003a, Heat shock protein 70 gene therapy combined with hyperthermia using magnetic nanoparticles. *Cancer Gene Ther* 10, 918-925.
- Ito, A., Matsuoka, F., Honda, H., Kobayashi, T., 2004, Antitumor effects of combined therapy of recombinant heat shock protein 70 and hyperthermia using magnetic nanoparticles in an experimental subcutaneous murine melanoma. *Cancer Immunol Immunother* 53, 26-32.
- Ito, A., Tanaka, K., Honda, H., Abe, S., Yamaguchi, H., Kobayashi, T., 2003b, Complete regression of mouse mammary carcinoma with a size greater than 15 mm by frequent repeated hyperthermia using magnetite nanoparticles. *J Biosci Bioeng* 96, 364-369.
- Ito, A., Tanaka, K., Kondo, K., Shinkai, M., Honda, H., Matsumoto, K., Saida, T., Kobayashi, T., 2003c, Tumor regression by combined immunotherapy and hyperthermia using magnetic nanoparticles in an experimental subcutaneous murine melanoma. *Cancer Sci* 94, 308-313.
- Jordan, A., 2009, Hyperthermia classic commentary: 'Inductive heating of ferrimagnetic particles and magnetic fluids: Physical evaluation of their potential for hyperthermia' by Andreas Jordan et al., *International Journal of Hyperthermia*, 1993;9:51-68. *Int J Hyperthermia* 25, 512-516.
- Jordan, A., Scholz, R., Maier-Hauff, K., van Landeghem, F.K., Waldoefner, N., Teichgraber, U., Pinkernelle, J., Bruhn, H., Neumann, F., Thiesen, B., von Deimling, A., Felix, R., 2006, The effect of thermotherapy using magnetic nanoparticles on rat malignant glioma. *J Neurooncol* 78, 7-14.
- Jordan, A., Maier-Hauff, K., 2007, Magnetic nanoparticles for intracranial thermotherapy. *J Nanosci Nanotechnol.*, 7, 4604-4606.
- Karle, P., Muller, P., Renz, R., Jesnowski, R., Saller, R., von Rombs, K., Nizze, H., Liebe, S., Gunzburg, W.H., Salmons, B., Lohr, M., 1998, Intratumoral injection of encapsulated cells producing an oxazaphosphorine activating cytochrome P450 for targeted chemotherapy. *Adv Exp Med Biol* 451, 97-106.
- Kubota, H., 2009, Quality control against misfolded proteins in the cytosol: a network for cell survival. *J Biochem* 146, 609-616.
- Lee, Y.J., Kim, J.H., Ryu, S., 1994, Comparison of heat shock gene expression in mild hyperthermia sensitive human prostatic carcinoma cells and heat-resistant human breast carcinoma cells, *J. Therm. Biol.* 19, 151-161.

-
- Lee, D.Y., Nam, J.H., Byun, Y., 2007, Functional and histological evaluation of transplanted pancreatic islets immunoprotected by PEGylation and cyclosporine for 1 year, *Biomaterials* 28, 1957–1966.
- Löhr, M., Hoffmeyer, A., Kroger, J., Freund, M., Hain, J., Holle, A., Karle, P., Knofel, W.T., Liebe, S., Muller, P., Nizze, H., Renner, M., Saller, R.M., Wagner, T., Hauenstein, K., Günzburg, W.H., Salmons, B., 2001, Microencapsulated cell-mediated treatment of inoperable pancreatic carcinoma. *Lancet* 357, 1591-1592.
- Löhr, M., Muller, P., Karle, P., Stange, J., Mitzner, S., Jesnowski, R., Nizze, H., Nebe, B., Liebe, S., Salmons, B., Günzburg, W.H., 1998, Targeted chemotherapy by intratumour injection of encapsulated cells engineered to produce CYP2B1, an ifosfamide activating cytochrome P450. *Gene Ther* 5, 1070-1078.
- Löhr, J.M., Kröger, J.C., Hoffmeyer, A., 2003; Safety, feasibility and clinical benefit of localized chemotherapy using microencapsulated cells for inoperable pancreatic carcinoma in a phase I/II trial. *Cancer Ther* 1, 121-131
- Luethy, J.D., Holbrook, N.J., 1992, Activation of the gadd153 promoter by genotoxic agents: a rapid and specific response to DNA damage. *Cancer Res.* 52, 5–10.
- Madeddu, P., 2005, Therapeutic angiogenesis and vasculogenesis for tissue regeneration. *Exp Physiol* 90, 315-326.
- Ma, M., Wu, Y., Zhou, J., Sun, Y., Zhang, Y., Gu, N., 2004, Size dependence of specific power absorption of Fe₃O₄ particles in AC magnetic field. *J Magnetism and Magnetic Materials* 268, 33–39
- Metzner, C., Salmons, B., Günzburg, W.H., Gemeiner, M., Miller, I., Gesslbauer, B., Kungl, A., Dangerfield, J.A., 2006, MMTV accessory factor Naf affects cellular gene expression. *Virology.* 346(1):139-50
- Mirazimi, A., Mousavi-Jazi, M., Sundqvist, V.A., Svensson, L., 1999, Free thiol groups are essential for infectivity of human cytomegalovirus. *J Gen Virol* 80 (Pt 11), 2861-2865.
- Moghimi, S.M., Hunter, A.C., Murray, J.C., 2005, Nanomedicine: current status and future prospects. *FASEB J* 19, 311-330.
- Mornet, S., Vasseur, S., Grasset, F., Duguet, E., 2004, Magnetic nanoparticle design for medical diagnosis and therapy. *J Mater Chem* 14, 2161-21752.

-
- Mostegl, M. 2009. Stable association of paramagnetic nanoparticles to retroviral vectors. Dissertation from the University of Veterinary Medicine. Chapter: Magnetic nanoparticles in biomedicine
- Motoyama, J., Hakata, T., Kato, R., Yamashita, N., Morino, T., Kobayashi, T., Honda, H., 2008, Size dependent heat generation of magnetite nanoparticles under AC magnetic field for cancer therapy. *Biomagn Res Technol* 6, 4.
- Orive, G., Hernandez, R.M., Gascon, A.R., Igartua, M., Rojas, A., Pedraz, J.L., 2001, Microencapsulation of an anti-VE-cadherin antibody secreting 1B5 hybridoma cells. *Biotechnol Bioeng* 76, 285-294.
- Orive, G., Hernández, R.M., Gascón, A.R., Calafiore, R., Chang, T.M.S., de Vos, P., Hortelano, G., Hunkeler, D., Lacík, I., Shapiro, A.M., Pedraz, J.L., 2003, Cell encapsulation: promise and progress. *Nat. Med.* 9 104–107.
- Orive, G., Hernandez, R.M., Rodriguez Gascon, A., Calafiore, R., Chang, T.M., de Vos, P., Hortelano, G., Hunkeler, D., Lacik, I., Pedraz, J.L., 2004, History, challenges and perspectives of cell microencapsulation. *Trends Biotechnol* 22, 87-92.
- Pankhurst, QAC., J.; Jones, S.K., and Dobson, J., 2003, Applications of magnetic nanoparticles in biomedicine. *Journal of Physics D: Applied Physics* 36: R176-R181
- Plank, C., Rosenecker, J., 2009, Magnetofection: the use of magnetic nanoparticles for nucleic acid delivery. *Cold Spring Harb Protoc* 2009, pdb prot5230.
- Plank, C., Scherer, F., Schillinger, U., Bergemann, C., Anton, M., 2003, Magnetofection: enhancing and targeting gene delivery with superparamagnetic nanoparticles and magnetic fields. *J Liposome Res* 13, 29-32.
- Rabanel, J.M., Banquy, X., Zouaoui, H., Mokhtar, M., Hildgen, P., 2009, Progress technology in microencapsulation methods for cell therapy. *Biotechnol Prog* 25, 946-963.
- Richter, K., Haslbeck, M., Buchner, J., 2010, The heat shock response: life on the verge of death. *Mol Cell* 40, 253-266.
- Rudolph, C., Lausier, J., Naundorf, S., Muller, R.H., Rosenecker, J., 2000, In vivo gene delivery to the lung using polyethylenimine and fractured polyamidoamine dendrimers. *J Gene Med* 2, 269-278.

-
- Sabel, M.S., Arora, A., Su, G., Mathiowitz, E., Reineke, J.J., Chang, A.E., 2007, Synergistic effect of intratumoral IL-12 and TNF-alpha microspheres: systemic anti-tumor immunity is mediated by both CD8+ CTL and NK cells. *Surgery* 142, 749-760.
- Saitoh, Y., Taki, T., Arita, N., Ohnishi, T., Hayakawa, T., 1995, Cell therapy with encapsulated xenogeneic tumor cells secreting beta-endorphin for treatment of peripheral pain. *Cell Transplant* 4 Suppl 1, S13-17.
- Salmons, B., Brandtner, E.M., Hettrich, K., Wagenknecht, W., Volkert, B., Fischer, S., Dangerfield, J.A., Gunzburg, W.H., 2010, Encapsulated cells to focus the metabolic activation of anticancer drugs. *Curr Opin Mol Ther* 12, 450-460.
- Salmons, B., Gunzburg, W.H., 2010, Therapeutic application of cell microencapsulation in cancer. *Adv Exp Med Biol* 670, 92-103.
- Salmons, B., Lohr, M., Gunzburg, W.H., 2003, Treatment of inoperable pancreatic carcinoma using a cell-based local chemotherapy: results of a phase I/II clinical trial. *J Gastroenterol* 38 Suppl 15, 78-84.
- Schäffellner, S., Stadlbauer, V., Stiegler, P., Hauser, O., Halwachs, G., Lackner, C., Iberer, F., Tscheliessnigg K.H., 2005, Porcine islet cells microencapsulated in sodium cellulose sulfate. *Transplant Proc.* 37, 248-52.
- Schmidt, J.J., Rowley, J., Kong, H.J., 2008, Hydrogels used for cell-based drug delivery. *J Biomed Mater Res A* 87, 1113-1122.
- Selvan, S.T., Patra, P.K., Ang, C.Y., Ying, J.Y., 2007, Synthesis of silica-coated semiconductor and magnetic quantum dots and their use in the imaging of live cells. *Angew Chem Int Ed Engl* 46, 2448-2452.
- Shamovsky, I., Nudler, E., 2008, New insights into the mechanism of heat shock response activation. *Cell Mol Life Sci* 65, 855-861.
- Shubayev, V.I., Pisanic, T.R., 2nd, Jin, S., 2009, Magnetic nanoparticles for theragnostics. *Adv Drug Deliv Rev* 61, 467-477.
- Somia, N., Verma, I.M., 2000, Gene therapy: trials and tribulations. *Nat Rev Genet* 1, 91-99.
- Stetter, K.O., 2006, Hyperthermophiles in the history of life. *Philos Trans R Soc Lond B Biol Sci* 361, 1837-1842; discussion 1842-1833.

-
- Stein, U., Walther, W., Wunderlich, V., 1994, Point mutations in the *mdr1* promoter region of human osteosarcomas are related with responsiveness to MDR relevant drugs, *Eur. J. Cancer* 30A, 1541–1545.
- Stiegler, P.B., Stadlbauer, V., Schäffellner, S., Halwachs, G., Lackner, C., Hauser, O., Iberer, F., Tscheliessnigg, K.H., 2006, Cryopreservation of insulin-producing cells microencapsulated in sodium cellulose sulfate. *Transplant Proc.* 38, 3026-3030
- Taylor, L., Midgley, A.W., Christmas, B., Madden, L.A., Vince, R.V., McNaughton, L.R., 2010, The effect of acute hypoxia on heat shock protein 72 expression and oxidative stress in vivo. *Eur J Appl Physiol* 109, 849-855.
- Teng, H., Zhang, Y., Wang, W., Ma, X., Fei, J., 2007, Inhibition of tumor growth in mice by endostatin derived from abdominal transplanted encapsulated cells. *Acta Biochim Biophys Sin (Shanghai)* 39, 278-284.
- Walther, W., Stein, U., 2009, Heat-responsive gene expression for gene therapy. *Adv Drug Deliv Rev* 61, 641-649.
- Wirth, M., Fritsche, P., Stojanovic, N., Brandl, M., Jaeckel, S., Schmid, R.M., Saur, D., Schneider, G., 2011, A simple and cost-effective method to transfect small interfering RNAs into pancreatic cancer cell lines using polyethylenimine. *Pancreas* 40, 144-150.

7. APPENDIX

7.1. Abbreviations

A	ampere
AMF	alternating magnetic field
ATP	adenosine-triphosphate
C	celsius
CLSM	confocal laser scanning microscope
CMV	cytomegalovirus
DAPI	4',6-diamidin-2-phenylindol
DMEM	Dulcecco`s modified eagle`s medium
DMSO	dimethyl-sulfoxide
dNTPs	desoxyribonucleotide-triphosphate
DPX	dibutyl phthalate - xylene
DTT	dithiothreitol
EDTA	ethylene-diamine-tetra-acetate
EGFP	enhanced green fluorescent protein
EM	electron microscopy
FCS	foetal calve serum
FITC	fluorescein-isothiocyanate
g	gram
GSK3 α	glycogen synthase kinase 3 α
h	hour
HEK293	human embryonic kidney cells
HS	heat shock
HSE	heat shock element
HSF1	heat shock factor 1
HSP70/90	heat shock protein 70/90
i.p.	intra-peritoneal
JNK	c-Jun N-terminal kinase

kDa	kilodalton
kHz	kiloherz
luc	luciferase
MAP	mitogen-activated protein kinase
MHz	megahertz
min	minute
ml	millilitre
μl	microlitre
MNPs	magnetic nanoparticles
MOPS	3-(N-Morpholino)propane sulfonic acid
MRI	magnet resonance imaging
1.9-NDT	1.9-nonanedithiol
ng	nanogram
NM	normal medium
p	plasmid
PBS	phosphate buffered saline
pDADMAC	poly diallyl dimethyl ammonium chloride
PEG	polyethylene glycol
PEI	polyethylenimine
pr	promoter
puro	puromycin
RT	room temperature
SAR	specific absorption rate
SCS	sodium cellulose sulphate
Ser	serine
SSA	specific surface area
TEM	transmission electron microscopy
Tris	tris(hydroxymethyl)aminomethane
UV	ultraviolet
V	voltage
w/w	weight per weight

7.2. List of figures

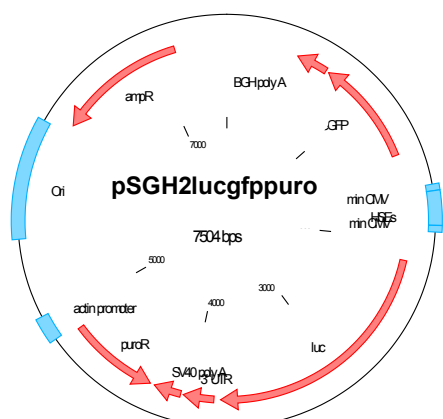
- Fig. 2.1.: Nanoparticle-mediated thermoregulation of gene expression within encapsulated cells by applying an alternating magnetic field.
- Fig. 2.2.: Concept of cell therapy and cell immunoisolation in microcapsules.
- Fig. 2.3.: Heat inducible expression construct.
- Fig. 2.4.: Regulation of heat shock response.
- Fig. 3.1.: Image of used encapsulator from Inotech (IE-50R).
- Fig. 3.2.: Schematic representation of the encapsulation process.
- Fig. 3.3.: Chemical structure of sodium cellulose sulphate and of poly-diallyl-dimethyl-ammonium-chloride.
- Fig. 3.4.: Custom-made magnetic field generator.
- Fig. 4.1.: Heat inducibility of cultured HEK293 pSGH2lucpuro C5 cells.
- Fig. 4.3.: Heat generation capacity of a set of different nanoparticles.
- Fig. 4.2.: Induction of GFP expression in HEK293 pSGH2lucpuro C5 cells.
- Fig. 4.4.: Nanoparticle aggregation.
- Fig. 4.5.: SCS capsules containing HEK293 pSGH2lucpuro C5 cells with and without nanoparticles.
- Fig. 4.6.: Capsule diameters of capsule with cells and with co-encapsulated nanoparticles.
- Fig. 4.7.: Capsule diameters.
- Fig. 4.8.: Analysis of size exclusion by capsule membranes manufactured with different SCS concentrations.
- Fig. 4.9.: Determination of membrane thickness.
- Fig. 4.10.: Coating material of selected nanoparticle formulations.
- Fig. 4.11.: Nanoparticle localisation.
- Fig. 4.12.: Viability of encapsulated cells during long-term cultivation
- Fig. 4.13.: Metabolic activity of encapsulated cells during long-term cultivation with or without nanoparticles.
- Fig. 4.14.: Growth of encapsulated cells with or without nanoparticles.
- Fig. 4.15.: Heat-inducible expression in encapsulated cells.
- Fig. 4.16.: Effect of heat treatment on metabolic activity of encapsulated cells.

-
- Fig. 4.17.: Induction of luciferase expression during long-term cultivation
- Fig. 4.18.: Multiple heat treatment during long-term cultivation of encapsulated cells.
- Fig. 4.19.: Effects of magnetic field treatment on cell integrity.
- Fig. 4.20.: Effects of magnetic field treatment on nuclear integrity and cell viability.
- Fig. 4.21.: Apoptosis in response to magnetic field treatment in encapsulated cells.
- Fig. 4.22.: Apoptosis in response to magnetic field treatment in encapsulated cells.
- Fig. 4.23.: Magnetic field-directed, nanoparticle-mediated, thermoregulation of luciferase expression in encapsulated cells.
- Fig. 4.24.: Magnetic field-directed, nanoparticle-mediated, thermoregulation of GFP expression in encapsulated cells.
- Fig. 4.25.: *In vivo* imaging of luciferase expression in implanted encapsulated cells.
- Fig. 5.1.: Heat generation capacity of a set of nanoparticles with different core sizes.

7.3. List of tables

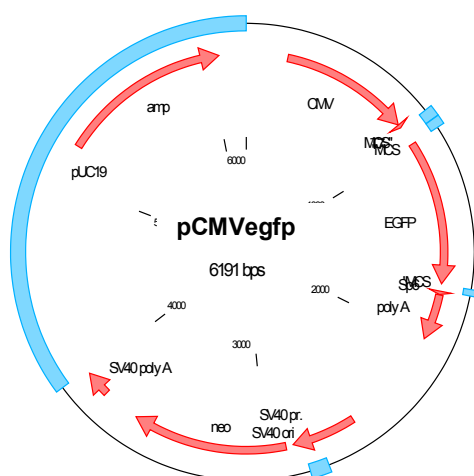
- Tab. 3.1.: Set of employed magnetite nanoparticles.
- Tab. 4.1.: Physicochemical characterisation of different nanoparticles.
- Tab. 4.2.: Magnetic field-directed, nanoparticle-mediated thermoregulation of GFP expression in encapsulated cells.
- Tab. 4.3.: *In vivo* thermoregulation of luciferase expression in encapsulated cells implanted into mice.

7.4. Plasmids



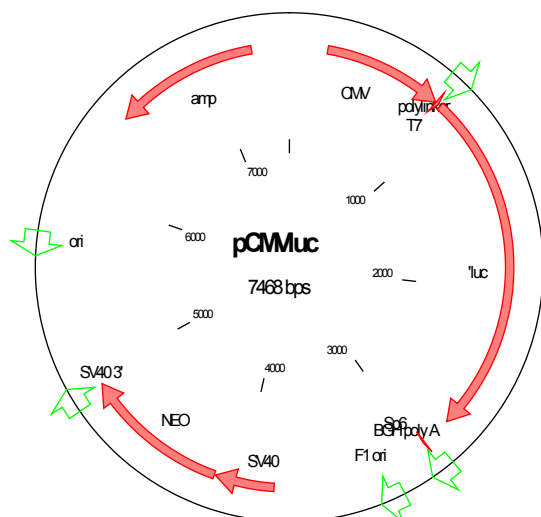
pSGH2lucgfp puro – heat inducible expression construct harbouring plasmid

Legend: minCMV: minimal cytomegalovirus promoter, HSE: heat shock elements. luc: gene encoding firefly luciferase, GFP: gene encoding green fluorescent protein, SV40 poly A: Simian Virus 40 polyA signal, BGH polyA: Bovine Growth Hormone polyA signal, ampR: gene encoding resistance for ampicillin, ori: origin of replication, puroR: gene encoding resistance against puromycin, 3`UTR: 3` untranslated region



pCMVegfp – control plasmid for constitutive EGFP expression

Legend: CMV: cytomegalovirus promoter, EGFP: gene coding for enhanced green fluorescent protein, neoR: gene encoding resistance for neomycin, SV40 pr: Simian Virus 40 promoter, SV40 poly A: Simian Virus 40 polyA signal, ampR: gene encoding resistance for ampicillin; MCS: multiple cloning site



pCMVluc – control plasmid for constitutive luciferase expression

Legend: CMV: cytomegalovirus promoter, luc: gene coding for firefly luciferase, neoR: gene encoding resistance for neomycin, SV40 pr: Simian Virus 40 promoter, SV40 poly A: Simian Virus 40 polyA signal, ampR: gene encoding resistance for ampicillin, T7: T7 promoter; ori: origin of replication, BGH polyA: Bovine Growth Hormone polyA signal, SP6: promoter of phage SP6

7.5. Own publications

7.5.1. Scientific paper

Journal of Controlled Release (article accepted)

Magnetic field-controlled gene expression of encapsulated cells

Ortner V.*^{1,2}, Kaspar C.*³, Halter C.¹, Töllner L.³, Mykhaylyk O.⁴, Walzer J.¹, Günzburg W.H.³, Dangerfield J.A.³, Hohenadl C.³, and Czerny T.^{1,2}

*Equal contributors; ¹University of Applied Sciences, FH Campus Wien, Department for Applied Life Sciences, Vienna, Austria; ²Department for Biomedical Sciences, Institute of Animal Breeding and ³Department for Pathobiology, Institute of Virology, University of Veterinary Medicine, Vienna, Austria ⁴Department for Pathobiology, Institute for Experimental Oncology, Klinikum Rechts der Isar, TU Munich, Munich, Germany

Abstract: Cell and gene therapies have an enormous range of potential applications, but as for most other therapies, dosing is a critical issue, which makes regulated gene expression a prerequisite for advanced strategies. Several inducible expression systems have been established, which mainly rely on small molecules as inducers, such as hormones or antibiotics. Here we describe a novel system for induction of gene expression in encapsulated cells. This involves the modification of cells to express potential therapeutic genes under the control of a heat inducible promoter and the co-encapsulation of these cells with magnetic nanoparticles. Magnetic nanoparticles produce heat when subjected to an alternating magnetic field, the elevated temperatures in the capsules then induce gene expression. In the present study we define the parameters of such systems and provide proof-of-principle using reporter gene constructs. The fine-tuned heating of nanoparticles in the magnetic field allows regulation of gene expression from the outside over a broad range and within short time. Such a system has great potential for advancement of cell and gene therapy approaches.

7.5.2. Oral presentation

ÖGBM, ÖGGGT, ÖGBT, ANGT Joint Annual Meeting 2008, Graz, 22. – 24.09.2008

Thermoregulation of gene expression in encapsulated cells by magnetic field-directed, nanoparticle-mediated heat induction

Kaspar, C.¹, Ortner, V.², Günzburg, W.H.¹, Kluger, C.⁴, Dangerfield, J.A.¹, Czerny, T.^{2,3}, Hohenadl, C.¹

¹Department of Pathobiology, Institute of Virology and ²Institute of Animal Breeding and Genetics, University of Veterinary Medicine, Vienna; ³University of Applied Sciences, FH Campus Vienna; ⁴Austrianova Biotechnology GmbH, Vienna; AUSTRIA

Abstract: For the treatment of metabolic disease using cell based therapies an externally controllable modulation of therapeutic gene expression is of great interest. In this respect we are evaluating a thermoregulatable expression system based on a synthetic heat shock promoter. Heat induction will be achieved by means of Fe₃O₄ nanoparticles treated with an alternating magnetic field. As a test system, HEK293 cells carrying a reporter gene construct driven by the respective promoter were encapsulated into sodium cellulose sulphate and analysed for heat inducible expression. Having successfully set up the optimum parameters for heat induction, cells were co-encapsulated with Fe₃O₄ nanoparticles and treated with a custom-made magnetic field generator. Preliminary analyses of reporter gene expression levels, cell viability, temperature limits and refraction times will be presented supporting proof of concept which will finally be demonstrated in a mouse model.

7.5.3. Poster presentations

ÖGMBT Annual Meeting 2009, Innsbruck, 21. – 23.09.2009

Magnetic nanoparticle induced gene expression in encapsulated cells

Kaspar C.¹ and Ortner V.², Halter C.³, Walzer J.³, Günzburg W.H.¹, Dangerfield J.A.¹, Czerny T.^{2,4}, Hohenadl C.¹

¹Department of Pathobiology, Institute of Virology and ²Department of Biomedical Sciences, Institute of Animal Breeding and Genetics, University of Veterinary Medicine, Vienna; ³Department of Technics and ⁴Department of Applied Life Sciences, FH Campus Vienna

Abstract: Microencapsulation of cells in biologically inert sodium cellulose sulphate allows implantation of heterologous cells, e.g. in cell-based therapy, without reaction of the host immune system. Combining different well established technologies, we here propose to regulate gene expression in encapsulated cells from outside the patient's body. Firstly, HEK293 cells were genetically modified to carry a synthetic bidirectional heat-inducible promoter which drives the expression of two different reporter genes. Secondly, these cells were co-encapsulated together with Fe₃O₄ nanoparticles. Finally, heat was generated within the capsules by application of an alternating magnetic field. We here provide a proof of concept *in vitro*, demonstrating robust induction of gene expression in magnetic field-treated samples.

BioNanoMed 2009, Krems, 26. – 27.01.2009**Magnetic nanoparticle mediated gene expression in cell therapy**

Ortner V.¹, Kaspar C.², Platzer T.¹, Halter C.³, Walzer J.³, Günzburg W.H.², Dangerfield J.A.², Hohenadl C.², Czerny T.^{1,4}

¹Department for Biomedical Sciences, Institute of Animal Breeding and Genetics, University of Veterinary Medicine, Veterinärplatz 1, 1210 Vienna; ²Department for Pathobiology, Institute of Virology, University of Veterinary Medicine, Veterinärplatz 1, 1210 Vienna; ³Department of Technics, FH Campus Wien, Daumegasse 3, 1100 Vienna; ⁴Department of Applied Life Sciences, FH Campus Wien, Campus Vienna Biocenter, Viehmarktgasse 2A, 1030 Vienna

Abstract: Cell therapy provides a strategy to administer genetically modified cells to patients. When incorporated into cellulose sulphate microcapsules, these cells are protected from the host immune system and localised to the area of implantation. Thus even heterologous cells survive in the patient and can produce therapeutic substances over several months to a targeted site.

We are developing a method to externally regulate the expression of the therapeutic gene inside the capsules. The basis for the project is a heat inducible promoter. Cells containing this promoter are encapsulated together with magnetic nanoparticles, which produce heat when exposed to an alternating magnetic field. After application of the capsules to the patient, the promoter is induced from the outside by a magnetic field which generates elevated temperatures in the encapsulated cells. Thus expression of the therapeutic genes can be regulated according to the requirements of the therapy.

In order to obtain a proof-of-principle for the project a stable HEK 293 cell line was generated, expressing the marker genes eGFP and Luciferase under the control of a bidirectional artificial heat shock promoter. A highly inducible cell clone was selected and characterised. Next, conditions for encapsulation in cellulose sulphate together with Fe₃O₄ magnetic nanoparticles were established. For application of the alternating magnetic field a generator with a power amplifier was built. The capsules

were incubated in cell culture medium in a water-cooled coil. Preliminary experiments gave proof-of-concept in vitro as ten-fold higher luciferase activity was measured in capsules containing magnetic nanoparticles compared to control capsules without nanoparticles.

ÖGMBT Annual Meeting 2009, Innsbruck, 21. – 23.09.2009

Characterisation of an artificial heat shock promoter for cell therapy applications

Ortner V.¹, Kaspar C.², Ludwig A.¹, Günzburg W.H.¹, Dangerfield J.A.², Hohenadl C.², Czerny T.^{1,3}

¹Department of Biomedical Sciences, Institute of Animal Breeding and Genetics and
²Department of Pathobiology, Institute of Virology, University of Veterinary Medicine, Vienna; ³Department of Applied Life Sciences, FH Campus Vienna

Abstract: The heat shock response is the most prominent reaction of cells to stress. Heat shock proteins form a large group of inducible proteins, which represent major players in this stress response. They are regulated by heat shock promoters which therefore can be applied for inducible expression systems. We generated an artificial heat shock promoter and present here its properties. As a reference serves endogenous heat shock protein expression. In addition we evaluated the promoter for gene therapy approaches, by comparing it to the well established natural HSP70B promoter. As a result, our artificial heat shock promoter leads to higher reporter gene expression with lower background levels. These superior properties make this promoter an ideal tool for gene therapy or cell therapy applications.

8. ACKNOWLEDGEMENTS

I owe special thanks to Professor Dr Ernst Wagner who gave me the opportunity to make my PhD thesis on the Ludwig-Maximilians-University and supported me. I want to thank PD Dr. Christine Hohenadl who was my supervisor and mentor and pushed the project forward at important moments.

I want to thank all the fluctuating people from the Institute of Virology and from the former company Austrianova. It was an exciting and instructive time and the companionship of the people was a strong support for me. Special thanks to Dr. Brian Salmons and Dr. John Dangerfield which brought me to Vienna. I want to thank Professor Dr. Walter Günzburg, who provided circumstances for an effective work against all adversities.

Furthermore, I want to thank the project leader Dr. Thomas Czerny for constructive advice. Many thanks to Victoria Ortner for good cooperativeness.

I want thank Dr. Olga Mykhaylyk and PD Dr. Plank for providing a set of nanoparticle dispersions which facilitated the accomplishment of the project. I want to thank Professor Dr. Christian Halter und Professor Dr. Johann Walzer for constructing and kindly providing the magnetic field generator.

Many thanks to Oliver Hauser and Dr. Lars Töllner for constructive discussions and advice by solving problems of encapsulation technology.

I want to thank the people from the Institute of Histology and Microanatomy for great assistance with my immunohistochemical experiments. I want to acknowledge Nora Dinhopf for help by performing electron-microscopic analysis. Many thanks to Helga Petznek and Isabelle Grosinger for excellent support with my animal experiments.

I give special thanks to my parents Gabriele and Jakob Kaspar and to my brothers Dominik and Tobias Kaspar for their help and life-long support and providing me all the means for my education.

9. CURRICULUM VITAE

Personal data

Date of birth: 10.10.1977
Place of birth: Munich, Germany
Marital status: unmarried

Education

- 07/2007 – present PhD thesis:** “Thermoregulation of gene expression in encapsulated cells by magnetic field-directed, nanoparticle-mediated heat induction“, external dissertation Department of Pharmaceutical Biology/Biotechnology, Ludwig-Maximilians-University, Munich, Germany; supervisor: Prof. Dr. Ernst Wagner, practical accomplishment Institute of Virology, University of Veterinary Medicine; Vienna, Austria
- 10/2000 – 08/2006 Diploma study of biology:** main subject: anthropology/human genetics, minor subjects: biochemistry, genetics and pharmacology/toxicology
Ludwig-Maximilians-University, Munich, Germany
diploma work: “Dynamic of hox gene clusters in differentiating murine stem cells by means of different development stages of embryoid bodies“
- 06/1999 Abitur,** main subjects: biology, economics and law,
Adolf-Weber-Gymnasium, Munich, Germany

Continuing education:

- 01/2003 – 12/2003 Intellectual Property Management** – extra-occupational training program in patent law,
Ludwig-Maximilians-University, Munich, Germany

Work experience:

- 03/2007 – 06/2007 and 06/2004 – 11/2004** **Student Assistant**, Association for Scientific Education, Ludwig-Maximilians-University, Munich, Germany
- 12/2004 – 06/2005 and 11/2001 – 08/2003** **Team Assistant**, Section of Patents and Licensing of the Research and Technology Transfer Office, Ludwig-Maximilians-University, Munich, Germany
- 08/2004 – 09/2004** **Research internship**: analytical detection of constituents from tobacco smoke, Analytical Biological Research laboratory, Munich, Germany
- 12/2003 - 03/2004** **Research internship**: genotyping of transgenic mice and investigation of the *in vivo* activity of the breast tissue-specific WAP promoter, Institute of Virology, University of Veterinary Medicine, Vienna, Austria
- 08/1999 – 06/2000** **Nursing practice** within the civilian service, section of urological diagnostics, Hospital of the Merciful Brethren, Munich, Germany

Scientific publications

Ortner V.*, Kaspar C.*, Halter C., Töllner L., Mykhaylyk O., Walzer J., Günzburg W.H., Dangerfield J.A., Hohenadl C., and Czerny T.. 2011. Magnetic field-controlled gene expression of encapsulated cells. J Controlled Release. Article accepted.

*Equal contributors.

Lanctot C., Kaspar C., Cremer C. 2007. Positioning of mouse Hox clusters in the nuclei of developing embryos and differentiating embryoid bodies. Exp Cell Res. 313 (7): 1449-59